ISSN: 2376-2136 (Print)
ISSN: 2376-2144 (Online)

Trends in Renewable Energy

Volume 1, Issue 2, August 2015

futureenergysp.com
thefutureenergy.org

Trends in Renewable Energy

ISSN: 2376-2136 (Print) ISSN: 2376-2144 (Online)

http://futureenergysp.com/

Trends in Renewable Energy is a quarterly, open accessed, peer-reviewed journal publishing reviews and research papers in the field of renewable energy technology and science.

The aim of this journal is to provide a communication platform that is run exclusively by scientists working in the renewable energy field. Scope of the journal covers: Renewable energy, Catalysis for energy generation, Biofuel, Bioenergy, Biomass, Biorefinery, Biological waste treatment, Bioprocessing, Energy conservation, Energy Resources, Energy transformation, Energy storage, Environmental impact, Feedstock utilization, Future energy development, Green chemistry, Green energy, Microbial products, Physico-chemical process for Biomass, Policy, Pollution, Thermo-chemical processes for biomass, etc.

The Trends in Renewable Energy publishes the following article types: peer-reviewed reviews, mini-reviews, technical notes, short-form research papers, and original research papers.

The article processing charge (APC), also known as a publication fee, is fully waived for the initial two years for the Trends in Renewable Energy.

Editorial Team of Trends in Renewable Energy

	University of the Basque Country, Spain
Dr. Nattaporn Chaiyat	Assist. Prof., School of Renewable Energy, Maejo University, Thailand
Dr. Nguyen Duc Luong	Institute of Environmental Science and Engineering, National University of Civil Engineering, Vietnam
Mohd Lias Bin Kamal	Faculty of Applied Science, Universiti Teknologi MARA, Malaysia
Dr. N.L. Panwar	Assistant Prof., Department of Renewable Energy Engineering, College of Technology and Engineering, Maharana Pratap University of Agriculture and Technology, India
Dr. Caio Fortes	BP BIOFUELS, Brazi
Dr. Flavio Prattico	Department of Methods and Models for Economics, Territory and Finance, Sapienza University of Rome, Italy
Dr. Wennan ZHANG	Docent (Associate Prof.) and Senior Lecturer in Energy Engineering, Mid Sweden University, Sweden
Dr. Ing. Stamatis S. Kalligeros	Assistant Prof., Hellenic Naval Academy, Greece
Carlos Rolz	Director of the Biochemical Engineering Center, Research Institute at Universidad del Valle, Guatemala
Ms. Lilias Makashini	Copperbelt University, Zambia
Dr. Ali Mostafaeipour	Assistant Prof., Industrial Engineering Department, Yazd University, Iran
Dr. Camila da Silva	Prof., Maringá State University, Brazil
Dr. Anna Skorek-Osikowska	Silesian University of Technology, Poland
Dr Shek Atiqure Rahman	Sustainable and Renewable Energy Engineering, College of Engineering, University of Sharjah, Bangladesh
Dr. Emad J Elnajjar	Associate Prof., Department of Mechanical Engineering, United Arab Emirates University, United Arab Emirates
Xianglin Zhai	Louisiana State University, United States
Dr. Adam Elhag Ahmed	National Nutrition Policy Chair, Department of Community Services, College of Applied Medical Sciences, King Saud University, Saudi Arabia
Dr. Srikanth Mutnuri	Associate Prof., Department of Biological Sciences, Associate Dean for International Programmes and Collaboration, Birla Institute of Technology & Science, India
Dr. Bashar Malkawi	S.J.D., Associate Prof., College of Law, University of Sharjah, United Arab Emirates
Dr. Simona Silvia Merola	Istituto Motori - National Research Council of Naples, Italy
Dr. Hakan Caliskan	Faculty of Engineering, Department of Mechanical Engineering, Usak University, Turkey

Table of Contents

Volume 1, Issue No. 2, August 2015

Trends in Renewable Energy
OPEN ACCESS ISSN: 2376-2144
EDITORIAL futureenergysp.com/index.php/tre

What Future for the Renewable Energy

Prof. Elio Santacesaria * (Professor of Industrial Chemistry; CEO of Eurochem Engineering Co.)

Eurochem Engineering srl, Via Codogno 5, 20139 Milano, Italy

Received April 9, 2015; Published April 10, 2015

In 1973, after the Kippur war, a considerable increase of the petroleum price occurred, because, Arabian countries decided to reduce the extraction and export of this raw material. It was the first time that petroleum price was imposed not by the market but as a consequence of a political unilateral decision. The governments of the occidental countries reacted to this situation by promoting researches on the use of coal as a possible substitute of petroleum. In Italy, for example, a national "Energy" project based on the use of coal had been launched and funded covering a period of about 10 years. Although, after some years the situation turned to the normality and the price of petroleum was consistently lowered rendering not convenient the use of coal, thanks to the performed studies, the scientists have learned to obtain from coal all the necessary components to satisfy the energetic needs. Coal was chosen as a possible alternative for the abundance of this raw material and, because, at that time the consume of petroleum was relatively limited and the environmental problems, deriving from a majestic use of petroleum, were not so important as today. In the last century, the petroleum consumption increased exponentially and the growing economy of the countries under development greatly contributed and still contributes to this increment. Gradually, the anxiety for the depletion of petroleum as raw material, which remedy could be clearly the use of coal, was substituted by the anxiety for the sustainability of the consequences of a continuous increase of the petroleum consumption on both the environment and the quality of the life. Under this aspect, coal is worse than petroleum and cannot be considered as a possible substitute.

Sustainability gradually became the cultural driving force for the development of the "Renewable Energy Sources" and new concepts like Bio-Refineries and Renewable Feedstock were diffused in a lot of publications and books and the governments funded many researches on the subject. However, it is opportune to remember that the consume of petroleum in the world is greater than 4 billion tons per year with only 4-5% destined to the chemicals production. The big economic interests, accompanying the commerce of petroleum, hold-down the development of any possible alternative. The recent intensive production of shale oil in United States, for example, has been contrasted by a strong decrease of the petroleum price produced in Arabia. In the meantime, a large availability of petroleum at low cost strongly reduced or blocked the production of bio-based fuels as biodiesel and bio-ethanol. The conclusion is that nowadays, Renewable Energy Sources cannot compete with petroleum for both the volume of production and price of the energy but remain the only feasible alternative if inserted in a revolutionary change of the way of life in which the man look for an equilibrium with the nature without renouncing to the

**Corresponding author:* info@eurochemengineering.com

Tr Ren Energy, 2015, Vol.1, No.2, 57-58. doi:10.17737/tre.2015.1.2.0010

wellness but certainly changing the previous habits. This is, at the same time a cultural, scientific but above all a political challenge to save the planet.

Trends in Renewable Energy
OPEN ACCESS ISSN: 2376-2144
Invited Review Article futureenergysp.com/index.php/tre

Designing Broadband over Power Lines Networks Using the Techno-Economic Pedagogical (TEP) Method – Part II: Overhead Low-Voltage and Medium-Voltage Channels and Their Modal Transmission Characteristics

Athanasios G. Lazaropoulos [1,2,*]

1: School of Electrical and Computer Engineering, National Technical University of Athens (NTUA), 9 Iroon Polytechniou Street, Zografou, Athens, Greece 15780
2: Department of Electrical and Electronic Engineering Educators, School of Pedagogical and Technological Education (ASPETE), Station Eirini HSAP, Heraklio Attikis, Athens, Greece 14121

Received February 8, 2015; Accepted March 25, 2015; Published April 11, 2015

Based on the techno-economic pedagogical (TEP) method proposed in [1] that is suitable for designing Broadband over Power Lines (BPL) networks in transmission and distribution power grids, this paper examines the broadband potential of overhead low-voltage/broadband over power lines (LV/BPL) and medium-voltage/broadband over power lines (MV/BPL) networks.

In this paper, on the basis of the set of linear simplifications and techno-economic metrics already presented in [1], TEP method demonstrates to undergraduate electrical and computer engineering (ECE) students the behavior of overhead LV/BPL and MV/BPL networks in terms of their modal transmission characteristics when different overhead LV/BPL and MV/BPL topologies occur.

The contribution of this paper is four-fold. First, the factors influencing modal transmission characteristics of overhead LV/BPL and MV/BPL networks are investigated with regard to their spectral behavior and end-to-end channel attenuation. Second, the impact of the multiplicity of branches at the same junction is first examined. In the light of cascaded two-way power dividers, TEP method is extended so as to cope with more complex BPL topologies offering a new simplified and accurate circuital approximation. Third, apart from the broadband transmission characteristics of the entire overhead distribution power grid, a consequence of the application of TEP method is that it helps towards the intraoperability/interoperability of overhead LV/BPL and MV/BPL systems under a common PHY framework in the concept of a unified distribution smart grid (SG) power network. Fourth, TEP method can be demonstrated to undergraduate ECE students as case study in order to stimulate their interest for Microwave Engineering and Circuit/System Engineering courses.

Keywords: Education, Educational Policy; Comparative Education; Faculty of Electrical and Computer Engineering; Microwave Engineering; Engineering Economics; Broadband over Power Lines (BPL) modeling; eigenvalue decomposition (EVD) modal analysis; Power Line Communications (PLC); overhead Low-Voltage (LV) power lines; overhead Medium-Voltage (MV) power lines

*Corresponding author: AGLazaropoulos@gmail.com

Tr Ren Energy, 2015, Vol.1, No.2, 59-86. doi:10.17737/tre.2015.1.2.006

I. Introduction

The need of bridging the digital gap between underdeveloped and developed areas signals the green light towards the deployment of broadband over power lines (BPL) networks across transmission –i.e., high-voltage (HV)– and distribution –i.e., low-voltage (LV) and medium-voltage (MV)– power grids [1]-[9]. Due to the ubiquitous nature of transmission and distribution power grids, BPL technology can offer real time information at any point of the entire power grid transforming it into an advanced IP-based interactive smart grid (SG) service network with a myriad of potential SG applications [10]-[14]. Recent findings demonstrate that the entire overhead distribution power grid may operate as an excellent communications medium offering low-loss characteristics, flat-fading features and low multipath dispersion on the vicinity of every power consumer [15]-[18].

To study overhead LV/BPL and MV/BPL networks, it is obvious that the development of efficient and accurate models to describe signal transmission at high frequencies across them is a challenging venture and imperative necessity. The behavior of BPL transmission channels installed on LV and MV multiconductor transmission line (MTL) structures is examined by employing the well-known hybrid method [3]. Briefly mentioned in [1], [63], this hybrid method follows: (i) a *bottom-up approach* consisting of an appropriate combination of the similarity transformation and MTL theory to determine the propagation constant and the characteristic impedance of the modes supported [19]-[23]; and (ii) a *top-down approach* –i.e., TM2 method– that is based on the concatenation of multidimensional *T*-matrices of network modules to evaluate the end-to-end channel attenuation of BPL connections [2], [3], [5], [19], [22], [24]-[26].

Although the hybrid method is characterized by experimental validation and high accuracy, it presents high complexity and demands advanced knowledge in Microwave and Circuit/System engineering so as to be understandable to ECE students. As it has already been mentioned in [1], [63], the set of linear simplifications allows the transformation of the complicated hybrid method into the straightforward techno-economic pedagogical (TEP) method without seriously affecting the validity and the accuracy of the used techno-economic metrics. Therefore, TEP method promotes the interaction between Microwave Engineering and Circuit/System Engineering courses facilitating the understanding of ECE students.

In contrast with overhead HV/BPL networks, overhead LV/BPL and MV/BPL networks are characterized by a significant variety of occurred topologies. This system peculiarity urges the need of upgrading the TEP method of [1], [63] so as to deal with different network topologies. Therefore, TEP method needs to be integrated with TM2 method of top-down approach of the hybrid method. Apart from a clear and consistent theoretical approach, this extended edition of TEP method is flexible and accurate determining, consequently, any changes of the transfer characteristics related to relevant factors of the system configuration in the 1-100 MHz frequency band. The influence of factors, such as the overhead power grid type –either LV or MV system configuration–, the physical properties of the conductors used, the MTL configuration, the end-to-end distance and the number, the electrical length, the terminations and the multiplicity of the branches encountered along the end-to-end BPL signal propagation are investigated based on numerical results concerning various simulated overhead LV/BPL and MV/BPL topologies. As it has already been presented in [1], [63], since the behavior of overhead BPL networks mainly depends on the behavior of modes supported by the examined overhead MTL configurations, the main interest of this paper is to highlight to ECE

students the influence of the aforementioned factors to modal channels of overhead LV and MV MTL configurations.

Through the comparative analysis of the numerical results of overhead distribution power grids, the common nature of overhead LV/BPL and MV/BPL networks is outlined to ECE students allowing their common handling as it concerns the BPL signal transmission through their power lines. On the basis of a unified PHY framework and in the light of cascaded two-way power dividers, TEP method further approximates end-to-end channel attenuation of each overhead BPL distribution network.

The applied transmission analysis reveals the low-loss nature of overhead BPL systems regardless of the overhead distribution power grid type and topology. A consequence of the proposed modeling is that it can facilitate the process of coexistence of overhead LV/BPL with MV/BPL systems; a preliminary step toward the intraoperability/interoperability of BPL systems in a SG environment.

The rest of this paper is organized as follows: In Section II, the overhead LV and MV configurations adopted in this paper are presented. Section III synopsizes the MTL theory and eigenvalue decomposition (EVD) modal analysis concerning overhead LV/BPL and MV/BPL transmission. In Section IV, numerical results are provided, aiming at marking out how the various features of the overhead distribution power grid influence BPL transmission. The common nature of overhead LV/BPL and MV/BPL systems is revealed permitting their further common PHY handling. Section V concludes the paper.

II. Overhead LV and MV Distribution power Networks

Either the overhead or the underground power grids are employed for new urban, suburban, and rural distribution power grid installations. The selection between overhead or underground power grid installation is made according to different technoeconomic criteria like cost requirements, existing grid topology and urban plan constraints. Overhead lines are essentially used in areas where the relatively low density of the population cannot justify the high cost of underground lines [27]-[29].

Since the power grid was not originally designed to serve the purpose of a transmission medium for communication signals, the overhead distribution power grids are subjected to the main aggravating factors that are attenuation, multipath due to various reflections, multimode propagation, noise and electromagnetic interference [2]-[7], [17], [24], [30]-[36]. Especially, as it concerns the multimode propagation, due to the assumption of the quasi-TEM mode of propagation, the traditional transmission-line (TL) theory is appropriate to model BPL propagation in the overhead case [30], [43], [53]. Good agreement between BPL models that are based on TL theory and a series of experiments [61], [62] has been confirmed for frequencies up to 100MHz, motivating either the extensive use of BPL models that are based on TL theory or the neglect of the higher-order modes of propagation that occur in the MHz frequency range. Except for the signal propagation and transmission drawbacks, in real distribution power grids, a number of “real life” anomalies further degrade the theoretical broadband communications performance of overhead power distribution grids: (i) overhead distribution poles do not only carry power distribution lines, but they also support street lighting and telecommunications cables, which are located near to overhead distribution lines, influencing BPL signal propagation; (ii) the presence of relatively large pole-mounted capacitor banks, MV/LV transformers, traps, shunt capacitors, and bypass

devices, which are mainly metallic elements, critically affect the BPL signal transmission; and (iii) neutral grounding and/or grounding of the wooden support poles and/or grounding of surge-diverters that are often provided by the utilities so as to deal with lightning strikes and voltage upsurges influence BPL system broadband potential. Hence, during the deployment of BPL networks in the "real life", these additional practical aggravating factors must be accounted for in the modeling or else the simulations and theoretical results may be proven to be optimistic [14], [25], [37]. Anyway, the analysis of this paper that has pedagogical purposes focuses on the basic theoretical analysis rather than "real network" problems [2], [25], [28]-[32], [35], [38]-[41].

A typical case of overhead LV distribution line is depicted in Fig. 1(a). Four non-insulated conductors are suspended one above the other spaced by Δ_{LV} in the range from 0.3m to 0.5m and located at heights h_{LV} ranging from 6m to 10m above ground for the lowest conductor. The upper conductor is the neutral, while the lower three conductors are the three phases. This three-phase four-conductor overhead LV distribution line configuration is considered in the present work consisting of ASTER 1×34.4mm^2+3×54.6mm^2 conductors [3], [21], [27], [28], [39]-[43].

Overhead MV distribution lines hang at typical heights h_{MV} ranging from 8m to 10m above ground. Typically, three parallel non-insulated phase conductors spaced by Δ_{MV} in the range from 0.3m to 1m are used above lossy ground. This three-phase three-conductor overhead MV distribution line configuration is considered in the present work consisting of ACSR 3×95mm^2 conductors –see Fig. 1(b)– [2]-[4], [25], [27], [28], [32], [39]-[41].

The ground is considered as the reference conductor. The conductivity of the ground is assumed $\sigma_g = 5$mS/m and its relative permittivity $\varepsilon_{rg} = 13$, which is a realistic scenario [2]-[7], [25], [32], [33]. The impact of imperfect ground on signal propagation over power lines was analyzed in [2], [4], [25], [32], [37], [39]-[41], [44]-[47].

III. MTL Theory and EVD Modal Analysis

As it has already been reported in [1]-[7], [12]-[14], [24], [30]-[33], [48], [49], [63], through a matrix approach, the standard TL analysis can be extended to the MTL case. MTL case involves more than two conductors. An MTL structure, which supports *n+1* conductors parallel to the *z* axis, as depicted in Figs. 1(a) and 1(b), may support *n* pairs of forward- and backward-traveling waves with corresponding propagation constants. A coupled set of *2n* first-order partial differential equations that relates the line voltages $V_i(z,t)$, $i = 1,\ldots,n$ to the line currents $I_i(z,t)$, $i = 1,\ldots,n$ may describe these forward- and backward-traveling waves. Each pair of these waves is referred to as a mode [2], [12]-[14], [21], [30]-[32].

Therefore, in the case of overhead LV ($n^{\mathrm{LV}} = 4$) and MV ($n^{\mathrm{MV}} = 3$) distribution power lines over lossy plane ground, it was found that n^{XV} modes are supported [2], [12]-[14], [19]-[22], [25], [27], [28], [32], [37], [42], [45]-[47]:

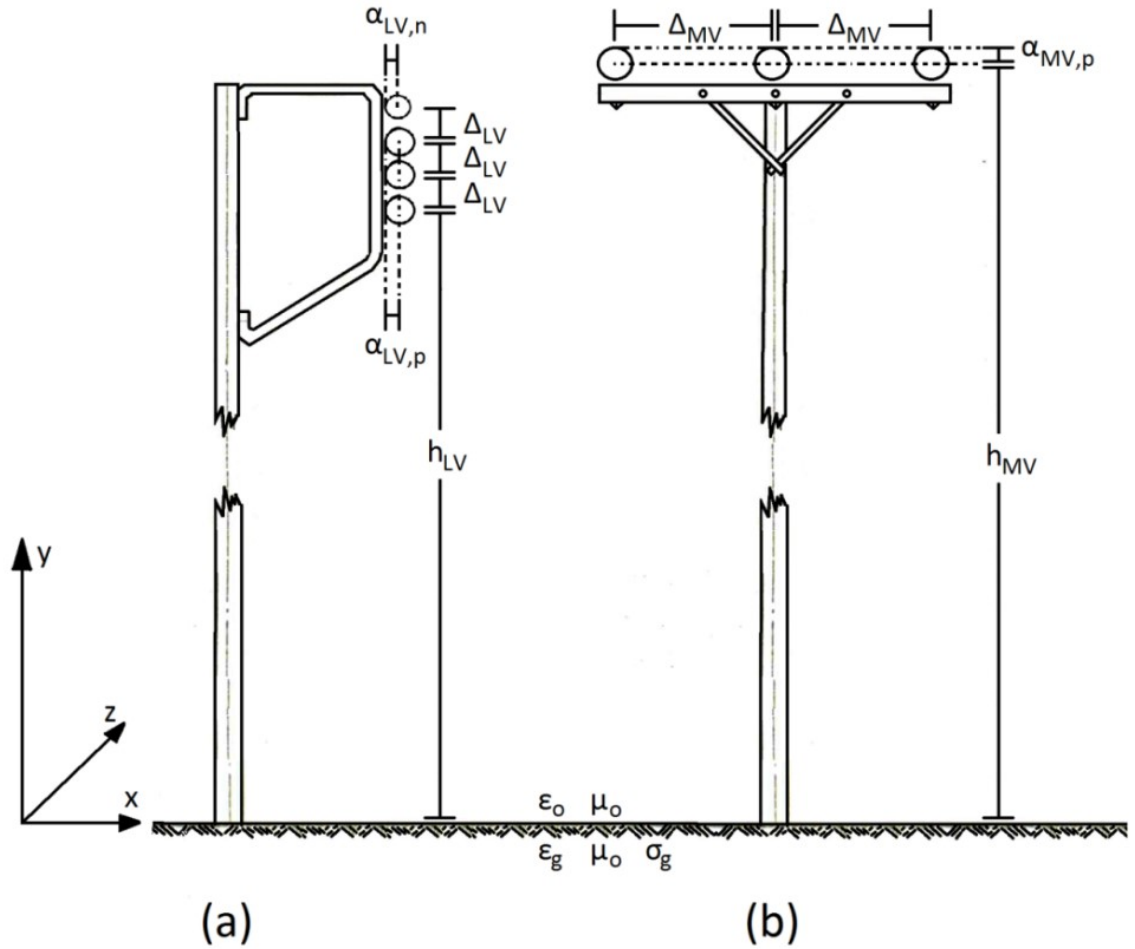

Figure 1. Typical overhead multiconductor structures [2], [3]. (a) LV. (b) MV.

- Common mode of overhead BPL transmission (CM^{XV}) which propagates via the n conductors and returns via the ground where $[\cdot]^{XV}$ indicates the overhead power grid type examined –either LV or MV grid–. γ_{CM}^{XV} constitutes the CM^{XV} propagation constant.
- Differential modes of overhead BPL transmission (DM_i^{XV}, $i=1,\ldots,n^{XV}-1$) which propagate and return via the n conductors. γ_{DMi}^{XV}, $i=1,\ldots,n^{XV}-1$ constitute the propagation constants of DM_i^{XV}, $i=1,\ldots,n^{XV}-1$, respectively.

Similarly to [1], [63], to bypass the complicated propagation analysis of the bottom-up approach of the hybrid method and to increase the ECE students' understanding of the following analysis, TEP method proposes that the attenuation coefficients and the phase delays of the CM and the DMs can be replaced by their respective linear approximations with satisfactory accuracy. More specifically, the modal attenuation coefficients can be replaced by their respective mean values while the modal phase delays can be replaced by their respective linear regressions.

The attenuation coefficients $\alpha_{CM}^{LV}=\mathrm{Re}\{\gamma_{CM}^{LV}\}$, $\alpha_{DMi}^{LV}=\mathrm{Re}\{\gamma_{DMi}^{LV}\}$, $i=1,2,3$, $\alpha_{CM}^{MV}=\mathrm{Re}\{\gamma_{CM}^{MV}\}$, and $\alpha_{DMj}^{MV}=\mathrm{Re}\{\gamma_{DMj}^{MV}\}$, $j=1,2$ of the CM^{LV}, the three DM^{LV}s, the CM^{MV}

and the two DM^{MV}s, respectively, are evaluated using the bottom-up approach of the hybrid method and are plotted versus frequency in Fig. 2(a) for the configurations depicted in Figs. 1(a) and 1(b). In Figs. 2(b)-(d), the absolute values of attenuation coefficient differences are also given versus frequency in the cases of: (i) CM^{LV} and CM^{MV}; (ii) DM_1^{LV} and DM_1^{MV}; and (iii) DM_2^{LV} and DM_2^{MV}, respectively, when the bottom-up approach of the hybrid method is adopted. In Figs. 2(e)-(h), the same plots are given when the TEP method is applied.

The phase delays $\beta_{CM}^{LV} = \mathrm{Im}\{\gamma_{\mathrm{CM}}^{\mathrm{LV}}\}$, $\beta_{\mathrm{DM}i}^{\mathrm{LV}} = \mathrm{Im}\{\gamma_{\mathrm{DM}i}^{\mathrm{LV}}\}$, $i = 1,2,3$, $\beta_{\mathrm{CM}}^{\mathrm{MV}} = \mathrm{Im}\{\gamma_{\mathrm{CM}}^{\mathrm{MV}}\}$, and $\beta_{\mathrm{DM}j}^{\mathrm{MV}} = \mathrm{Im}\{\gamma_{\mathrm{DM}j}^{\mathrm{MV}}\}$, $j = 1,2$ of the CM^{LV}, the three DM^{LV}s, the CM^{MV} and the two DM^{MV}s, respectively, are linear functions of frequency, coincide and are plotted versus frequency in Fig. 3(a) for the configurations depicted in Figs. 1(a) and 1(b) when the bottom-up approach of the hybrid method is adopted. In Figs. 3(b)-(d), the absolute values of phase delay differences are also given versus frequency in the cases of: (i) CM^{LV} and CM^{MV}; (ii) DM_1^{LV} and DM_1^{MV}; and (iii) DM_2^{LV} and DM_2^{MV}, respectively, when the bottom-up approach of the hybrid method is adopted. In Figs. 3(e)-(h), the same plots are given when the TEP method is applied.

As far as the spectral behavior of the modes is concerned, the following characteristics should be noted.

- As it concerns overhead BPL propagation in overhead LV and MV MTL configurations, according to the hybrid method, in the lower part of the frequency spectrum –up to approximately 20MHz–, the attenuation of the CM^{XV}s is higher compared to that of the DM^{XV}s. At frequencies above 20MHz, propagation takes place entirely above the ground as in the lossless case. Therefore, the CM^{XV}s and the DM^{XV}s coexist resulting to multimode propagation [2], [12], [14], [32], [45]-[47]. Similarly to [1], [63], TEP method provides an adequate approximation of the behavior of modal attenuation coefficients that, however, facilitates the ECE students to the following circuit analysis. Anyway, the occurred differences between hybrid and TEP method slightly affect the generality of the following analysis (see also in Section IV).
- The phase delays of CM^{XV} and DM^{XV}s exhibit a linear behavior with respect to frequency across the entire frequency range 1-100MHz and depend mainly on the surrounding media (air) properties. This almost identical spectral behavior of phase delays has also been observed in overhead and underground MV/BPL and HV/BPL transmission [1], [2], [12], [14], [32], [45]-[47]. Based on the results of the linear regression, TEP method accurately describes the behavior of modal phase delays.
- In accordance with the hybrid method, the plots corresponding to the spectral behavior of the difference between CM^{LV} and CM^{MV} reveal the close behavior of CM^{XV}s. The slight divergence existing between CM^{LV} and CM^{MV} is attributed to the differences between the overhead LV and MV configurations considered in the present paper. As to DM^{XV}s of overhead BPL transmission, since the relevant

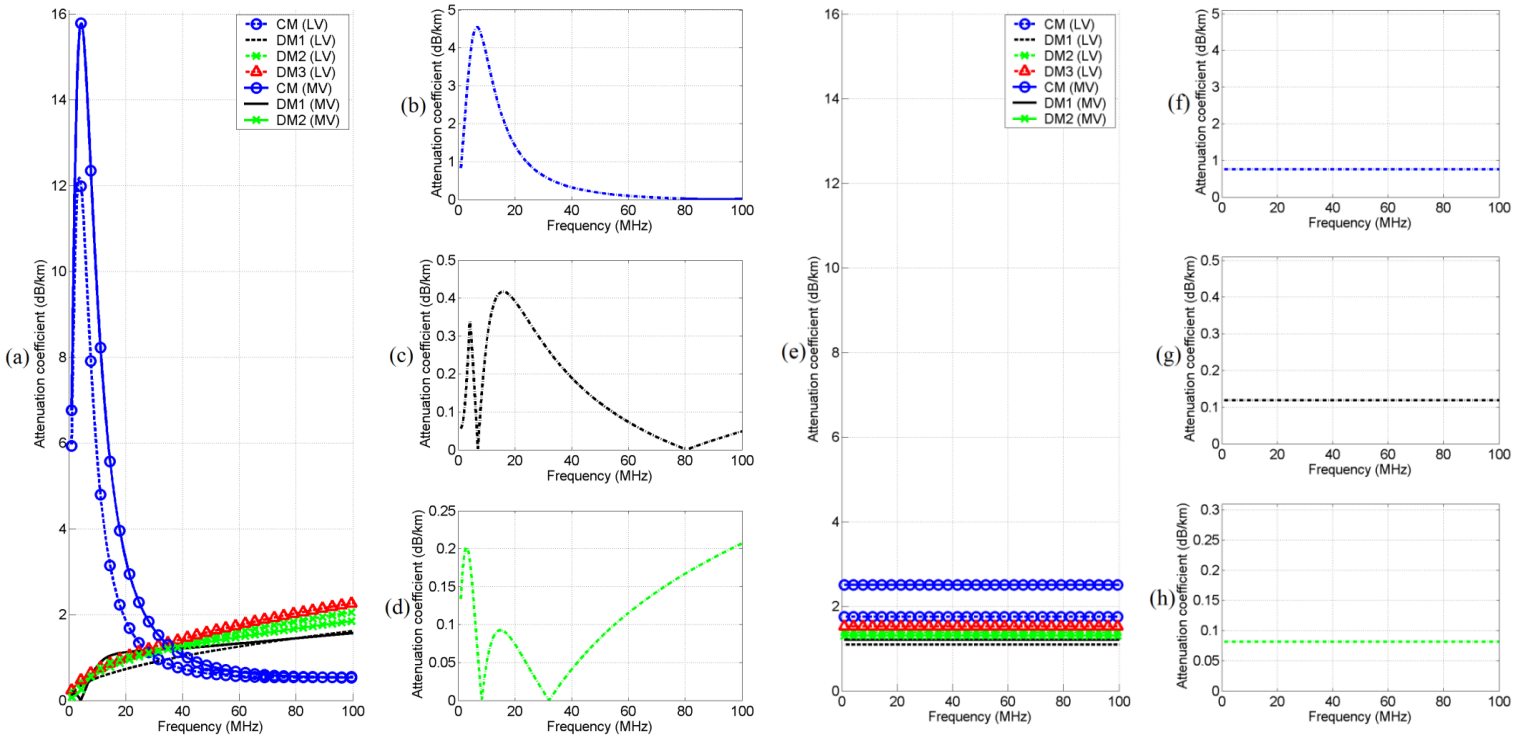

Figure 2. Attenuation coefficients of overhead LV/BPL and MV/BPL distribution lines when hybrid and TEP methods are applied (the subchannel frequency spacing is equal to 0.1MHz). (a) All the modes –hybrid method–. (b) Difference between CM^{LV} and CM^{MV} –hybrid method–. (c) Difference between DM_1^{LV} and DM_1^{MV} –hybrid method–. (d) Difference between DM_2^{LV} and DM_2^{MV} –hybrid method–. (e) All the modes –TEP method–. (f) Difference between CM^{LV} and CM^{MV} –TEP method–. (g) Difference between DM_1^{LV} and DM_1^{MV} –TEP method–. (h) Difference between DM_2^{LV} and DM_2^{MV} –TEP method–.

influence of the lossy ground is negligible, the spectral behaviors of DM^{XV}s are very close to each other; their curves are almost identical either between DMs of the same overhead power grid type or between DMs of different distribution power grids. According to TEP method, the basic differences between the aforementioned modes are maintained so that ECE students could recognize the effect of MTL configurations and ground/air properties to the propagation phenomena.

- As usually done to simplify the analysis [2]-[7], [12]-[14], [24], [30]-[33], due to their almost identical spectral behavior, only one DM of the same overhead power grid type will be examined, hereafter.

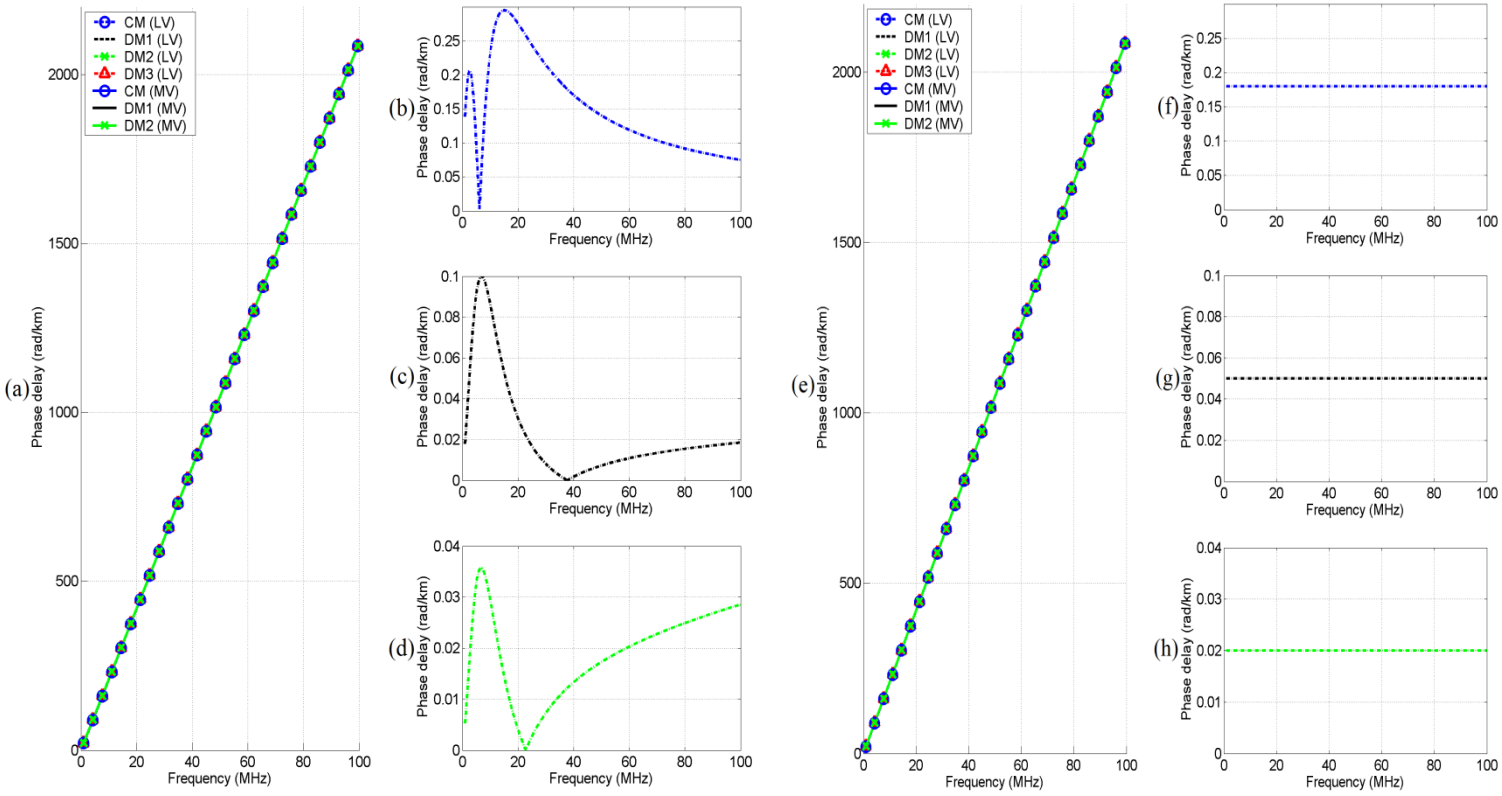

Figure 3. Phase delays of overhead LV/BPL and MV/BPL distribution lines when hybrid and TEP methods are applied (the subchannel frequency spacing is equal to 0.1MHz). (a) All the modes –hybrid method–. (b) Absolute difference between CM^{LV} and CM^{MV} –hybrid method–. (c) Absolute difference between DM_1^{LV} and DM_1^{MV} –hybrid method–. (d) Absolute difference between DM_2^{LV} and DM_2^{MV} –hybrid method–. (e) All the modes –TEP method–. (b) Absolute difference between CM^{LV} and CM^{MV} –TEP method–. (c) Absolute difference between DM_1^{LV} and DM_1^{MV} –TEP method–. (d) Absolute difference between DM_2^{LV} and DM_2^{MV} –TEP method–.

As it has already been presented in [1], [2], [4], [19], [21], [30]-[32], the EVD modal voltages $\mathbf{V}^{XV,\mathrm{m}}(z)=\left[V_1^{XV,\mathrm{m}}(z)\ \cdots\ V_n^{XV,\mathrm{m}}(z)\right]^{\mathrm{T}}$ and the EVD modal currents $\mathbf{I}^{XV,\mathrm{m}}(z)=\left[I_1^{XV,\mathrm{m}}(z)\ \cdots\ I_n^{XV,\mathrm{m}}(z)\right]^{\mathrm{T}}$ may be related to the respective line quantities $\mathbf{V}^{XV}(z)=\left[V_1^{XV}(z)\ \cdots\ V_n^{XV}(z)\right]^{\mathrm{T}}$ and $\mathbf{I}^{XV}(z)=\left[I_1^{XV}(z)\ \cdots\ I_n^{XV}(z)\right]^{\mathrm{T}}$ via the similarity transformations

$$\mathbf{V}^{XV}(z)=\mathbf{T}_{\mathrm{V}}^{XV}\cdot\mathbf{V}^{XV,\mathrm{m}}(z) \quad (1)$$

$$\mathbf{I}^{XV}(z)=\mathbf{T}_{\mathrm{I}}^{XV}\cdot\mathbf{I}^{XV,\mathrm{m}}(z) \quad (2)$$

where $[\cdot]^{\mathrm{T}}$ denotes the transpose of a matrix, $\mathbf{T}_{\mathrm{V}}^{XV}$ and $\mathbf{T}_{\mathrm{I}}^{XV}$ are $n^{XV}\times n^{XV}$ matrices depending on the overhead power grid type, the frequency, the physical properties of the conductors and the geometry of the MTL configuration. Through the aforementioned

equations, the line voltages and currents are expressed as appropriate superpositions of the respective EVD modal quantities. From eq. (1)

$$\mathbf{V}^{XV,\mathrm{m}}(0)=\left[\mathbf{T}_{\mathrm{V}}^{XV}\right]^{-1}\cdot\mathbf{V}^{XV}(0) \tag{3}$$

The TM2 method –based on the scattering matrix theory formalism [2], [3], [5]-[7], [12]-[14], [24], [26], [32], [33], [50] and presented analytically in [3], [5]– models the spectral relationship between $V_i^{XV,\mathrm{m}}(z)$, $i=1,\ldots,n^{XV}$ and $V_i^{XV,\mathrm{m}}(0)$, $i=1,\ldots,n^{XV}$ proposing operators $H_{ij}^{XV,\mathrm{m}}\{\cdot\}$, $i,j=1,\ldots,n^{XV}$ so that

$$\mathbf{V}^{XV,\mathrm{m}}(z)=\mathbf{H}^{XV,\mathrm{m}}\left\{\mathbf{V}^{XV,\mathrm{m}}(0)\right\} \tag{4}$$

where

$$\mathbf{H}^{XV,\mathrm{m}}\{\cdot\}=\begin{bmatrix}H_{11}^{XV,\mathrm{m}}\{\cdot\} & \cdots & H_{1n}^{XV,\mathrm{m}}\{\cdot\}\\ \vdots & \ddots & \vdots\\ H_{n1}^{XV,\mathrm{m}}\{\cdot\} & \cdots & H_{nn}^{XV,\mathrm{m}}\{\cdot\}\end{bmatrix} \tag{5}$$

is a $n^{XV}\times n^{XV}$ matrix operator whose elements $H_{ij}^{XV,\mathrm{m}}\{\cdot\}$, $i,j=1,\ldots,n^{XV}$ are the EVD modal transfer functions, and $H_{i,j}^{\mathrm{XV,m}}$ denotes the element of matrix $\mathbf{H}^{\mathrm{XV,m}}\{\cdot\}$ in row i of column j [2]-[7], [12]-[14], [24], [30]-[33]. Combining eqs. (1) and (5), the $n^{XV}\times n^{XV}$ matrix channel transfer function $\mathbf{H}^{XV}\{\cdot\}$ relating $\mathbf{V}^{XV}(z)$ with $\mathbf{V}^{XV}(0)$ through

$$\mathbf{V}^{XV}(z)=\mathbf{H}^{XV}\left\{\mathbf{V}^{XV}(0)\right\} \tag{6}$$

is determined from

$$\mathbf{H}^{XV}\{\cdot\}=\mathbf{T}_{\mathrm{V}}^{XV}\cdot\mathbf{H}^{XV,\mathrm{m}}\{\cdot\}\cdot\left[\mathbf{T}_{\mathrm{V}}^{XV}\right]^{-1} \tag{7}$$

Based on eq. (7), the $n^{XV}\times n^{XV}$ matrix transfer functions $\mathbf{H}^{XV}\{\cdot\}$ of the overhead BPL distribution networks are determined [2]-[7], [12]-[14], [24], [30]-[33].

As it has already been mentioned in [3], [5], TM2 method is extremely resultful since it is able to calculate EVD modal transfer functions associated with complex networks including various types of overhead BPL configurations, any type of interconnection at the branches and any type of branch termination. In contrast with its ancestor methods, TM2 method does not consider specific transmission assumptions that reduce the generality of the method [2], [3], [5]-[8], [12]-[14], [24], [26], [32], [33], [50]-[52]. Moreover, applying TM2 method, the problem of mode mixture is fully investigated through the definition of the EVD matrix channel transfer function –as given in eq. (7)–. Also, TM2 method is a pure microwave engineering technique that can be easily detailed to ECE students during the course of Microwave Engineering.

With reference to eq. (7), $\mathbf{T}_{\mathrm{V}}^{XV}$ is $n^{XV}\times n^{XV}$ matrix that describes the power allocation of each modal transfer function to the transfer functions of the line quantities. Similarly to [1], [63], in order to completely bypass the application of the bottom-up approach of the hybrid method and to simplify the following analysis to ECE students, TEP method argues that the real parts of the elements of matrix $\mathbf{T}_{\mathrm{V}}^{XV}$ can be replaced by their mean values while their imaginary parts can be assumed equal to 0 in the BPL operation frequency range. For the sake of clarity and terseness, these figures are omitted in this companion paper since they resemble to Figs. 3(a)-(j) of [1]. Anyway, since the main interest of this paper is concentrated on the behavior of modal channels as described in eqs. (4) and (5), the further examination of matrix $\mathbf{T}_{\mathrm{V}}^{XV}$ is omitted.

With reference to eqs. (4) and (5), the $n^{XV} \times n^{XV}$ matrix transfer functions $\mathbf{H}^{XV,m}\{\cdot\}$ of the overhead BPL distribution networks can be determined combining the set of linear simplifications of TEP method, concerning modal attenuation coefficients and modal phase delays, and TM2 method without using the complicated bottom-up approach of the hybrid method.

IV. Numerical Results and Discussion

First of all, the numerical results of this Section focus on identifying the TEP method as an efficient pedagogical tool that can be comfortably presented to ECE students during the courses of Microwave and Circuit/System Engineering of their ECE program. TEP method succeeds in providing the general concept of designing overhead BPL networks without deviating from the "real world" conditions and confusing ECE students. In addition, except for the pedagogical purposes of TEP method, the simulations of various types of overhead LV/BPL and MV/BPL transmission channels aim at revealing to ECE students: (a) their broadband transmission characteristics; (b) how their spectral behavior is affected by several factors, such as the type/topology of the overhead power grid and the multiplicity of branches; (c) the introduction of appropriate simplified approximations; and (d) the common PHY handling perspective among different types of BPL distribution power grids.

Conversely to [1], this paper mainly focuses on the modal behavior and the modal transmission characteristics of overhead LV/BPL and MV/BPL networks. As mentioned in Section III, since the modes supported by the overhead LV/BPL and MV/BPL configurations may be examined separately, it is assumed for simplicity that the BPL signal is injected directly into the modes [2]-[7], [12]-[14], [19]-[25], [30]-[33]; thus, the complicated EVD modal analysis of [21], briefly described in Section III, is avoided to be presented in ECE students. Hence, after the presentation of linear simplifications of TEP method, which concern bottom-up approach, that are available *ab initio* for given overhead LV and MV MTL configuration and TM2 method, concerning the integration of TEP method, ECE students directly enter into the findings of this Section.

For the following numerical computations, the three-phase four-conductor overhead LV and the three-phase three-conductor overhead MV distribution line configurations depicted in Figs. 1(a) and 1(b), respectively, have been considered.

The following discussion will focus on the transmission characteristics related to the CM^{XV} and to the DM^{XV}s of the overhead BPL systems, as well. Since, as mentioned in Section III, the DMs of the same overhead power grid type exhibit an almost identical spectral behavior, the transmission characteristics of only one DM of each overhead power grid type, say that of DM_1^{LV} and DM_1^{MV}, will be examined, hereafter.

The simple overhead topology of Fig. 4(a) of [1], having N branches has been considered. With reference to Fig. 4(a) of [1], the transmitting and the receiving ends are assumed matched to the characteristic impedance of the mode considered, whereas the branch terminations are assumed open circuit [2]-[7], [24], [27], [30]-[33], [64]. Also, five indicative overhead topologies, which are common for both overhead LV/BPL and MV/BPL systems, concerning end-to-end connections of average lengths equal to 1000m are examined [3], [5]-[7], [17]-[19], [22], [24], [25], [27], [28], [33], [34], [37], [43], [53]-[55]. Their topological characteristics are reported in Table I.

A. End-to-End Channel Attenuation – Comparison of the TEP Method with the Hybrid Method – Comparison between Overhead LV/BPL and MV/BPL Topologies

As it concerns the hybrid method, in Figs. 4(a) and 4(d), the end-to-end channel attenuation from A to B is plotted with respect to frequency for the aforementioned five indicative topologies for the propagation of CM^{LV} and DM_1^{LV}, respectively. In Figs. 4(b) and 4(e), similar plots are given for the propagation of CM^{MV} and DM_1^{MV}, respectively. In Figs. 4(c), 4(f), 4(g), and 4(h), the absolute difference of the end-to-end channel attenuations from A to B is also drawn versus frequency for the aforementioned indicative topologies in the cases of: (i) CM^{LV} and CM^{MV}; (ii) DM_1^{LV} and DM_1^{MV}; (iii) CM^{LV} and DM_1^{LV}; and (iv) CM^{MV} and DM_1^{MV}; respectively. In Figs. 5(a)-(h), same plots are given in the case of the TEP method.

From Figs. 4(a)-(h) and 5(a)-(h), several interesting remarks can be pointed out regarding the convergence of TEP and hybrid method as well as the transmission characteristics of overhead LV/BPL and MV/BPL networks:

- In all the cases examined, TEP method efficiently approximates the hybrid method. As it has already been identified in [2]-[7], [12]-[14], [18], [24], [29]-[33], [51], [53], [54], [56], overhead BPL networks are mainly affected by the multipath environment rather than "LOS" attenuation. Actually, these notches are superimposed on the exponential "LOS" attenuation of each mode. Since TM2 method is responsible for dealing with overhead BPL topologies, the TEP and hybrid methods present similarities either in the positions of spectral notches or in the extent of these notches despite the fact that different bottom-up approaches are assumed.
- Since the dominant factor that affect signal propagation in overhead LV/BPL and MV/BPL channels is the superimposed multipath, an indicative picture of the transmission characteristics of the modes can be obtained studying the transmission characteristics of only one mode of each power grid type. This is a rather typical procedure in BPL analysis [2]-[7], [12], [14], [24], [27], [32], [33], [54].
- Regardless of the method considered, the spectral behavior of end-to-end channel attenuation of modes depends drastically on the frequency, the mode considered, the physical properties of the conductors used, the end-to-end –"LOS"– distance and the number and the electrical length of the branches encountered along the end-to-end transmission path. This is a critical point of the analysis that should be highlighted to ECE students.
- Already mentioned in [3]-[7], [12]-[14], [24], [30], [31], [33], [57], there are three major channel classes for LV/BPL and MV/BPL channels: (i) *"LOS" channels*, when no branches are encountered and, consequently, no spectral notches are observed; (ii) *Good channels*, when the number of branches is small and their electrical length is large. Shallow spectral notches are observed. Suburban case will represent good channel class, hereafter; and (iii) *Bad channels*, when the number of branches is large and their electrical length is small. Deep spectral notches are observed. Urban case B will represent bad channel class, hereafter.

Table I. Five Indicative Overhead Topologies [3], [4], [8], [24].

Denotation	Description	Number of Branches (N)	Lengths of Distribution TLs [L_1 ... L_{N+1}]	Lengths of Branch TLs [L_{b1} ... L_{bN}]
Urban case A	A typical urban topology	3	[500m 200m 100m 200m]	[8m 13m 10m]
Urban case B	An aggravated urban topology	5	[200m 50m 100m 200m 300m 150m]	[12m 5m 28m 41m 17m]
Suburban case	A typical suburban topology	2	[500m 400m 100m]	[50m 10m]
Rural case	A typical rural topology	1	[600m 400m]	[300m]
"LOS" case*	"LOS" transmission	0	[1000m]	–

(*: "LOS" topology corresponds to Line of Sight transmission in wireless channels)

- Regardless of the considered method, the channel attenuation differences between same modes of overhead LV/BPL and MV/BPL networks remain limited. This is due to the fact that the different modal transmission performances of overhead LV/BPL and MV/BPL channels are only marginally influenced by different wire positioning in the longitudinal cross-section of the line. Actually, this is an evidence for their common PHY handling that is further analyzed in the following subsections.
- MTL theory and EVD modal analysis are definitely useful tools to face the problem. Nevertheless, it is mandatory to consider that modal transmission characteristics of overhead LV/BPL and MV/BPL channels are strongly influenced by load characteristics, on the one hand, and by modem connection, on the other [64]. Since this analysis is mainly focused on ECE students, the assumption of optimal data transmission is acceptable; say, each mode (CM^{XV} and DM^{XV}s) can propagate along a fictitious two-conductor transmission line with matched terminations.

On the basis of the previous findings and as it concerns the modal transmission characteristics, only one mode of each overhead power grid type is going to be examined; say that of DM_1^{LV} and DM_1^{MV}. As it regards the topological features, "LOS" transmission case, good channel case and bad channel case are going to be representative cases for the rest of this paper.

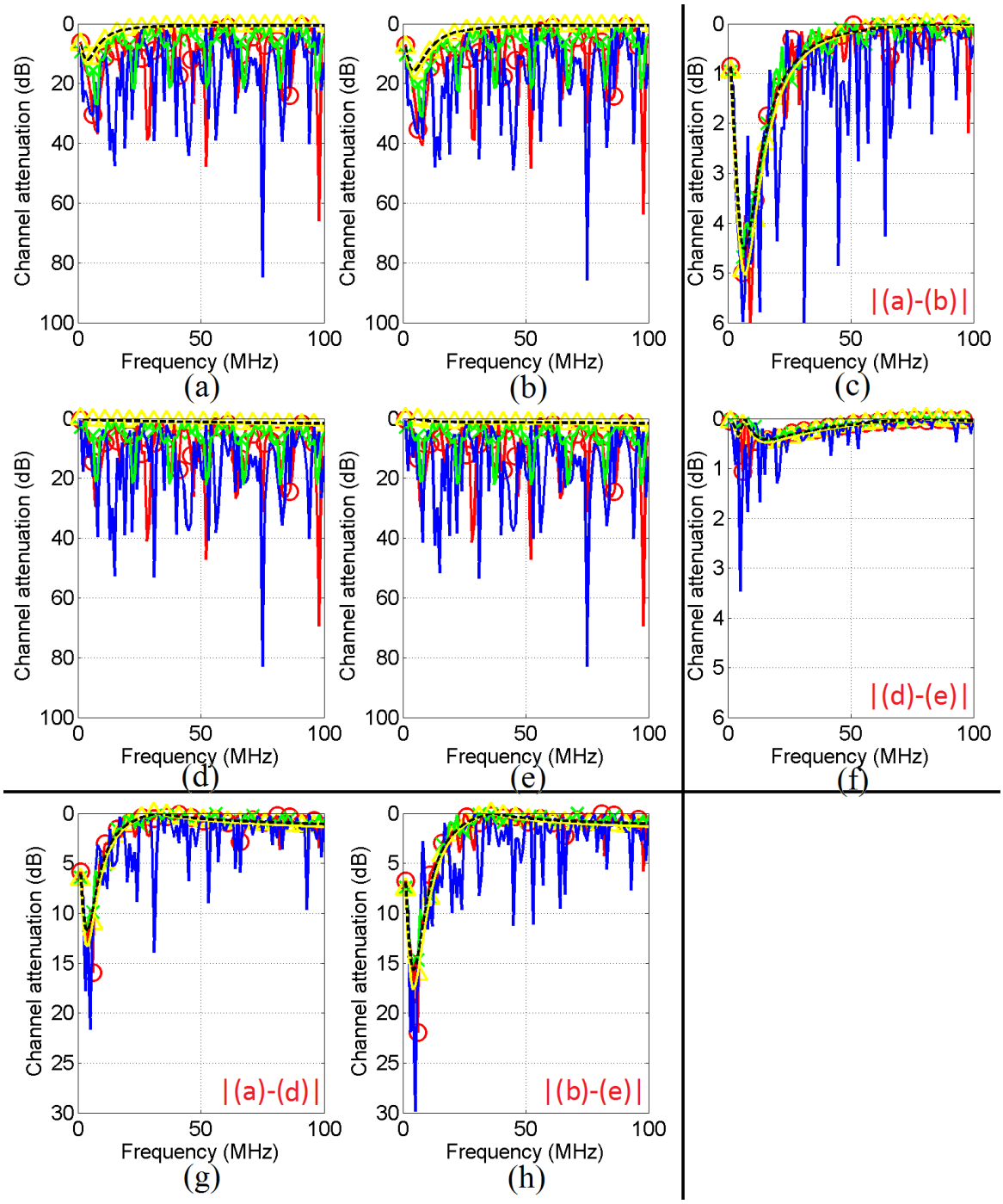

Figure 4. End-to-end channel attenuation versus frequency for urban case A (⊖), urban case B (—), suburban case (×), rural case (△), and "LOS" transmission case (-----) when the hybrid method is adopted (the subchannel frequency spacing is equal to 1MHz). (a) $\mathrm{CM}^{\mathrm{LV}}$. (b) $\mathrm{CM}^{\mathrm{MV}}$. (c) Absolute difference between $\mathrm{CM}^{\mathrm{LV}}$ and $\mathrm{CM}^{\mathrm{MV}}$. (d) $\mathrm{DM}_1^{\mathrm{LV}}$. (e) $\mathrm{DM}_1^{\mathrm{MV}}$. (f) Absolute difference between $\mathrm{DM}_1^{\mathrm{LV}}$ and $\mathrm{DM}_1^{\mathrm{MV}}$. (g) Absolute difference between $\mathrm{CM}^{\mathrm{LV}}$ and $\mathrm{DM}_1^{\mathrm{LV}}$. (h) Absolute difference between $\mathrm{CM}^{\mathrm{MV}}$ and $\mathrm{DM}_1^{\mathrm{MV}}$.

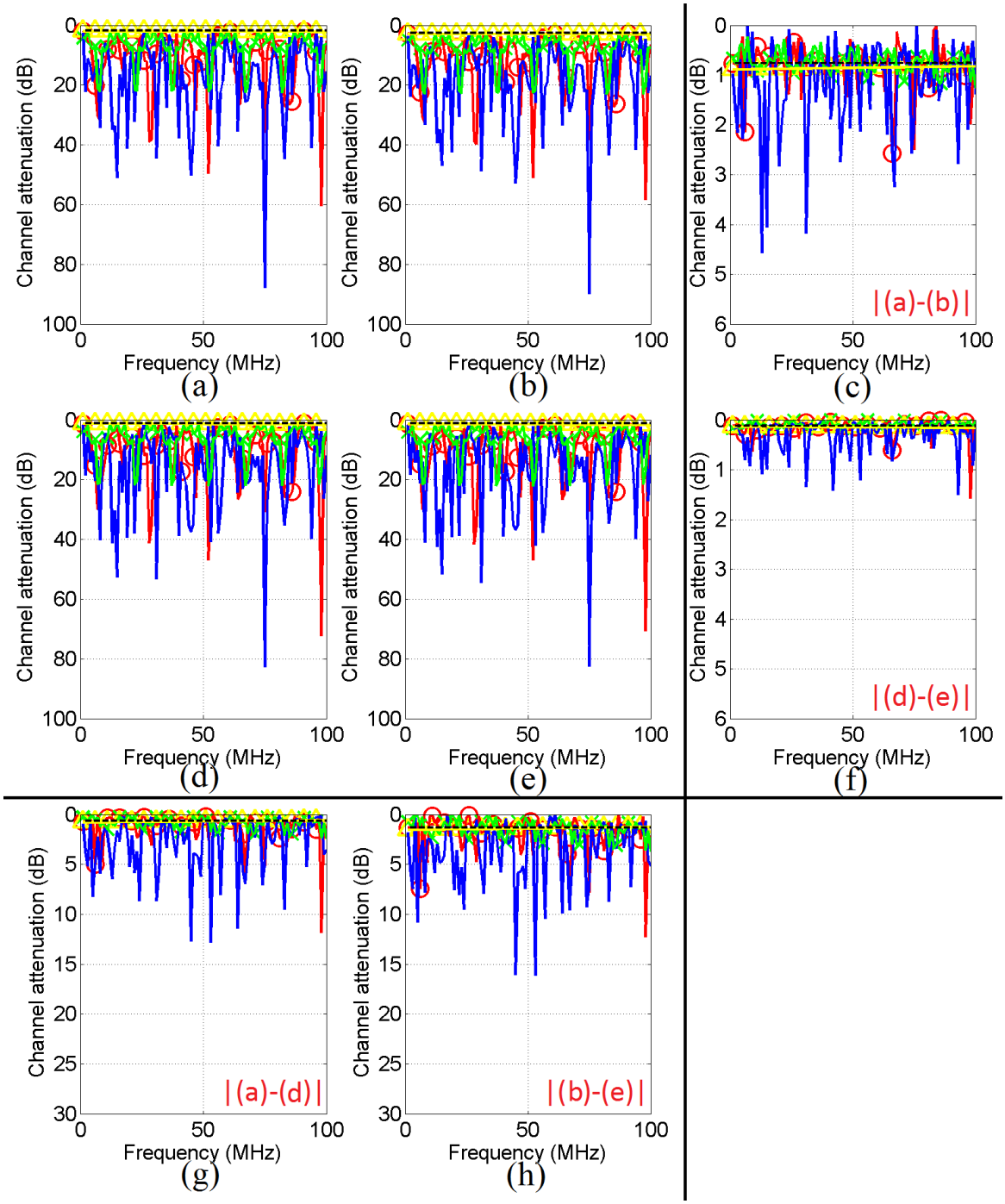

Figure 5. Same plots with Fig. 4 but for the TEP method.

B. The Effect of Branch Length – Introduction of Simplified Approach with Two-Way Power Dividers – Comparison between Overhead LV/BPL and MV/BPL Topologies

As it has already been identified in [2], [12], [14], [32], apart from causing spectral notches, the various branches also cause additional stepwise discontinuities to the channel attenuation at each branch encountered along the end-to-end transmission path.

The effect of the branch length on the attenuation discontinuity at each branch is examined in Figs 6(a) and 6(d), where the channel attenuation of DM_1^{LV} is plotted versus the distance from the transmitting end –see Fig. 4(a) of [1], point A– for good channel class case, Topology 1 –see Table II–, bad channel class case, Topology 2 –see Table II–, and the "LOS" transmission case at f=25MHz and f=76MHz, respectively. In Figs. 6(b) and 6(e), similar plots are given for the propagation of DM_1^{MV}. In Figs. 6(c) and 6(f), the absolute difference of the channel attenuations between DM_1^{LV} and DM_1^{MV} is also drawn with respect to the distance from the transmitting end for the same topologies at f=25MHz and f=76MHz, respectively. Note that in Figs. 6(a)-(f), hybrid method is applied whereas in Figs. 7(a)-(f), same plots are given when TEP method is applied.

Comparing Figs. 6(a)-(f) with 7(a)-(f), the channel attenuation discontinuity results of TEP method are very close to respective ones of the hybrid method. This is due to the fact that multipath aggravation is described in both methods by the TM2 method. In addition, ECE students can easily understand that the attenuation discontinuity at each branch primarily depends on the frequency and on its electrical length rather than overhead distribution power grid type. Actually, from Figs. 6(c), 6(f), 7(c) and 7(f), it is demonstrated that the attenuation differences between overhead LV/BPL and MV/BPL channels are lower than 0.5dB in the majority of the cases for a given overhead power grid topology.

Moreover, observing Figs. 6(a)-(e) and 7(a)-(e), it is noticed that as the branches become longer, the spectral behavior of the BPL networks tends to converge to the spectral behavior of the respective BPL networks with branch terminations matched to the characteristic impedance of the mode examined; say approximately a two-way power divider or 3.01dB superimposed attenuation per each single branch [18], [29], [35], [51], [53], [55], [58]-[60]. This result defines the first interesting circuital approximation of TEP method and, at the same time, it is easily understandable by ECE students since power dividers are essential part of the material of their Microwave Engineering and Circuit/System Engineering courses.

Finally, from Figs. 4(a)-(h), 5(a)-(h), 6(a)-(f) and 7(a)-(f), it is obvious that TEP method provides accurate results in comparison with the respective ones of the hybrid method. Therefore, only TEP method is considered for the rest of this paper.

C. Multiple Branches at given Junction – Comparison between Overhead LV/BPL and MV/BPL Topologies

A typical urban overhead LV topology can serve 10-60 household customers while a typical urban overhead MV topology may support 2-8 MV/LV transformers. These typical overhead topologies are mainly of radial configuration either with a single branch or with multiple branches at the same junction [18], [19], [22], [27], [28], [53]-[55], [57]-[60].

To demonstrate the effect of multiple branches at given junction on the channel attenuation, the end-to-end channel attenuation of DM_1^{LV} from A to B is plotted versus frequency for good channel class case, Topology 3 –see Table III–, bad channel class case, Topology 4 –see Table III–, and "LOS" transmission case in Fig. 8(a). In Fig. 8(b), similar plots are given for the propagation of DM_1^{MV}. In Fig. 8(c), the absolute difference

of the channel attenuations between DM_1^{LV} and DM_1^{MV} is also drawn with respect to frequency for the same topologies.

Table II. Two Indicative Overhead Topologies with Longer Branches

Denotation	Description	Times of longer branches	Lengths of Distribution TLs [L_1 ... L_{N+1}]	Lengths of Branch TLs [L_{b1} ... L_{bN}]
Topology 1	Same as good channel class case but with twenty times longer branches	20	[500m 400m 100m]	[1000m 200m]
Topology 2	Same as bad channel class case but with twenty times longer branches	20	[200m 50m 100m 200m 300m 150m]	[240m 100m 560m 820m 340m]

D. Multiple Branch Attenuation Discontinuity and the Extension of Simplified Approach with Two-Way Power Dividers – Comparison between Overhead LV/BPL and MV/BPL Topologies

From Figs. 8(a)-(c), it is evident that the multiple branches at each junction cause additional stepwise attenuation to the stepwise attenuation that already exists due to the single branches. In order to examine the effect of the multiple branches on the attenuation discontinuity at the each junction and the newly proposed simplified approximation method of cascaded two-way power dividers, in Figs 9(a) and 9(d), the channel attenuation of DM_1^{LV} is plotted versus the distance from the transmitting end

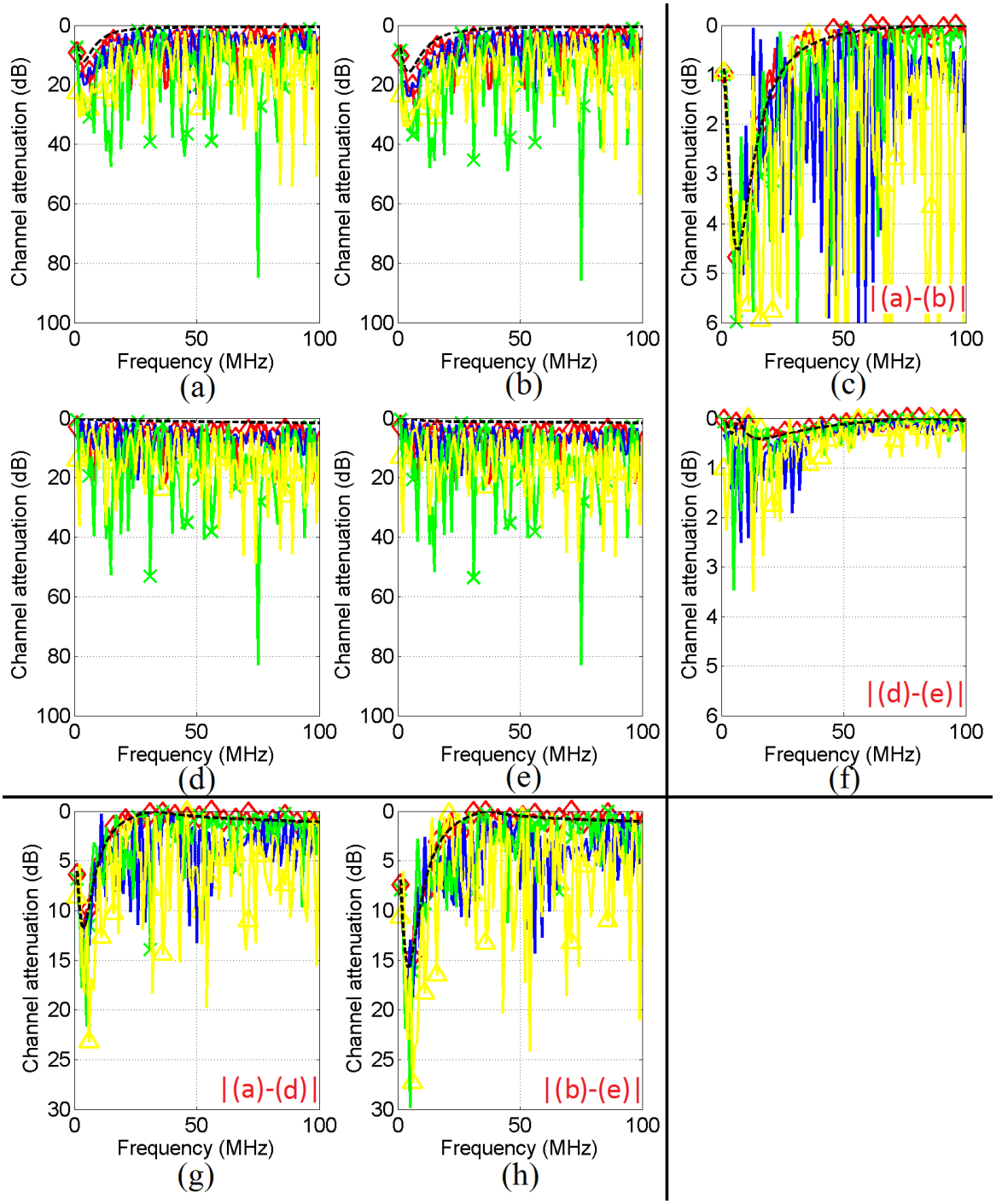

Figure 6. Channel attenuation versus the distance from the transmitting end (see Fig. 4, point A) for good channel class case (—x—), Topology 1 (—◇—), bad channel class case (—), Topology 2 (—□—), and "LOS" transmission case (----) when hybrid method is adopted (the distance span is equal to 1m). (a) DM_1^{LV} at f=25MHz. (b) DM_1^{MV} at f=25MHz. (c) Absolute difference between DM_1^{LV} and DM_1^{MV} at f=25MHz. (d) DM_1^{LV} at f=76MHz. (e) DM_1^{MV} at f=76MHz. (e) Absolute difference between DM_1^{LV} and DM_1^{MV} at f=76MHz.

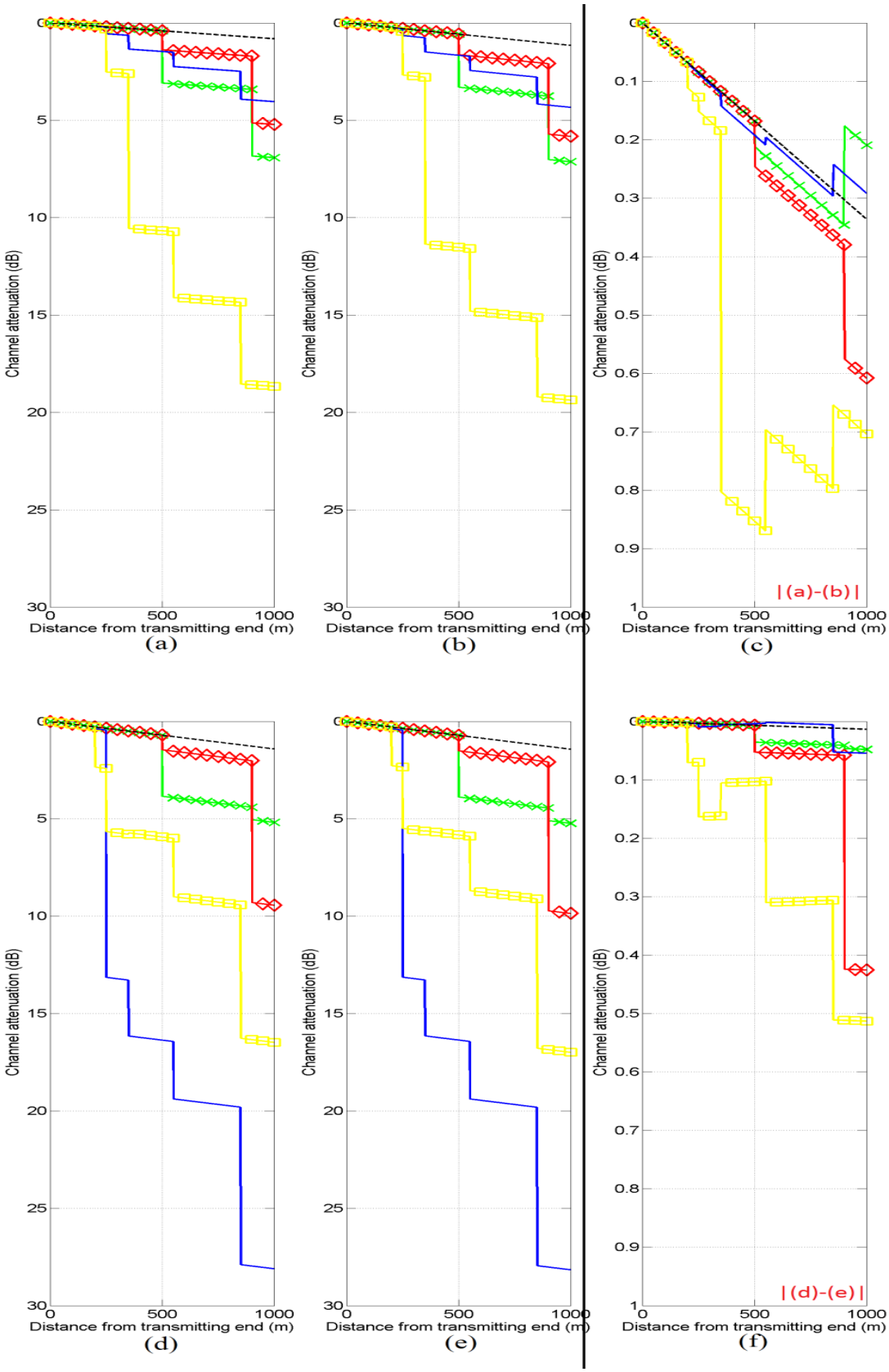

Figure 7. Same plots with Fig. 6 but for the TEP method.

TABLE III. Two Indicative Overhead Topologies with Multiple Branches at the same Junction.

Denotation	Description	Number of Multiple Branches at the same Junction	Lengths of Distribution TLs [L_1 ... L_{N+1}]	Lengths of Branch TLs [L_{b1} ... L_{bN}]
Topology 3	Same as good channel class case but with five times more, same branches at each junction	5	[500m 0m 0m 0m 0m 400m 0m 0m 0m 0m 100m]	[50m 50m 50m 50m 50m 10m 10m 10m 10m 10m]
Topology 4	Same as bad channel class case but with five times more, same branches at each junction	5	[200m 0m 0m 0m 0m 50m 0m 0m 0m 0m 100m 0m 0m 0m 0m 200m 0m 0m 0m 0m 300m 0m 0m 0m 0m 150m]	[12m 12m 12m 12m 12m 5m 5m 5m 5m 5m 28m 28m 28m 28m 28m 41m 41m 41m 41m 41m 17m 17m 17m 17m 17m]

–see Fig. 4(a) of [1], point A– for good channel class case, Topology 3, bad channel class case, Topology 4, and the "LOS" transmission case at f=25MHz and f=76MHz, respectively. In Figs. 9(a) and 9(d), each of the aforementioned topologies is accompanied by its corresponding equivalent concatenation of K two-way power divider per each K-multiple-branch junction. In Figs 9(b) and 9(e), similar plots are given for the propagation of DM_1^{MV}. In Figs. 9(c) and 9(f), the absolute difference of the channel attenuations between DM_1^{LV} and DM_1^{MV} is also drawn with respect to the distance from the transmitting end for the same topologies at f=25MHz and f=76MHz, respectively.

From Figs. 9(a)-(e), it is clearly demonstrated that the superimposed attenuation due to the multiple branches at each junction depends on the frequency, the number, and the electrical length of each of these multiple branches. As the branches become longer,

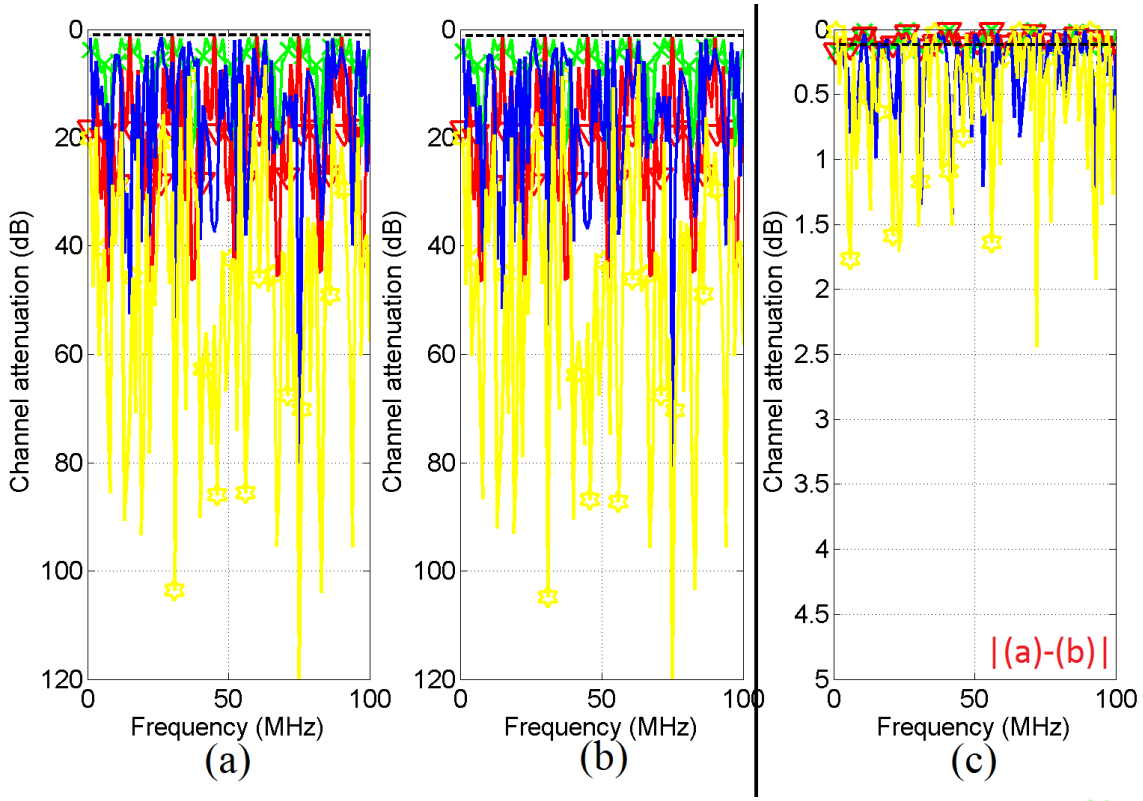

Figure 8. End-to-end channel attenuation versus frequency for good channel class case ( ), Topology 3 ( ), bad channel class case ( ), Topology 4 ( ), and "LOS" transmission case ( ) when TEP method is applied (the subchannel frequency spacing is equal to 1MHz). (a) DM_1^{LV}. (b) DM_1^{MV}. (c) Absolute difference between DM_1^{LV} and DM_1^{MV}.

the spectral behavior of the BPL networks tends to converge to the spectral behavior of the respective BPL networks with branch terminations matched to the characteristic impedance of the mode examined; say, approximately a 3.01dB superimposed attenuation per each single branch or K×3.01dB superimposed attenuation per each K-branch junction. Actually, the convergence between numerical results and approximation method is better, as the number of branches per junction and the length of branches increase. On the basis of the satisfactory accuracy between numerical results and results from the simplified approximation method, the concatenation of K two-way power divider per each K-multiple-branch junction is validated [2], [30]-[32], [53], [55]. This result defines the second circuital approximation of TEP method and, at the same time. Similarly to the first circuital approximation, it is easily understandable by ECE students since power dividers are presented during the Microwave Engineering and Circuit/System Engineering courses.

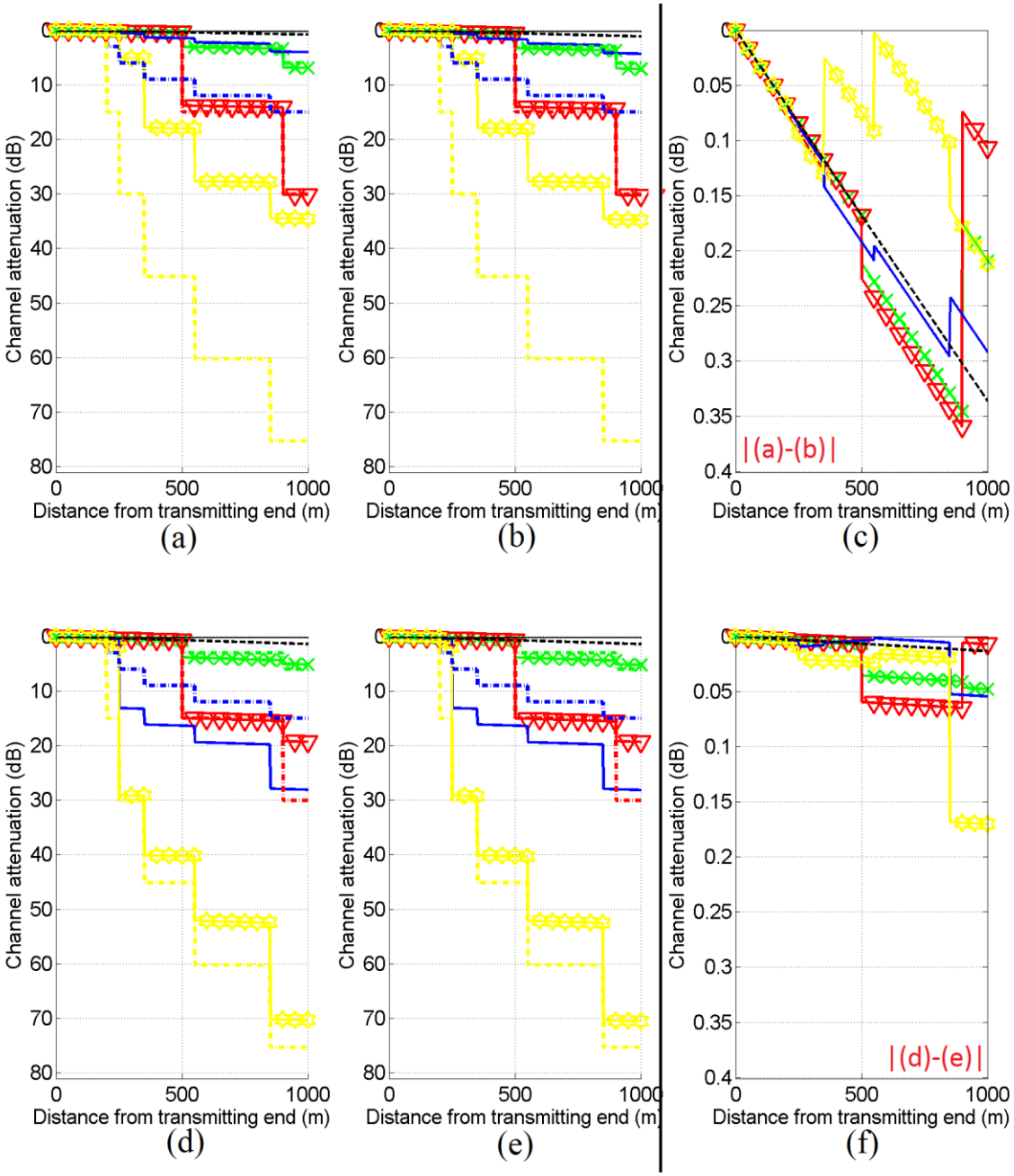

Figure 9. Channel attenuation versus the distance from the transmitting end –see Fig. 4(a) of [1], point A– for good channel class case (—x—) with its equivalent concatenation of two-way power dividers (—·—·—), Topology 3 (—▽—) with its equivalent concatenation of two-way power dividers (—··—··—), bad channel class case (——) with its equivalent concatenation of two-way power dividers (— — —), Topology 4 (—○—) with its equivalent concatenation of two-way power dividers (—·—·—), and "LOS" transmission case (----) when the TEP method is adopted (the distance span is equal to 1m). (a) DM_1^{LV} at f=25MHz. (b) DM_1^{MV} at f=25MHz. (c) Absolute difference between DM_1^{LV} and DM_1^{MV} at f=25MHz. (d) DM_1^{LV} at f=76MHz. (e) DM_1^{MV} at f=76MHz. (e) Absolute difference between DM_1^{LV} and DM_1^{MV} at f=76MHz.

E. Synopsizing the Comparison Results between Overhead LV/BPL and MV/BPL Topologies – The Common PHY Framework

Concluding this exhaustive comparative EVD modal analysis concerning the behavior of overhead LV/BPL and MV/BPL distribution power grid, several interesting remarks can be pointed out:

- TEP method can comfortably replace hybrid method for educational purposes. In fact, TEP method maintains the required simplicity so as to be understandable from ECE students without lacking of the basic elements of propagation and transmission analysis that should be highlighted. This result has been verified in overhead LV/BPL and MV/BPL modal channels.
- ECE students can recognize that though determined for 1km long LV and MV connections, BPL transmission via the overhead distribution grid exhibits low-loss characteristics regardless of the overhead power grid type favoring the exploitation of LV/BPL and MV/BPL bandwidth.
- The CM^{LV} and the CM^{MV} exhibit: (i) an almost identical spectral behavior regarding their attenuation coefficients and phase delays as it has already mentioned in Section III –see Figs. 2(b), 2(f), 3(b) and 3(f)–; and (ii) very close end-to-end channel attenuation for a great number of indicative overhead BPL topologies –see Figs. 4(c) and 5(c)–. Hence, the transmission characteristics of only one CM^{XV} –either CM^{LV} or CM^{MV}– may be examined for both overhead LV/BPL and MV/BPL systems with significant accuracy.
- As to the DM^{XV}s, since the DM^{LV}s and DM^{MV}s exhibit: (i) an almost identical spectral behavior regarding their attenuation coefficients and phase delays as it has already mentioned in Section III –see Figs. 2(c), 2(d), 2(g), 2(h), 3(c), 3(d), 3(g) and 3(h)–; (ii) very close end-to-end channel attenuation for a plethora of indicative overhead LV/BPL and MV/BPL topologies –see Figs. 4(f), 5(f), 6(f), and 8(c)–; and (iii) identical attenuation discontinuity for a plethora of indicative overhead LV/BPL and MV/BPL topologies either at single-branch junctions –see Figs. 7(c) and 7(f)– or at multi-branch junctions –see Figs. 9(c) and 9(f)–. Thus, the transmission characteristics of only one DM^{XV} –only one of either DM^{LV} or DM^{MV}– may be examined giving results with excellent accuracy for both overhead LV/BPL and MV/BPL systems.
- As the branches become longer and the number of branches per junction increases, the spectral behavior of the overhead BPL networks tends to converge to the spectral behavior of an equivalent circuit which consists of the concatenation of the N K_i-two-way power dividers, $i = 1,\ldots,N$ where K_i is the number of multiples branches at the junction i, $i = 1,\ldots,N$ –see Fig. 4(a) of [1], point A_i–. This approach is a simple channel modelling approximation further facilitating the analysis of overhead LV/BPL and MV/BPL networks.
- Apart from the multiplicity of the various branches encountered along the end-to-end BPL signal propagation, ECE students can identify that the end-to-end channel attenuation in overhead BPL modal channels depends on the frequency, the physical properties of the MTL configurations used, the "LOS" attenuation, and the number, the electrical length, and the terminations of the various branches.
- ECE students can finally realize the common nature between overhead LV/BPL and MV/BPL systems. This permits their common handling under a unified PHY

framework as it concerns their BPL signal transmission through their power lines. The consideration of only one mode –say DM_1^{XV} – for both overhead LV/BPL and MV/BPL systems defines the final step of the common handling PHY approach of overhead distribution power systems. Anyway, the application of a unified PHY framework in real BPL networks using more sophisticated channel approximation techniques is going to be further analyzed in the oncoming research works [65], [66].

V. Conclusions

This companion paper has presented the extension of TEP method that is suitable for the study and the design of overhead LV/BPL and MV/BPL networks from ECE students. This paper has focused on the perspective of common handling of overhead LV/BPL and MV/BPL distribution power systems during BPL signal transmission analysis. This approach offers a valuable tool towards the unified BPL distribution network design when different topologies occur.

Apart from the educational character of this paper, it has been demonstrated that the broadband transmission capability of such networks depends on the frequency, the physical properties of the overhead MTL configuration used, the end-to-end –"LOS"– distance, and the number, the electrical length, the terminations, and the multiplicity of the branches along the end-to-end BPL signal propagation. Furthermore, under the aegis of the unified PHY framework, a simple approximation suitable for the modelling of overhead BPL distribution networks when multiple branches at the same junction occur has been proposed. The simplified approach of TEP method suggests that the spectral behavior of overhead BPL distribution power networks may be satisfactorily described by using equivalent circuits which consist of concatenations of two-way power dividers.

Finally, the results demonstrate to ECE students the low-loss nature of overhead BPL systems over a 1km repeater span well beyond 100MHz. Concluding this paper, ECE students realize that overhead distribution power lines can operate as a promising broadband last mile technology permitting the further exploitation of overhead BPL bandwidth regardless of the overhead power grid type and the overhead power grid topology.

Conflicts of Interest

The author declares that there is no conflict of interests regarding the publication of this paper.

References

[1] A. G. Lazaropoulos, "Designing Broadband over Power Lines Networks Using the Techno-Economic Pedagogical (TEP) Method – Part I: Overhead High Voltage Networks and Their Capacity Characteristics," *Trends in Renewable Energy*, vol. 1, no. 1, pp. 16-42, Mar. 2015. DOI: 10.17737/tre.2015.1.1.002

[2] A. G. Lazaropoulos and P. G. Cottis, "Transmission characteristics of overhead medium voltage power line communication channels," *IEEE Trans. Power Del.*, vol. 24, no. 3, pp. 1164–1173, Jul. 2009. DOI: 10.1109/tpwrd.2008.2008467

[3] A. G. Lazaropoulos, "Towards Modal Integration of Overhead and Underground Low-Voltage and Medium-Voltage Power Line Communication Channels in the Smart Grid Landscape: Model Expansion, Broadband Signal Transmission

Characteristics, and Statistical Performance Metrics (Invited Paper)," *ISRN Signal Processing*, vol. 2012, Article ID 121628, pp. 1-17, 2012. DOI: 10.5402/2012/121628

[4] A. G. Lazaropoulos and P. G. Cottis, "Capacity of overhead medium voltage power line communication channels," *IEEE Trans. Power Del.*, vol. 25, no. 2, pp. 723–733, Apr. 2010. DOI: 10.1109/tpwrd.2009.2034907

[5] A. G. Lazaropoulos, "Review and Progress towards the Common Broadband Management of High-Voltage Transmission Grids: Model Expansion and Comparative Modal Analysis," *ISRN Electronics*, vol. 2012, Article ID 935286, pp. 1-18, 2012. DOI: 10.5402/2012/935286

[6] A. G. Lazaropoulos, "Broadband Transmission Characteristics of Overhead High-Voltage Power Line Communication Channels," *Progress in Electromagnetics Research B*, vol. 36, pp. 373-398, 2012. DOI: 10.2528/PIERB11091408

[7] A. G. Lazaropoulos, "Broadband Transmission and Statistical Performance Properties of Overhead High-Voltage Transmission Networks (Invited Paper)," *Hindawi Journal of Computer Networks and Commun.*, vol. 2012, Article ID 875632, pp. 1-16, 2012. DOI: 10.1155/2012/875632

[8] A. G. Lazaropoulos, "Green Overhead and Underground Multiple-Input Multiple-Output Medium Voltage Broadband over Power Lines Networks: Energy-Efficient Power Control," *Springer Journal of Global Optimization*, 57(3), 997-1024, 2013. DOI: 10.1007/s10898-012-9988-y

[9] M. U. Rehman, S. Wang, Y. Liu, S. Chen, X. Chen, and C. G. Parini, "Achieving High Data Rate in Multiband-OFDM UWB Over Power-Line Communication System," *IEEE Trans. on Power Del.*, vol. 27, no. 3, pp. 1172–1177, Jul. 2012. DOI: 10.1109/TPWRD.2012.2193902

[10] A. M. Sarafi, G. I. Tsiropoulos, and P. G. Cottis, "Hybrid Wireless-Broadband over Power Lines: A Promising Broadband Solution in Rural Areas," *IEEE Comm. Mag.*, pp. 140–147, Nov. 2009. DOI: 10.1109/MCOM.2009.5307478

[11] G. N. S. Prasanna, A. Lakshmi, S. Sumanth, V. Simha, J. Bapat, and G. Koomullil, "Data Communication over the Smart Grid," in *Proc. IEEE Int. Symp. Power Line Communications and Its Applications*, Dresden, Germany, Mar./Apr. 2009, pp. 273–279. DOI: 10.1109/ISPLC.2009.4913442

[12] S. Galli, A. Scaglione, and Z. Wang, "For the grid and through the grid: the role of power line communications in the smart grid," in *Proc. IEEE*, vol. 99, no. 6, pp. 998–1027, Jun. 2011.

[13] S. Liu and L. J. Greenstein, "Emission characteristics and interference constraint of overhead medium-voltage broadband power line (BPL) systems," in *Proc. IEEE Global Telecommunications Conf.*, New Orleans, LA, USA, Nov./Dec. 2008, pp. 1-5. DOI: 10.1109/GLOCOM.2008.ECP.560

[14] P. Amirshahi and M. Kavehrad, "High-frequency characteristics of overhead multiconductor power lines for broadband communications," *IEEE J. Sel. Areas Commun.*, vol. 24, no. 7, pp. 1292–1303, Jul. 2006. DOI: 10.1109/jsac.2006.874399

[15] A. G. Lazaropoulos, "Review and Progress towards the Capacity Boost of Overhead and Underground Medium-Voltage and Low-Voltage Broadband over Power Lines Networks: Cooperative Communications through Two- and Three-Hop Repeater Systems," *ISRN Electronics*, vol. 2013, Article ID 472190, pp. 1-19, 2013. DOI: 10.1155/2013/472190

[16] S. Galli, and Oleg Logvinov, "Recent developments in the standardization of power line communications within the IEEE," *IEEE Communications Magazine,* vol. 46, no. 7, pp. 64-71, 2008. DOI: 10.1109/MCOM.2008.4557044

[17] P. S. Henry, "Interference characteristics of broadband power line communication systems using aerial medium voltage wires," *IEEE Commun. Mag.*, vol. 43, no. 4, pp. 92–98, Apr. 2005. DOI: 10.1109/MCOM.2005.1421910

[18] J. Anatory, N. Theethayi, R. Thottappillil, M. M. Kissaka, and N. H. Mvungi, "The effects of load impedance, line length, and branches in typical low-voltage channels of the BPLC systems of developing countries: transmission-line analyses," *IEEE Trans. Power Del.*, vol. 24, no. 2, pp. 621–629, Apr. 2009. DOI: 10.1109/TPWRD.2008.923395

[19] T. Sartenaer, "Multiuser communications over frequency selective wired channels and applications to the powerline access network" Ph.D. dissertation, Univ. Catholique Louvain, Louvain-la-Neuve, Belgium, Sep. 2004.

[20] T. Calliacoudas and F. Issa, ""Multiconductor transmission lines and cables solver," An efficient simulation tool for plc channel networks development," presented at the *IEEE Int. Conf. Power Line Communications and Its Applications*, Athens, Greece, Mar. 2002.

[21] C. R. Paul*, Analysis of Multiconductor Transmission Lines*. New York: Wiley, 1994.

[22] T. Sartenaer and P. Delogne, "Deterministic modelling of the (Shielded) outdoor powerline channel based on the multiconductor transmission line equations," *IEEE J. Sel. Areas Commun.*, vol. 24, no. 7, pp. 1277–1291, Jul. 2006. DOI: 10.1109/jsac.2006.874423

[23] S. Galli and T. Banwell, "A deterministic frequency-domain model for the indoor power line transfer function," *IEEE J. Sel. Areas Commun.*, vol. 24, no. 7, pp. 1304–1316, Jul. 2006. DOI: 10.1109/jsac.2006.874428

[24] A. G. Lazaropoulos and P. G. Cottis, "Broadband transmission via underground medium-voltage power lines-Part II: capacity," *IEEE Trans. Power Del.*, vol. 25, no. 4, pp. 2425-2434, Oct. 2010. DOI: 10.1109/tpwrd.2010.2052113

[25] P. Amirshahi, "Broadband access and home networking through powerline networks" Ph.D. dissertation, Pennsylvania State Univ., University Park, PA, May 2006.

[26] H. Meng, S. Chen, Y. L. Guan, C. L. Law, P. L. So, E. Gunawan, and T. T. Lie, "Modeling of transfer characteristics for the broadband power line communication channel," *IEEE Trans. Power Del.*, vol. 19, no. 3, pp. 1057–1064, Jul. 2004. DOI: 10.1109/tpwrd.2010.2048929

[27] OPERA1, D44: Report presenting the architecture of plc system, the electricity network topologies, the operating modes and the equipment over which PLC access system will be installed, IST Integr. Project No 507667, Dec. 2005.

[28] DLC+VIT4IP, D1.2: Overall system architecture design DLC system architecture. FP7 Integrated Project No 247750, Jun. 2010.

[29] K. Dostert*, Powerline Communications*. Upper Saddle River, NJ: Prentice-Hall, 2001.

[30] A. G. Lazaropoulos and P. G. Cottis, "Broadband transmission via underground medium-voltage power lines—Part I: transmission characteristics," *IEEE Trans. Power Del.*, vol. 25, no. 4, pp. 2414–2424, Oct. 2010. DOI: 10.1109/tpwrd.2010.2048929

[31] A. G. Lazaropoulos, "Towards Broadband over Power Lines Systems Integration: Transmission Characteristics of Underground Low-Voltage Distribution Power Lines," *Progress in Electromagnetics Research B*, vol. 39, pp. 89-114, 2012. DOI: 10.2528/PIERB12012409

[32] A. G. Lazaropoulos, "Factors Influencing Broadband Transmission Characteristics of Underground Low-Voltage Distribution Networks," *IET Commun.*, vol. 6, no. 17, pp. 2886-2893, Nov. 2012. DOI: 10.1049/iet-com.2011.0661

[33] A. G. Lazaropoulos, "Deployment Concepts for Overhead High Voltage Broadband over Power Lines Connections with Two-Hop Repeater System: Capacity Countermeasures against Aggravated Topologies and High Noise Environments," *Progress in Electromagnetics Research B*, vol. 44, pp. 283-307, 2012. DOI: 10.2528/PIERB12081104

[34] A. G. Lazaropoulos, "Underground Distribution BPL Connections with (N + 1)-hop Repeater Systems: A Novel Capacity Mitigation Technique," Elsevier *Computers and Electrical Engineering*, vol. 40, pp. 1813-1826, 2014. DOI: 10.1016/j.compeleceng.2014.06.001

[35] M. Gebhardt, F. Weinmann, and K. Dostert, "Physical and regulatory constraints for communication over the power supply grid," *IEEE Commun. Mag.*, vol. 41, no. 5, pp. 84–90, May 2003. DOI: 10.1109/mcom.2003.1200106

[36] A. G. Lazaropoulos, "Broadband over Power Lines Systems Convergence: Multiple-Input Multiple-Output Communications Analysis of Overhead and Underground Low-Voltage and Medium-Voltage BPL Networks," ISRN Power Engineering, vol. 2013, Article ID 517940, 30 pages, 2013. DOI: 10.1155/2013/517940

[37] P. Amirshahi and M. Kavehrad, "Medium voltage overhead power-line broadband communications; Transmission capacity and electromagnetic interference," in *Proc. IEEE Int. Symp. Power Line Commun. Appl.*, Vancouver, BC, Canada, Apr. 2005, pp. 2–6. DOI: 10.1109/ISPLC.2005.1430454

[38] M. Götz, M. Rapp, and K. Dostert, "Power line channel characteristics and their effect on communication system design," *IEEE Commun. Mag.*, vol. 42, no. 4, pp. 78–86, Apr. 2004. DOI: 10.1109/mcom.2004.1284933

[39] T. A. Papadopoulos, G.K. Papagiannis, and D.P. Labridis, "A generalized model for the calculation of the impedances and admittances of overhead power lines above stratified earth." *Electric Power Systems Research*, 80(9), 1160-1170. DOI: 10.1016/j.epsr.2010.03.009

[40] T. A. Papadopoulos, C. G. Kaloudas, and G. K. Papagiannis, "A multipath channel model for PLC systems based on nodal method and modal analysis," in *Proc. 2007 IEEE Int. Symp. Power Line Communications and Its Applications (ISPLC'07)*, Pisa, Italy, Mar. 2007, pp. 278–283. DOI: 10.1109/ISPLC.2007.371137

[41] T. A. Papadopoulos, B. D. Batalas, A. Radis, and G. K. Papagiannis, "Medium voltage network PLC modeling and signal propagation analysis," in *Proc. 2007 IEEE Int. Symp. Power Line Communications and its Applications (ISPLC'07)*, Pisa, Italy, Mar. 2007, pp. 284–289. DOI: 10.1109/ISPLC.2007.371138

[42] F. Issa, D. Chaffanjon, E. P. de la Bâthie, and A. Pacaud, "An efficient tool for modal analysis transmission lines for PLC networks development," presented at the *IEEE Int. Conf. Power Line Communications and Its Applications*, Athens, Greece, Mar. 2002.

[43] J. Anatory and N. Theethayi, "On the efficacy of using ground return in the broadband power-line communications—A transmission-line analysis," *IEEE Trans. Power Del.*, vol. 23, no. 1, pp. 132–139, Jan. 2008. DOI: 10.1109/TPWRD.2007.910987

[44] A. I. Chrysochos, T. A. Papadopoulos, and G. K. Papagiannis, "Enhancing the frequency-domain calculation of transients in multiconductor power transmission lines," *Electric Power Systems Research*, vol. 122, pp. 56-64, 2015. DOI: 10.1016/j.epsr.2014.12.024

[45] M. D'Amore and M. S. Sarto, "A new formulation of lossy ground return parameters for transient analysis of multiconductor dissipative lines," *IEEE Trans. Power Del.*, vol. 12, no. 1, pp. 303–314, Jan. 1997. DOI: 10.1109/61.568254

[46] *M.* D'Amore and M. S. Sarto, "Simulation models of a dissipative transmission line above a lossy ground for a wide-frequency range—Part I: Single conductor configuration," *IEEE Trans. Electromagn. Compat.,* vol. 38, no. 2, pp. 127–138, May 1996. DOI: 10.1109/15.494615

[47] M. D'Amore and M. S. Sarto, "Simulation models of a dissipative transmission line above a lossy ground for a wide-frequency range—Part II: Multi-conductor configuration," *IEEE Trans. Electromagn. Compat.*, vol. 38, no. 2, pp. 139–149, May 1996. DOI: 10.1109/15.494616

[48] W. H. Wise, "Propagation of High Frequency Currents in Ground Return Circuits," *Proc. Inst. Radio Eng.*, vol. 22, pp. 522-527, Apr., 1934. DOI: 10.1109/JRPROC.1934.225868

[49] W. H. Wise, "Potential coefficients for ground return circuits," *Bell Syst. Tech. J.*, vol. 27, pp. 365-371, Apr., 1948. DOI: 10.1002/j.1538-7305.1948.tb00913.x

[50] S. Barmada, A. Musolino, and M. Raugi, "Innovative model for time-varying power line communication channel response evaluation," *IEEE J. Sel. Areas Commun.*, vol. 24, no. 7, pp. 1317–1326, Jul. 2006. DOI: 10.1109/JSAC.2006.874426

[51] M. Zimmermann and K. Dostert, "A multipath model for the powerline channel," *IEEE Trans. Commun.*, vol. 50, no. 4, pp. 553–559, Apr. 2002. DOI: 10.1109/26.996069

[52] D. Sabolić, R. Malarić, and A. Bažant, "A Practical Method for Extraction of High-Frequency Parameters of Distribution Cables," *IEEE Trans. on Power Del.*, vol. 27, no. 4, pp. 1877–1884, Oct. 2012. DOI: 10.1109/TPWRD.2012.2211899

[53] J. Anatory, N. Theethayi, R. Thottappillil, M. M. Kissaka, and N. H. Mvungi, "The influence of load impedance, line length, and branches on underground cable Power-Line Communications (PLC) systems," *IEEE Trans. Power Del.*, vol. 23, no. 1, pp. 180–187, Jan. 2008. DOI: 10.1109/TPWRD.2007.911020

[54] OPERA1, D5: Pathloss as a function of frequency, distance and network topology for various LV and MV European powerline networks. IST Integrated Project No 507667, Apr. 2005.

[55] J. Anatory, N. Theethayi, and R. Thottappillil, "Power-line communication channel model for interconnected networks—Part II: Multiconductor system," *IEEE Trans. Power Del.*, vol. 24, no. 1, pp. 124–128, Jan. 2009. DOI: 10.1109/TPWRD.2008.2005681

[56] P. A. A. F. Wouters, P. C. J. M. van der Wielen, J. Veen, P. Wagenaars, and E. F. Steennis, "Effect of cable load impedance on coupling schemes for MV power line

communication," *IEEE Trans. Power Del.*, vol. 20, no. 2, pt. 1, pp. 638–645, Apr. 2005. DOI: 10.1109/TPWRD.2005.844334

[57] L. M. Kuhn, S. Berger, I. Hammerström, and A. Wittneben, "Power line enhanced cooperative wireless communications," *IEEE J. Sel. Areas Commun.*, vol. 24, no. 7, pp. 1401–1410, Jul. 2006. DOI: 10.1109/JSAC.2006.874407

[58] Y. Xiaoxian, Z. Tao, Z. Baohui, Y. Fengchun, D. Jiandong, and S. Minghui, "Research of impedance characteristics for medium-voltage power networks," *IEEE Trans. Power Del.*, vol. 22, no. 2, pp. 870-878, Apr. 2007. DOI: 10.1109/TPWRD.2006.881573

[59] Y. Xiaoxian, Z. Tao, Z. Baohui, N. Xu, W. Guojun, and D. Jiandong, "Investigation of transmission properties on 10-kV medium voltage power lines—part I: general properties," *IEEE Trans. on Power Del.*, vol. 22, no. 3, pp. 1446–1454, 2007. DOI: 10.1109/TPWRD.2007.900290

[60] Z. Tao, Y. Xiaoxian, Z. Baohui, C. Jian, Y. Zhi, and T. Zhihong, "Research of noise characteristics for 10-kV medium-voltage power lines," *IEEE Trans. on Power Del.*, vol. 22, no. 1, pp. 142–150, 2007. DOI: 10.1109/TPWRD.2006.881414

[61] J. Anatory, N. Theethayi, R. Thottappillil, M. M. Kissaka, and N. H. Mvungi, "An experimental validation for Broadband Power-Line Communication (BPLC) model," *IEEE Trans. Power Del.*, vol. 23, no. 3, pp. 1380–1383, Jul. 2008. DOI: 10.1109/TPWRD.2008.916739

[62] J. Anatory, N. Theethayi, R. Thottappillil, M. M. Kissaka, and N. H. Mvungi, "Broadband power-line communication channel model: Comparison between theory and experiments," in *Proc. IEEE Int. Symp. Power Line Communications and Its Applications*, Jeju Island, Korea, Apr. 2008, pp. 322–324. DOI: 10.1109/ISPLC.2008.4510447

[63] A. G. Lazaropoulos, "Numerical Evaluation of Broadband Transmission Characteristics of Underground Low-Voltage Networks – Introducing Techno-Pedagogical (TP) Method," *Elsevier Int. Journal of Electrical Power & Energy Systems*, vol. 55, pp. 253-260, 2014. DOI: 10.1016/j.ijepes.2013.09.009

[64] T. A. Papadopoulos, A. I. Chrysochos, A. I. Nousdilis, and G. K. Papagiannis, "Simplified measurement-based black-box modeling of distribution transformers using transfer functions," *Electric Power Systems Research*, vol. 121, pp. 77-88, 2015. DOI: 10.1016/j.epsr.2014.12.003

[65] I. C. Demetriou, "Algorithm 742: L2CXFT: a Fortran subroutine for least-squares data fitting with nonnegative second divided differences," *ACM Transactions on Mathematical Software (TOMS)*, vol. 21, no. 1, pp. 98-110, 1995. DOI: 10.1145/200979.201039

[66] S. S. Papakonstantinou and I. C. Demetriou, "Data Engineering by the Best l1 Convex Data Fitting Method," in *Proceedings of the World Congress on Engineering*, vol. 1, 2014.

Trends in Renewable Energy
OPEN ACCESS ISSN: 2376-2144
Peer-Reviewed Article futureenergysp.com/index.php/tre

Policies for Carbon Energy Footprint Reduction of Overhead Multiple-Input Multiple-Output High Voltage Broadband over Power Lines Networks

Athanasios G. Lazaropoulos*

School of Electrical and Computer Engineering, National Technical University of Athens (NTUA), 9 Iroon Polytechniou Street, Zografou, Athens, Greece 15780

Received April 11, 2015; Accepted May 12, 2015; Published May 15, 2015

The impact of different environmental policies on the broadband performance of overhead multiple-input multiple-output high-voltage/broadband over power lines (MIMO/HV/BPL) networks is investigated in this paper. The examined environmental policies focus on the carbon energy footprint reduction of overhead MIMO/HV/BPL networks while respecting their broadband character.
The contribution of this paper is three-fold. First, the spectral and environmental performance of various configurations and topologies of overhead MIMO/HV/BPL networks is assessed with regard to respective spectral efficient (SE) and newly presented environmental efficient (EE) metrics. Second, further insights regarding the performance of overhead MIMO/HV/BPL networks highlight the better spectral and environmental performance of these networks against other today's overhead HV/BPL networks, such as single-input single-output (SISO), single-input multiple-output (SIMO), or multiple-input single-output (MISO) ones. Third, the definition of appropriate environmental policies that optimize the coexistence of the three main sectors of concern, which are the Quality of Service (QoS) requirements, protection of existing radioservices and promotion of environmentally aware limits, is promoted. Towards that direction, the proposed SE/EE trade-off relation of this paper is expected to prove an extremely helpful SE/EE optimization technique.

Keywords: Broadband over Power Lines (BPL) modeling; modal analysis; Power Line Communications (PLC); overhead High-Voltage (HV) power lines; capacity; green technology

I. Introduction

The deployment of broadband over power lines (BPL) networks across the entire transmission and distribution grid –i.e., high-voltage (HV), medium-voltage (MV) and low-voltage (LV) grids– may critically facilitate the role of sensing, communications and control across the existing power grid [1]-[4]. On the basis of the modernization of today's power grid towards a smart power network with state-of-the-art communications capabilities, a plethora of potential smart grid (SG) applications, such as grid monitoring, protection and automatic optimization of operations related to network interconnected elements, can be available [5]-[11].

Until now, significant efforts have been made to exploit the broadband potential of HV/BPL, MV/BPL and LV/BPL networks [12]-[30]. Apart from the fervent interest towards the adoption of BPL technology in future's SG installations, new interest arises due to the recent developments regarding multiple-input multiple-output (MIMO)

*Corresponding author: AGLazaropoulos@gmail.com

Tr Ren Energy, 2015, Vol.1, No.2, 87-118. doi:10.17737/tre.2015.1.2.0011

transmission technology for BPL networks and the interoperability of the BPL technology with other already established broadband technologies intended to be installed in upcoming SG installations [31]-[33]. Since today's single-input single-output (SISO) HV/BPL systems lack of providing adequate transmission rates so as to cover future SG application requirements in a trustworthy way, the deployment of MIMO configuration schemes in overhead HV/BPL networks, which is firstly presented in [14], [32], [34]-[41], is imminent. Nevertheless, a major disadvantage of overhead HV/BPL systems –either SISO or single-input multiple-output (SIMO) or multiple-input single-output (MISO) or MIMO scheme configurations– is their high energy consumption with regards to their spectral performance.

At the same time, carbon energy footprint reduction in information and communications technology (ICT) becomes a growing concern for providers in order not only to reduce their environmental effect [42] but also to enhance their profitability [7], [43], [44]. Actually, the strong interest of telecom and energy regulatory authorities towards the reduction of ICT carbon energy footprint –including carbon and energy use embodied in the ICT infrastructure– encourages technological innovations so that environmental efficient (EE) improvements can be achieved without significantly affecting the quality of service (QoS) [7], [45]-[52]. In fact, a possible reduction of energy consumption through appropriate techniques may also entail the carbon energy footprint reduction. To define an environmental high-bitrate MIMO/HV/BPL network design, the coexistence of injected power spectral density mask (IPSDM) limits, which assure electromagnetic interference (EMI) protection to primary wireless services that operate at the same frequency bands with BPL systems [17], [19], with environmental policies, which regulate carbon energy footprint and the energy consumption of MIMO/HV/BPL systems, needs to be examined in this paper. On the basis of [7], a modification to the fixed IPSDM limits through the insertion of an appropriate "green factor" is proposed so that the three main sectors of concern, which are the Quality of Service (QoS) requirements, protection of the existing radioservices and promotion of environmentally aware limits, can be compromised.

To assess the spectral and environmental performance of overhead HV/BPL networks, the well-established hybrid method that is usually employed to examine the behavior of BPL transmission channels installed on HV multiconductor transmission line (MTL) structures is also used in this paper. The hybrid method is based on: (i) a bottom-up approach consisting of an appropriate combination of the similarity transformation and MTL theory [12], [16], [21]-[23], [31], [53]-[63]; and (ii) a top-down approach consisting of the exact version of multidimensional chain scattering matrix method [5]-[7], [16]-[23], [53], [58], [59]. Through the bottom-up approach, the modes that may be supported by an overhead HV/BPL configuration are determined concerning their propagation constants and their characteristic impedances whereas, through the top-down approach, the end-to-end attenuation of overhead HV/BPL channels is defined.

With reference to the numerical results of the aforementioned hybrid method, the performance of overhead MIMO/HV/BPL networks is assessed using appropriate transmission, spectral efficient (SE) and EE metrics [5], [16]-[20], [41], [52], [64]-[68]. Extending the energy efficient metrics of [7] to the EE metrics of this paper, the proposed trade-offs between spectral and environmental performance highlight a novel wiser compromise among throughput performance, EMI regulations and environmental awareness. Further insights, such as how to improve the occurred trade-off curves

through proper environmental policies and how to tune the operation points of overhead MIMO/HV/BPL networks at the trade-off curves to balance the aforementioned compromise, are expected to influence the practical system design of future's overhead MIMO/HV/BPL networks [42], [45], [66]. Moreover, the strategic turn of countries towards cleaner energy sources is studied through the lens of the proposed trade-off curves. Consequently, this paper introduces a multidisciplinary approach towards a greener sustainable development of overhead MIMO/HV/BPL networks by appropriately combining a wide range of research areas, such as communications and electrical engineering, economic management and environmental planning.

The rest of the paper is organized as follows: In Section II, the overhead HV configuration adopted in this paper is demonstrated. Section III highlights the main features of MIMO/HV/BPL transmission that are MTL theory, eigenvalue decomposition (EVD), singular value decomposition (SVD) modal analyses and hybrid method. Section IV emphasizes to the electromagnetic compatibility (EMC) of overhead HV/BPL systems with other already licensed radioservices, the proposed green modification of existing IPSDM limits, the HV/BPL system power consumption and carbon energy footprint. Section V provides a description of the transmission, SE and EE metrics applied in this paper for the MIMO/HV/BPL network analysis. In Section VI, numerical results and conclusions are presented, aiming at marking out how the various EMI regulations, EE policies and MIMO scheme configurations influence overhead MIMO/HV/BPL transmission, SE and EE metrics. On the basis of the proposed SE/EE trade-off curves, appropriate EE high-bitrate policies are proposed. Section VII concludes the paper.

II. Overhead HV Transmission Power Networks

The overhead HV power grid differs considerably from transmission via twisted-pair, coaxial, or fiber-optic cables due to the significant differences of the network structure and the physical properties of the power transmission cables used [5], [6], [16], [18], [22], [23], [25], [54], [69]-[75].

Overhead 400kV double-circuit overhead HV transmission phase lines with radii r_p^{400kV} =15.3mm hang at typical heights h_p^{400kV} equal to 20m above ground –i.e., conductors 1, 2, 3, 4, 5, and 6–. These six phase conductors are divided into three bundles; the phase conductors of each bundle are connected by non-conducting spacers and are separated by Δ_{p1}^{400kV} equal to 400mm, whereas bundles are spaced by Δ_{p2}^{400kV} equal to 10m. Moreover, two parallel neutral conductors with radii r_n^{400kV} =9mm spaced by Δ_n^{400kV} equal to 12m hang at heights h_n^{400kV} equal to 23.7m –i.e., conductors 7 and 8–. This double-circuit eight-conductor ($n^{400kV}=8$) overhead HV distribution line configuration is considered in the present work consisting of ACSR conductors –see Fig. 1– [5], [6], [23], [73]-[80].

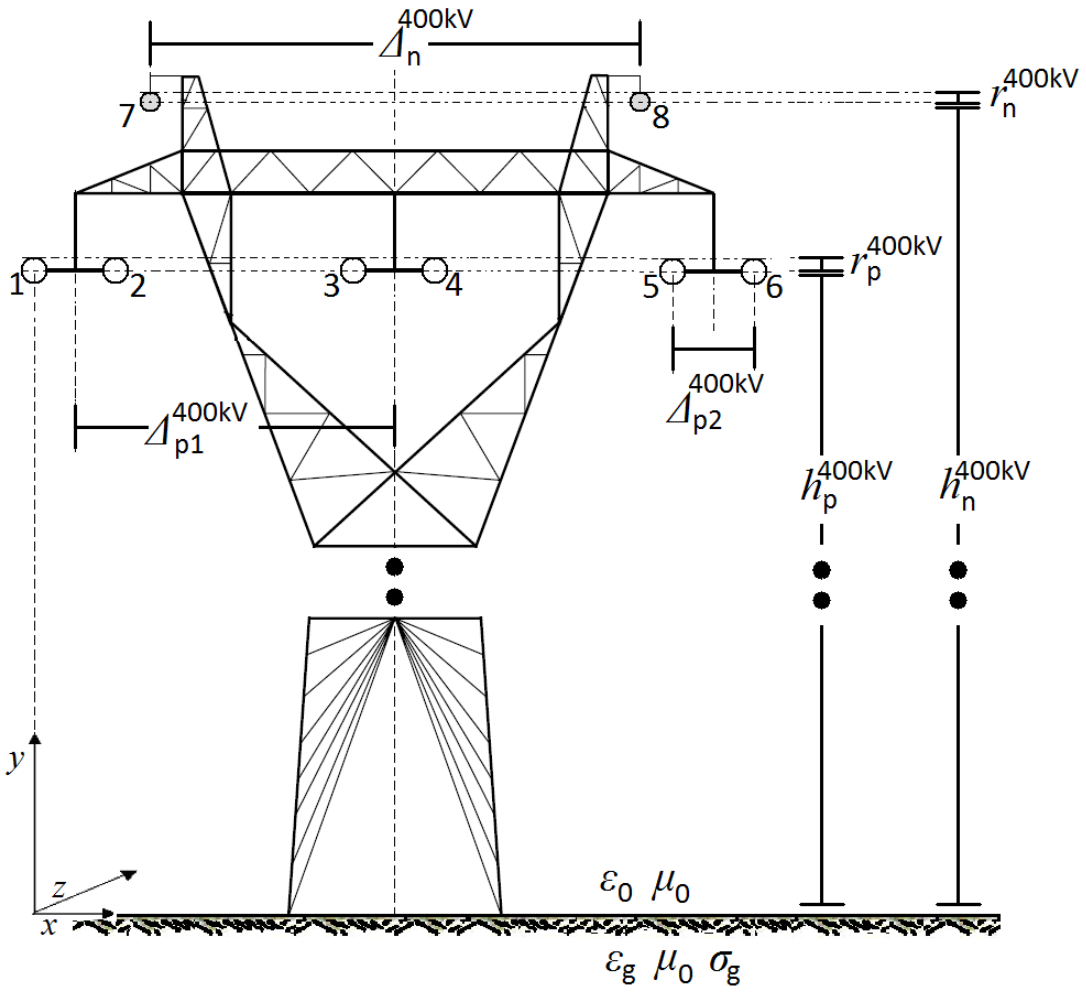

Figure 1. Typical overhead 400kV double-circuit HV multiconductor structures [1], [76]-[80].

The ground is considered as the reference conductor. The conductivity of the ground is assumed σ_g=5mS/m and its relative permittivity ε_{rg}=13, which is a realistic scenario [5], [6], [16], [17], [23], [54], [72]. The impact of imperfect ground on signal propagation via overhead power lines was analyzed in [16], [17], [54], [72], [81]-[84]. Contrary to other available models for overhead power lines [85]-[88], this formulation is suitable for transmission at high frequencies [5], [6], [7], [16]-[20], [23].

III. An Overview of the Modal Analysis of Overhead MIMO/HV/BPL Systems

Through a matrix approach, the standard TL analysis can be extended to the MTL case which involves more than two conductors. Compared to a two-conductor line supporting one forward- and one backward-traveling wave, an MTL structure with eight plus one conductors parallel to the z axis as depicted in Fig. 1 may support eight pairs of forward- and backward-traveling waves with corresponding propagation constants. These waves may be described by a coupled set of sixteen first-order partial differential equations relating the line voltages $V_i(z,t)$, $i=1,\ldots,8$ to the line currents

$I_i(z,t),\ i=1,\ldots,8$. Each pair of forward- and backward-traveling waves is referred to as a mode [5]-[7], [16]-[23], [60], [61]. Consequently, in the case of overhead HV transmission lines involving eight conductors over lossy plane ground, eight modes may be supported, namely:

- Common mode of overhead BPL transmission (CM) with propagation constant $\gamma_{\mathrm{CM}} \equiv \gamma_1$. Its spectral behavior is thoroughly investigated in [1], [5], [6].
- Differential modes of overhead BPL transmission (DM_i , $i=1,\ldots,7$) with corresponding propagation constants $\gamma_{\mathrm{DM}i} \equiv \gamma_{\mathrm{i+1}}$, $i=1,\ldots,7$. Their spectral behavior is thoroughly investigated in [1], [5], [6].

The EVD modal voltages $\mathbf{V}^{\mathrm{m}}(z)=\left[V_1^{\mathrm{m}}(z)\ \cdots\ V_8^{\mathrm{m}}(z)\right]^{\mathrm{T}}$ and the EVD modal currents $\mathbf{I}^{\mathrm{m}}(z)=\left[I_1^{\mathrm{m}}(z)\ \cdots\ I_8^{\mathrm{m}}(z)\right]^{\mathrm{T}}$ may be related to the respective line quantities $\mathbf{V}(z)=\left[V_1(z)\ \cdots\ V_8(z)\right]^{\mathrm{T}}$ and $\mathbf{I}(z)=\left[I_1(z)\ \cdots\ I_8(z)\right]^{\mathrm{T}}$ via the similarity transformations

$$\mathbf{V}(z)=\mathbf{T}_{\mathrm{V}}\cdot\mathbf{V}^{\mathrm{m}}(z) \tag{1}$$

$$\mathbf{I}(z)=\mathbf{T}_{\mathrm{I}}\cdot\mathbf{I}^{\mathrm{m}}(z) \tag{2}$$

where $[\cdot]^{\mathrm{T}}$ denotes the transpose of a matrix, $\mathbf{T}_{\mathrm{V}}$ and $\mathbf{T}_{\mathrm{I}}$ are 8×8 matrices depending on the overhead power grid type, the frequency, the physical properties of the cables and the geometry of the MTL configuration [1], [5], [6], [16], [18], [23], [53], [60], [61], [76]-[95].

On the basis of eqs (1) and (2), the line voltages and currents are expressed as appropriate superpositions of the respective EVD modal quantities, namely:

$$\mathbf{V}^{\mathrm{m}}(0)=\left[\mathbf{T}_{\mathrm{V}}\right]^{-1}\cdot\mathbf{V}(0) \tag{3}$$

The TM2 method, which is module of the top-down approach of the hybrid method, is based on the scattering matrix theory and is presented analytically in [7], models the spectral relationship between $V_i^{\mathrm{m}}(z),\ i=1,\ldots,8$ and $V_j^{\mathrm{m}}(0),\ j=1,\ldots,8$ proposing operators $H_{i,j}^{\mathrm{m}}\{\cdot\},\ i,j=1,\ldots,8$ so that

$$\mathbf{V}^{\mathrm{m}}(z)=\mathbf{H}^{\mathrm{m}}\left\{\mathbf{V}^{\mathrm{m}}(0)\right\} \tag{4}$$

where $\mathbf{H}^{\mathrm{m}}\{\cdot\}$ is the 8×8 EVD modal transfer function matrix whose elements $H_{i,j}^{\mathrm{m}}\{\cdot\},\ i,j=1,\ldots,8$ with $i=j$ are the EVD modal co-channel (CC) transfer functions, while those $H_{i,j}^{\mathrm{m}}\{\cdot\}$, $i,j=1,\ldots,8$ with $i\neq j$ are the EVD modal cross-channel (XC) transfer functions and $H_{i,j}^{\mathrm{m}}$ denotes the element of matrix $\mathbf{H}^{\mathrm{m}}\{\cdot\}$ in row i of column j [5]-[7], [16]-[23], [55], [91]. Combining eqs. (1) and (4), the 8×8 transfer function matrix $\mathbf{H}\{\cdot\}$ of overhead HV/BPL transmission network relating $\mathbf{V}(z)$ with $\mathbf{V}(0)$ through

$$\mathbf{V}(z)=\mathbf{H}\{\mathbf{V}(0)\} \tag{5}$$

is determined from

$$\mathbf{H}\{\cdot\}=\mathbf{T}_{\mathrm{V}}\cdot\mathbf{H}^{\mathrm{m}}\{\cdot\}\cdot\left[\mathbf{T}_{\mathrm{V}}\right]^{-1} \tag{6}$$

Since in overhead MIMO/HV/BPL networks, the number of active transmit ports n_T and receive ports n_R may vary from one to eight, through a similar matrix expression

to eq. (6), $\min\{n_T, n_R\}$ parallel and independent SISO/HV/BPL channels may occur, appropriately decomposing channel transfer function matrix $\mathbf{H}\{\cdot\}$ using the SVD transformation [32], [35]-[37], [39], [96], [97]:

$$\widetilde{\mathbf{H}}^m\{\cdot\} = \widetilde{\mathbf{T}}_V^H \cdot \mathbf{H}^+\{\cdot\} \cdot \widetilde{\mathbf{T}}_I \tag{7}$$

where

$$H_{ij}^+\{\cdot\} = \begin{Bmatrix} H_{ij}\{\cdot\} & ,\text{if } (i \in \mathbf{n}_T \text{ and } j \in \mathbf{n}_R) \\ 0 & ,\text{otherwise} \end{Bmatrix} \quad i, j = 1,\ldots,8 \tag{8}$$

denotes the element of matrix $\mathbf{H}^+\{\cdot\}$ in row i of column j. From eqs. (7) and (8), $\mathbf{H}^+\{\cdot\}$ is the 8×8 extended channel transfer function matrix whose elements $H_{ij}^+\{\cdot\}$, $i, j = 1,\ldots,8$ are the extended channel transfer functions, $\widetilde{\mathbf{H}}^m\{\cdot\}$ is a diagonal matrix operator whose elements $\widetilde{H}_i^m\{\cdot\}$, $i = 1,\ldots,\min\{n_T, n_R\}$ are the singular values of $\mathbf{H}^+\{\cdot\}$ and, at the same time, the SVD modal transfer functions, $\min\{x, y\}$ returns the smallest value between x and y, $\mathbf{n}_T$ and $\mathbf{n}_R$ are the active transmit port and the active receive port sets, respectively, $[\cdot]^H$ denotes the Hermitian conjugate of a matrix, and $\widetilde{\mathbf{T}}_V$ and $\widetilde{\mathbf{T}}_I$ are 8×8 unitary matrices [36], [39], [98]. Combining eqs. (6)-(8), SVD modal transfer function matrix $\widetilde{\mathbf{H}}^m\{\cdot\}$ may be determined given EVD modal transfer function matrix $\mathbf{H}^m\{\cdot\}$.

IV. Brief Description of Overhead MIMO/HV/BPL Channels

A. Power Constraints due to EMI and Environmental Constraints

A critical issue related to the operation of overhead MIMO/HV/BPL networks has to do with the power constraints (i.e., IPSDM limits) that should be imposed in order to ensure their successful coexistence with other already existing wireless and telecommunication services at the same frequency band of operation [17], [19], [26], [99]. Among regulatory bodies that have established proposals concerning the safe EMI BPL operation, the most important are those of FCC Part 15, German Reg TP NB30, the Norwegian Proposal and the BBC/NATO Proposal [71], [100]-[102].

Especially, the IPSDM limits proposed by Ofcom for compliance with FCC Part 15 that are presented in [71], [100]-[102] are the most cited due to their proneness towards the deployment of high-bitrate BPL networks. More specifically, for overhead HV/BPL networks, according to Ofcom, in the 1.705-30MHz frequency range, maximum levels -60 dBm/Hz constitute appropriate IPSDM limits $p(f)$ providing presumption of compliance with the current FCC Part 15 limits [17], [19], [103], [104]. To extend the capacity analysis in the 30-88MHz range, maximum IPSDM limits $p(f)$ that are equal to -77 dBm/Hz for overhead HV/BPL networks are assumed to provide a presumption of compliance in this frequency range [17], [19], [103], [104]. Note that as it regards the above power constraints of overhead MIMO/HV/BPL scheme configurations, to extend the analysis in the 1.705-88MHz range, common IPSDM limits $p(f)$ between HV/BPL and MV/BPL systems have been assumed exploiting the significant similarities regarding overhead HV/BPL and MV/BPL transmission without

harming the generality of the following MIMO analysis [17], [19], [54], [72], [103]-[105].

Different IPSDM limits may provide to the authorities the necessary alternative options in protecting services and, at the same time, permitting energy efficient high-bitrate MIMO/HV/BPL system operation. In accordance with [7], power spectral regulation through the insertion of a suitable green multiplicative factor $[1+\Phi(f)]$ to the existing IPSDM limits (in dBm/Hz) may offer significant flexibility options; since existing IPSDM limits receive negative values, new IPSDM limits $p^*(f)=p(f)\cdot[1+\Phi(f)]$ can assure both BPL compatibility with other wireless services and the required energy efficiency. Note that the green factor $\Phi(f)$ that may be defined by both regulatory bodies and network operators can take only positive values in order to maintain the necessary EMC of overhead HV/BPL networks. The factors that determine the imposed green factor depend on the required degree of energy consumption (carbon energy footprint saving), the local traffic, the type of services delivered and QoS threshold criterion imposed. Since lower energy consumption implies higher carbon energy footprint savings, the higher the value of the green factor $\Phi(f)$, the higher the influence of EE policies is. In contrast, when the green factor is equal to 0, no concern for EE policies is taken.

Without affecting the generality of the following analysis, only the class of continuous EE policies will be taken into consideration; this class contains all the EE policies where a constant value of green factor $\Phi\equiv\Phi(f)$ across the entire 1.705-88MHz frequency range is assumed [7].

B. Noise Characteristics

According to [17], [19], [25], [54], [72], [106], [107], two types of noise are dominant in overhead HV/BPL channels:

- *Colored background noise*: This type of noise is dominant in BPL channels. It is the environmental noise that depends on weather conditions, humidity, geographical location, height of cables above the ground, etc. Corona discharge is a major source of colored background noise, especially under humid and severe weather conditions [54], [72], [82], [101], [108], [109].
- *Narrowband noise*: This type of noise is the result of the narrowband interferences from other wireless services operating at the same frequency bands with overhead HV/BPL networks. This kind of noise exhibits local variations and is time-dependent [17], [19], [72], [108], [109].

As it regards the noise properties of overhead MIMO/HV/BPL scheme configurations, to extend this analysis in the 1.705-88MHz range, uniform additive white Gaussian noise (AWGN) PSD level $N(f)$ will be assumed [17], [19], [54], [72], [103]-[105], [110]. In detail, to evaluate the capacity of overhead MIMO/HV/BPL systems, a uniform AWGN/PSD level is assumed equal to -105dBm/Hz [17], [19], [54], [72]. The noise AWGN/PSD of each power grid type is assumed common to all MIMO channels of the MTL configuration. Note that as it regards the above noise features of overhead MIMO/HV/BPL scheme configurations, to extend the analysis in the 1.705-88MHz frequency range, common AWGN PSD level $N(f)$ between HV/BPL and MV/BPL systems has been assumed exploiting the significant similarities regarding

overhead HV/BPL and MV/BPL transmission without harming the generality of MIMO analysis.

C. Power Consumption

According to [66], [111]-[114], two types of power consumption occur in overhead MIMO/HV/BPL systems, namely:

- *Power Consumption due to Power Amplifiers.* Power amplifiers are the main power consumption blocks in any advanced communication system due to their needed high RF power amplifier efficiency. This class of power consumption depends mainly on the imposed EE policy [66], [112].
- *Power Consumption due to all other Circuit Blocks.* Apart from power amplifiers, overhead MIMO/HV/BPL systems consist of the Digital-to-Analog Converter (DAC), the mixer, the active filters at the transmitting end, the frequency synthesizer, the low-noise amplifier (LNA), the intermediate frequency amplifier (IFA), the active filters at the receiver side and the Analog-to-Digital Converter (ADC). This type of power consumption is related to all these circuit blocks and depends on the number of active transmit and receive ports of MIMO/HV/BPL systems [66], [112].

The total average power consumption P_{tot} of overhead MIMO/HV/BPL systems is given by the sum of the aforementioned two types of power consumption. Based on the related circuit and system parameters, which are detailed in [66], [111]-[114], an approximation of the actual MIMO/HV/BPL system power consumption is computed.

D. Carbon Emissions

The carbon energy footprint of an overhead MIMO/HV/BPL network depends on its power consumption and on the origin of the electricity production [115]. A metric of carbon energy footprint, which is subject to each country's energy sources, is given by converting power consumption into *gr* of CO_2 per each *kWh* of energy consumption. For anthracite electricity production and gas electricity production of this paper, the carbon energy footprint of an overhead MIMO/HV/BPL system is computed according to

$$K^{CO_2} = 8.64 \cdot 10^{-6} \cdot P_{tot} \cdot X \tag{9}$$

where K^{CO_2} is expressed in *tons* of CO_2 per *year* and X is the conversion metric that is equal to $870 grCO_2/kWh$ and $360 grCO_2/kWh$ for anthracite electricity production and gas electricity production, respectively [115], [116].

V. SE and EE Metrics of Overhead MIMO/HV/BPL Networks

To assess the spectral and environmental performance of overhead MIMO/HV/BPL networks, respective SE and EE metrics are used. SE metrics describe how efficiently BPL networks exploit their allocated frequency band whereas EE metrics correspond each bit per second (bps) to a carbon energy footprint. In this Section, several useful SE and EE metrics are introduced in order to examine the properties of the overhead MIMO/HV/BPL networks, namely:

a. *Capacity.* Capacity is the maximum achievable transmission rate in bps over a BPL channel and depends on the applied configuration of MIMO/HV/BPL

network, the system features, the imposed EE policy and the noise characteristics. In this paper, capacity is the considered QoS criterion.

More specifically, the capacity of the SISO/HV/BPL system from transmit port *j* to receive port *i* is given by [7], [17], [19]

$$C_{ij}^{SISO} = f_s \sum_{q=0}^{K-1} \log_2 \left\{ 1 + \left[SNR(qf_s) \cdot \left| H_{ij,q}^{+} \right|^2 \right] \right\}, i, j = 1,\ldots,8 \tag{10}$$

where

$$SNR(f) = \left\langle \left[1 + \Phi(f) \right] p^*(f) \right\rangle_L / \left\langle N(f) \right\rangle_L \tag{11}$$

is the BPL signal-to-noise ratio (SNR), $\langle \cdot \rangle_L$ is an operator that converts dBm/Hz into a linear power ratio (W/Hz), K is the number of subchannels in the BPL signal frequency range of interest and f_s is the flat-fading subchannel frequency spacing [17], [19], [99]. As it concerns the characterization of overhead SISO/HV/BPL systems, the elements C_{ij}^{SISO}, $i, j = 1,\ldots,8$ with $i = j$ and $i \neq j$ characterize SISO/CC HV/BPL and SISO/XC HV/BPL system capacities, respectively.

Similarly, the capacity of the $1 \times n_R$ SIMO HV/BPL systems from the transmit port *j* with n_R receive ports –ranging from two to eight– is given by

$$C_j^{SIMO} = f_s \sum_{q=0}^{K-1} \log_2 \left\{ 1 + SNR(qf_s) \cdot \sum_{i \in \mathbf{n}_R} \left| H_{ij}^{+}(qf_s) \right|^2 \right\} \tag{12}$$

In the case of $n_T \times 1$ MISO HV/BPL system, the capacity to the receiving port *i* with n_T transmit ports –ranging from two to eight– is given by [7], [64], [117]

$$C_i^{MISO} = f_s \sum_{q=0}^{K-1} \log_2 \left\{ 1 + \frac{SNR(qf_s)}{n_T} \cdot \sum_{j \in \mathbf{n}_T} \left| H_{ij}^{+}(qf_s) \right|^2 \right\} \tag{13}$$

Finally, in the general case of $n_T \times n_R$ MIMO/HV/BPL systems with n_T and n_R ranging both from two to eight, the capacity is determined by [7], [32], [36], [37], [39], [40], [64], [117]

$$C^{MIMO} = f_s \sum_{q=0}^{K-1} \sum_{i=1}^{\min\{n_R, n_T\}} \log_2 \left\{ 1 + \frac{SNR(qf_s)}{n_T} \cdot \left| \tilde{H}_i^m(qf_s) \right|^2 \right\} \tag{14}$$

Note that both eqs. (13) and (14) are based on equal power uncorrelated sources as the common case is adopted where the transmitting end does not have channel state information (CSI).

According to the different SISO, SIMO, MISO and MIMO scheme configurations, the resulting single- and multi-port diversities may be classified into two major classes:

- *Pure Scheme Configuration Class*. This class contains the elementary single- and multi-port implementations, namely: 8×8 MIMO, 1×8 SIMO, 8×1 MISO, and all SISO systems –either SISO/CCs or SISO/XCs–.
- *Mixed Scheme Configuration Class*. This class contains all the other multi-port implementations that may be deployed, namely: $n_T \times n_R$ MIMO systems with $1 < n_T, n_R < 8$.

b. *The EE capacity*. It denotes the maximum achievable transmission rate of Mbps that the system can deliver per ugr of CO_2 emitted from it. This EE capacity metric is obtained as the ratio of the capacity to the carbon energy footprint for given EE policy, circuit/system parameters and country's energy sources for electricity production. This EE capacity metric provides a macroscopic qualitative estimate of the role of EE policies and system power consumption during BPL system operation.

VI. Numerical Results and Discussion

The simulation results of various configurations of overhead MIMO/HV/BPL networks aim at investigating: (a) their broadband performance; (b) how the applied SE and EE capacity metrics are influenced by the implementation of various MIMO/HV/BPL scheme configurations; and (c) the occurred SE/EE dynamic equilibria due to the different EE policies.

As mentioned in Section III, since the modes supported by the overhead HV/BPL configurations may be examined separately, it is assumed for simplicity that the BPL signal is injected directly into the EVD modes [5]-[7], [16]-[23], [53]-[56], [58]-[62], [72], [117].

For the numerical computations, the 400kV double-circuit overhead HV transmission line configuration, depicted in Fig. 1, has been considered. The simple overhead topology of Fig. 2(a), having N branches, has been assumed. In order to simplify the following analysis without affecting its generality, the branching cables are assumed identical to the transmission cables and the interconnections between the transmission and branch conductors are fully activated. With reference to Fig. 2(b), the transmitting and the receiving ends are assumed matched to the characteristic impedance of the modal channels supported, whereas the branch terminations $\mathbf{Z}_{bk}$, $k = 1,2,\ldots,N$ are assumed open circuit [5]-[8], [16]-[19], [54], [76]-[79], [92].

With reference to Fig. 2(b), four indicative overhead HV topologies concerning end-to-end connections of average lengths equal to 25km are examined. These topologies are [5]-[8], [22]-[24], [69], [73], [74], [76]-[79], [92], [118]-[120]:

(1) A typical urban topology (urban case) with N=3 branches (L_1=1.15km, L_2=12.125km, L_3=8.425km, L_4=3.3km, L_{b1}=27.6km, L_{b2}=17.2km, L_{b3}=33.1km).
(2) A typical suburban topology (suburban case) with N=2 branches (L_1=9.025km, L_2=12.75km, L_3=3.225km, L_{b1}=46.8km, L_{b2}=13.4 km).
(3) A typical rural topology (rural case) with only N=1 branch (L_1=3.75km, L_2=21.25km, L_{b1}=21.1km).
(4) The "LOS" transmission along the average end-to-end distance $L=L_1+\ldots+L_{N+1}$=25km when no branches are encountered. This topology corresponds to Line-of-Sight transmission in wireless channels.

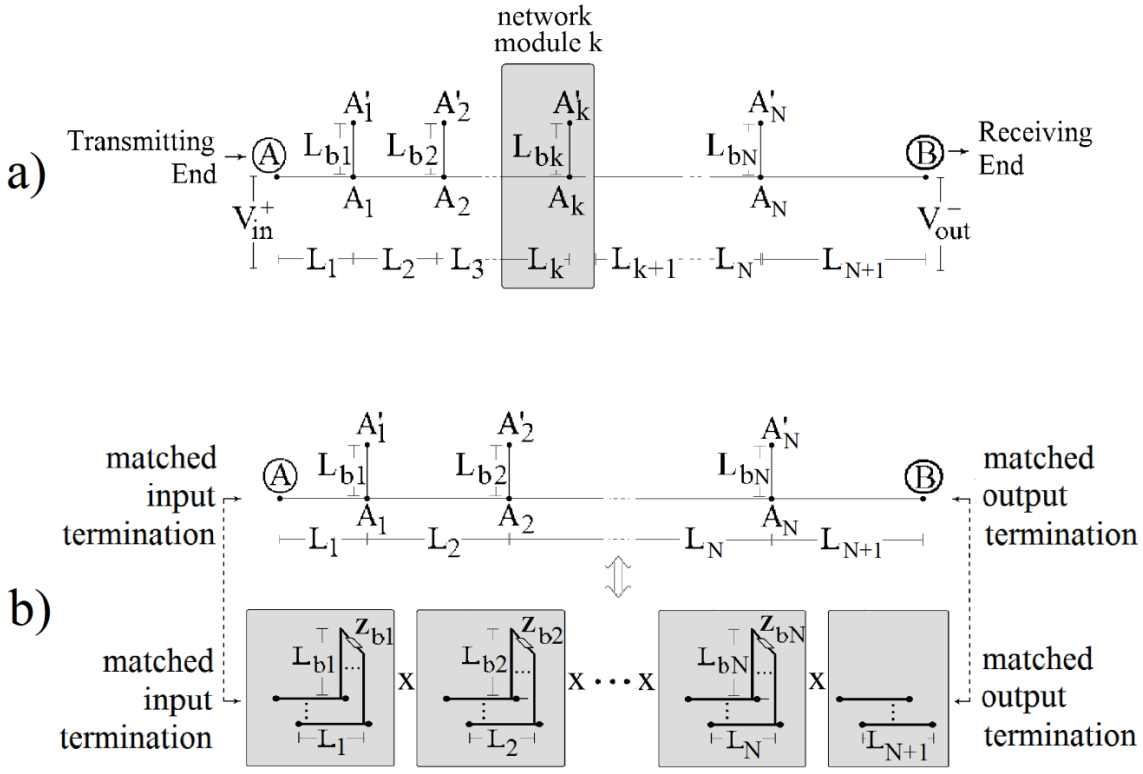

Figure 2. (a) End-to-end overhead HV/BPL connection with *N* branches. (b) An indicative HV/BPL topology considered as a cascade of *N*+1 modules corresponding to *N* branches [5]-[7], [16], [17], [19]-[23].

As it concerns the MIMO transmission scheme assumptions, in the common case, the transmitter does not have CSI –as it has already mentioned– whereas the channel is perfectly known to the receiver (i.e., channel knowledge at the receiver can be maintained via training and tracking). The flat-fading subchannel frequency spacing is assumed equal to $f_s = 10\,\text{kHz}$. The proposed MIMO/HV/BPL system analysis, which is outlined in Section III, is used in the rest of this paper.

As it has already been mentioned in Section IV, to evaluate the capacity of overhead MIMO/HV/BPL networks, a uniform AWGN PSD level is assumed equal to -105dBm/Hz [17], [19], [54], [72]. As it concerns the power consumption of overhead MIMO/HV/BPL systems, the related circuit and system parameters are detailed in [66], [111]-[114] providing a satisfactory approximation towards the actual HV/BPL system power consumption.

A. Effect of HV Grid Topology and MIMO Scheme Configuration on Overhead MIMO/HV/BPL Capacity Performance

The spectral performance in terms of capacity in the 3-88MHz frequency band is evaluated based on the application of FCC Part 15 under the assumption of Ofcom/IPSDM limits when different overhead HV/BPL network configurations occur. In this subsection, it is assumed that only the highest values (upper bound) of capacity of each MIMO/HV/BPL configuration of the same class for each of the aforementioned indicative overhead HV/BPL topologies are going to be presented.

In Figs. 3(a)-(d), the capacity of the overhead MIMO networks for the aforementioned indicative overhead topologies is plotted with respect to the active transmit and receive ports of different MIMO scheme configurations. Moreover, the relative capacity gain concerning each MIMO scheme configuration in relation with the corresponding SISO one for the aforementioned indicative overhead topologies is also demonstrated.

From Figs. 3(a)-(d), it is observed that:

- The high IPSDM limits of FCC Part 15, combined with the relatively low end-to-end channel attenuation and the low noise characteristics of overhead MIMO/HV/BPL networks, reveal their significant broadband potential. Regardless of the high average end-to-end transmission distances occurred in overhead HV grids, capacity and relative capacity gain maintain sufficient high values for all the future's SG applications.
- Observing capacity and relative capacity gain results, SIMO/HV/BPL networks present better results than the corresponding ones of MISO/HV/BPL networks regardless of the topology and the MIMO configuration scheme. This is due to the fact that, in the SIMO cases, all the transmitted power is concentrated at one transmit port and collected from multiple receive ports whereas, in the MISO cases without CSI, the transmitted power is equally allocated among the available transmit ports and collected from one receive port [121].
- Due to the common bus-bar system topology [7], [40], [122], in overhead BPL networks, end-to-end channel attenuation curves between CCs and XCs present similarities indicating the strong coupling among the individual MIMO channels. However, the XC channels present significantly higher end-to-end channel attenuation than CC ones regardless of the network topology [35], [37], [50].
- The increase of the available transmit ports in MISO systems entails higher influence of XC channels in the occurred capacity results and, consequently, lower capacity results in comparison with the upper bound of SISO systems.
- When the number of transmit n_T and receive n_R ports increases, the capacity differences among $n_T \times n_R$ and $n_R \times n_T$ MIMO networks tend to be mitigated.
- MIMO configuration schemes provide dramatic improvement in the capacity results rendering their installation preferable in comparison with the other available SISO, SIMO and MISO alternatives.

Due to their similar capacity behavior, only one overhead HV topology, say "LOS" case, will be examined hereafter.

B. Impact of EE Policies on SE and EE Metrics

Until now, MIMO/BPL research has mainly focused on determining the optimum number of transmit and receive ports, which succeeds the best compromise among system complexity, capacity and system availability [35], [123]-[125]. However, the recent growing communications concern is not only to maximize the spectral efficiency

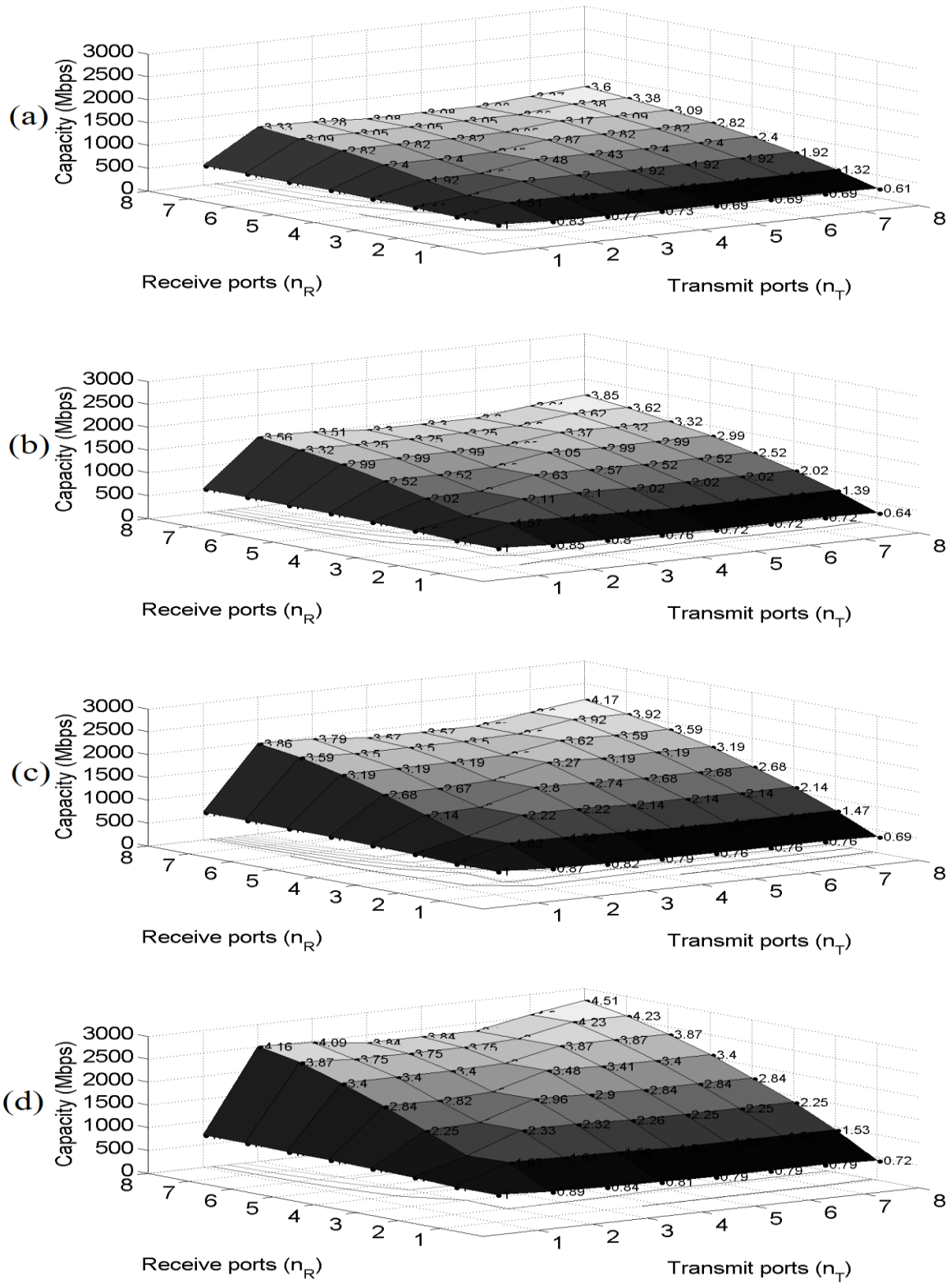

Figure 3. Capacity and relative capacity gain of overhead MIMO/HV/BPL networks for the four indicative topologies (IPSDM limits of the FCC Part 15 limits are applied and the subchannel frequency spacing is equal to 10kHz). (a) Urban case. (b) Suburban case. (c) Rural case. (d) "LOS" case.

of networks and systems but also to increase profitability through energy consumption savings while protecting the environment [42]. Towards that direction, different MIMO/HV/BPL networks arrangements are investigated in this paper when different EE policies are adopted. In the rest of this paper, it is assumed that only the maximum values of all possible SIMO, MISO and MIMO system capacities will be studied in the 3-88MHz frequency band.

As it has already been analyzed in Fig. 3(d), the capacity and relative capacity gain of overhead MIMO/HV/BPL "LOS" case have been plotted for various MIMO scheme configurations when FCC Part 15 is applied. These results define the optimum capacity case when no environmental concern is taken into account (EE1 policy).

Apart from EE1 policy, other five indicative EE policies given in Table 1 have been applied in order to examine how their application affect the SE and EE metrics of this paper (i.e., capacity, carbon energy footprint and EE capacity). Note that as the number x of EEx policy increases so does the environmental awareness. In Table 1, green factor Φ of each EE policy is also reported.

To examine the impact of EE policies on spectral performance of overhead MIMO/HV/BPL networks, in Figs. 4(a)-(g), the capacity and the relative capacity gain of overhead MIMO/HV/BPL networks for the "LOS" case are plotted with respect to the active transmit and receive ports of different MIMO scheme configurations when the six indicative EE policies of Table 1 are applied, respectively. The influence of EE policies on the EE performance of overhead MIMO/HV/BPL networks is examined in Figs. 5(a)-(g) where the corresponding carbon energy footprint is plotted for the above six indicative EE policies, respectively.

The interaction between SE and EE metrics can be examined through the use of suitable combined SE/EE metrics such as EE capacity. In Figs. 6(a)-(g), the corresponding EE capacity and relative EE capacity gain are given for the above six indicative EE policies, respectively. Note that as it regards the carbon emissions of overhead MIMO/HV/BPL scheme configurations, in Figs. 5(a)-(f) and 6(a)-(f), only anthracite electricity production is assumed.

From Figs. 4(a)-(f), 5(a)-(f) and 6(a)-(f), several interesting conclusions may be drawn as follows.

- Capacity and carbon energy footprint of overhead MIMO/HV/BPL networks are very sensitive to IPSDM limit changes as these are imposed by the applied EE policy [17], [19]. However, the strategic choice of the countries to achieve significant carbon emission reductions pushes towards the adoption of EE policies that can diminish the broadband perspectives of overhead MIMO/HV/BPL networks. On the other hand, EE policies that are not environmentally oriented lead to waste of energy since the capacity improvement becomes marginal above a capacity threshold. Therefore, ecologically aware EE policies should be promoted that can lead to energy savings and reduction of carbon emissions while their corresponding capacity results may be carefully adjusted so as to satisfy certain capacity requirements. In fact, it can be seen that by reducing the IPSDM limits by 5% –see EE2 in Table 1 and in Figs. 4(a) and 4(b)–, the capacity reduction of overhead MIMO/HV/BPL networks

Table 1. EE Policies Used

EE Policy (type)	EE1	EE2	EE3	EE4	EE5	EE6
Green factor Φ	0	0.05	0.10	0.20	0.50	1

is ranging from 14.05% to 21.45% while carbon emissions decrease and EE capacity increase are ranging from 44.85%-48.99% and 42.44%-64.59%, respectively. Similar results for the other EE policies reveal the importance of the selection of proper IPSDM limits, capacity threshold and carbon emissions reduction goal.

- Carbon emissions depend drastically on the IPSDM limits that are imposed by the applied EE policy as well as the applied MIMO configuration scheme.
- The traditional belief that MIMO networks are always more energy-efficient and, subsequently, more environmentally friendly in comparison with SISO, MISO and SIMO ones may be misleading when the carbon emissions of overhead MIMO/HV/BPL networks are considered [64], [66], [111], [112]. More specifically, depending on the MIMO configuration scheme, applied EE policy, and SE and EE thresholds imposed, various trade-offs among SE and EE metrics may occur, namely: (i) in approximately 85% of the cases examined, given the number of transmit n_T and receive n_R ports, overhead $n_T \times n_R$ MIMO/HV/BPL networks with $n_T = n_R$ present better EE capacity values in comparison with other equivalent pure and mixed configurations, i.e. $i \times j$ MIMO networks with $1 \le i \le n_T$, $1 \le j \le n_R$; and (ii) Similarly to capacity results, in all the cases examined, overhead $1 \times n_R$ SIMO/HV/BPL networks demonstrate a more environmentally friendly behavior rather than equivalent $n_R \times 1$ MISO/HV/BPL networks. However, in general, by adopting suitable EE policies, the superiority of MIMO systems in terms of EE metrics may be further enhanced [64], [66], [111], [112].
- On the basis of capacity and EE capacity, the exact knowledge of the trade-off relation among IPSDM limits, EE policies and MIMO scheme configurations is essential for the overhead MIMO/HV/BPL network design.

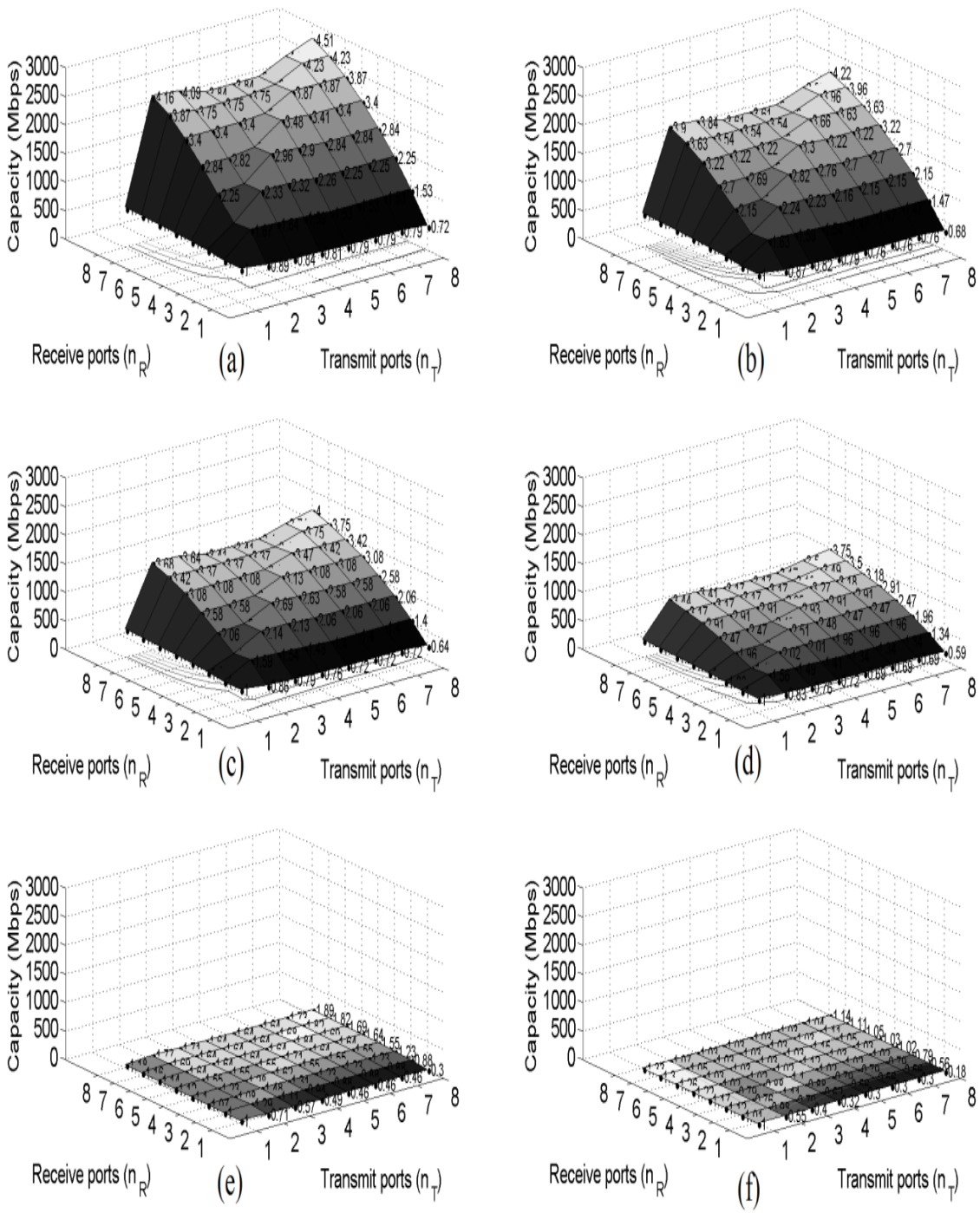

Figure 4. Capacity and relative capacity gain of overhead MIMO/HV/BPL "LOS" case networks for the EE policies of Table 1 (the subchannel frequency spacing is equal to 10kHz). (a) EE1. (b) EE2. (c) EE3. (d) EE4. (e) EE5. (f) EE6.

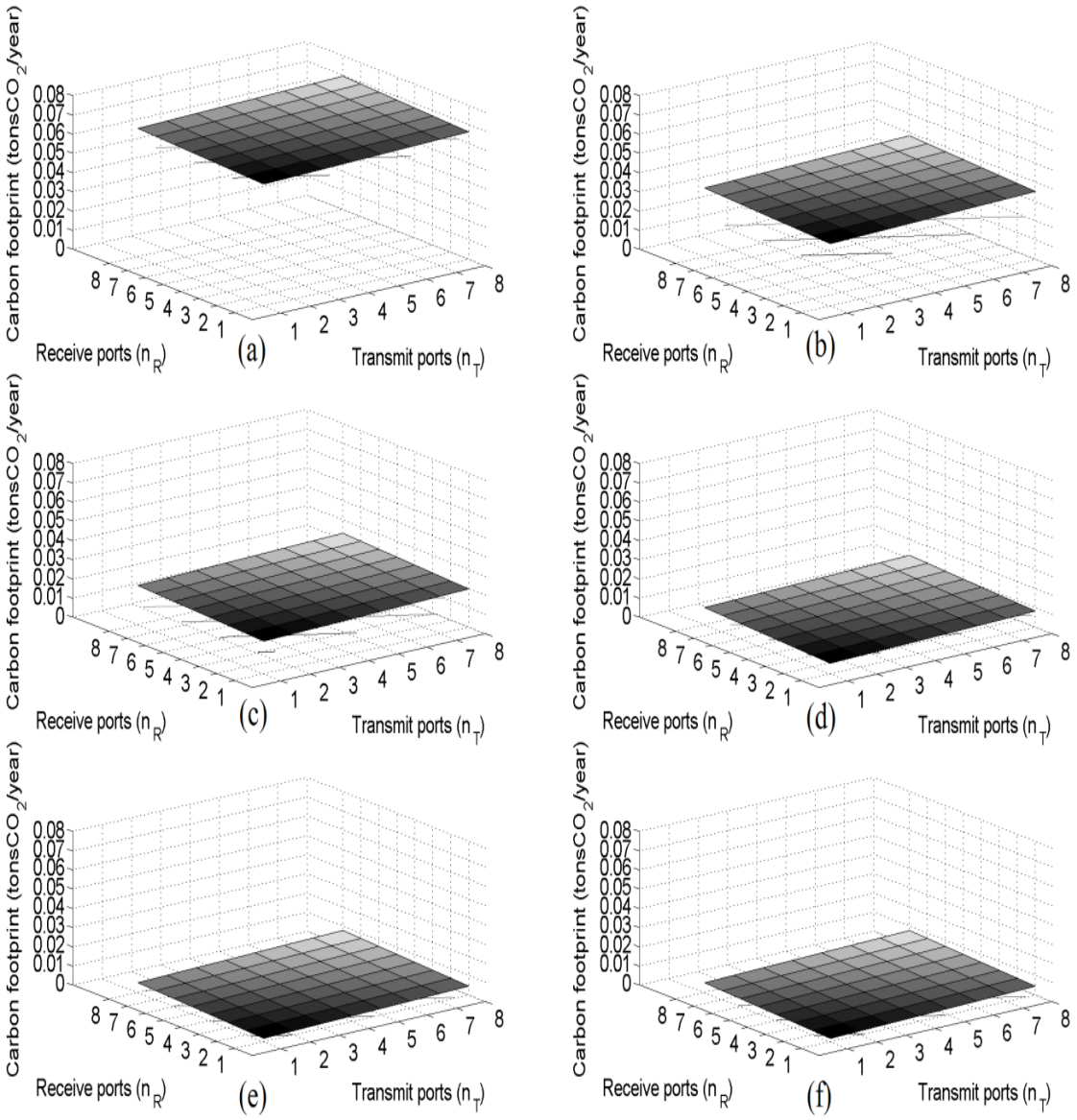

Figure 5. Carbon emissions of overhead MIMO/HV/BPL "LOS" case networks for the EE policies of Table 1 (the subchannel frequency spacing is equal to 10kHz). (a) EE1. (b) EE2. (c) EE3. (d) EE4. (e) EE5. (f) EE6.

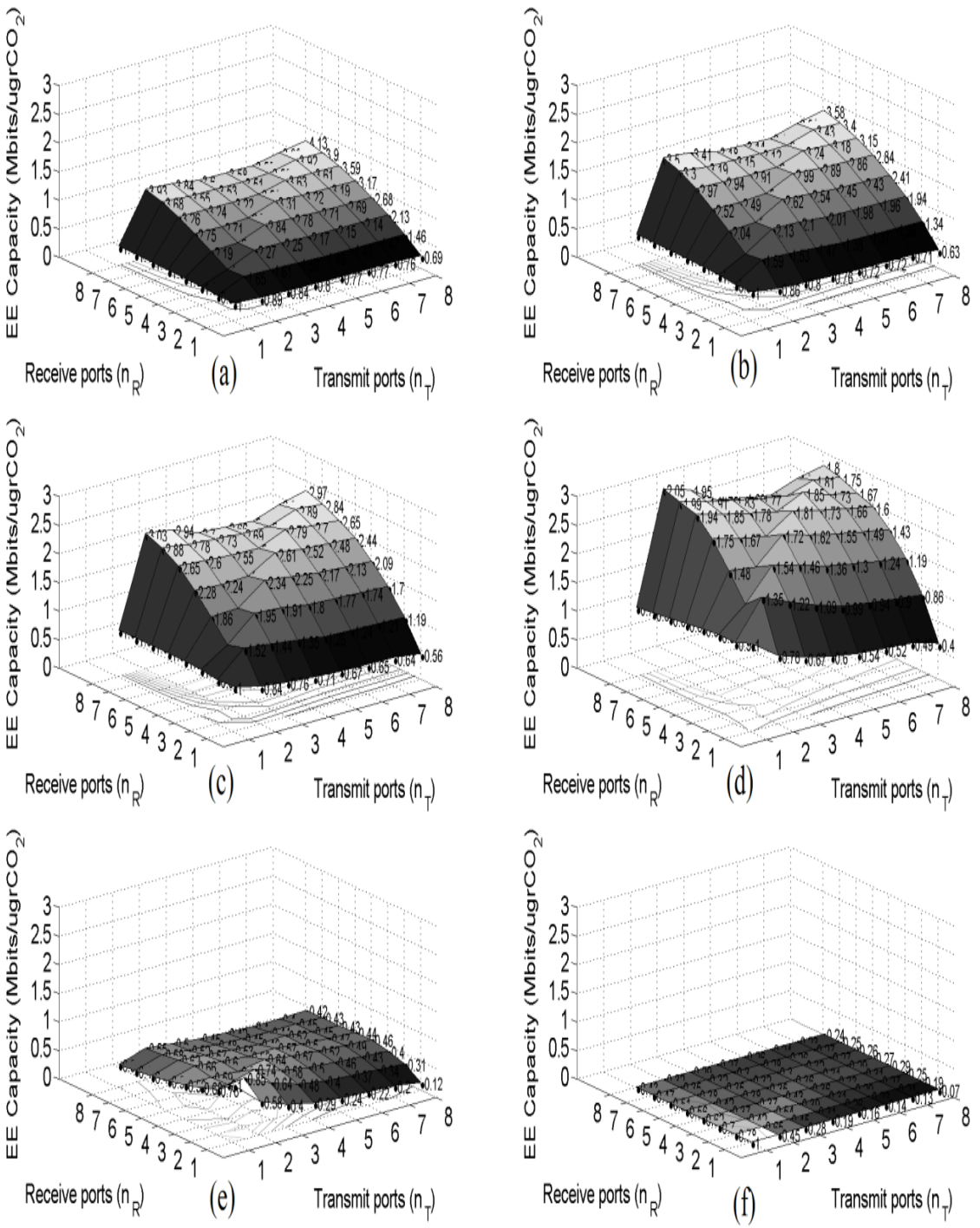

Figure 6. EE capacity and relative EE capacity gain of overhead MIMO/HV/BPL "LOS" case networks for the EE policies of Table 1 (the subchannel frequency spacing is equal to 10kHz). (a) EE1. (b) EE2. (c) EE3. (d) EE4. (e) EE5. (f) EE6.

- Carbon emissions savings in overhead MHMO/HV/BPL networks can be adjusted by appropriately regulating the capacity threshold requirements. Carbon emissions savings decrease as the capacity threshold increases. Therefore, at lower capacity thresholds, MIMO configuration schemes of lower cardinality can be used. As the capacity threshold increases, MIMO configuration schemes of higher cardinality are encouraged to be deployed [67].

C. Capacity and EE Capacity Trade-Off Curves

The aforementioned analysis has focused on the behavior of SE and EE metrics as well as their interaction through the lens of the carbon energy footprint. In fact, the relation between capacity and EE capacity in overhead MIMO/HV/BPL networks has been investigated for different MIMO configuration schemes and EE policies. Their interaction is important for designing greener overhead MIMO/HV/BPL networks since a better balance between spectral performance and environmental awareness can be achieved. In the rest of this paper, it is assumed that only the maximum values of pure scheme configurations (8×8 MIMO, 1×8 SIMO, 8×1 MISO, and SISO systems –either SISO/CCs or SISO/XCs–) of overhead MIMO/HV/BPL "LOS" case networks are going to be studied in the 3-88MHz frequency band.

Until now, the proposal of suitable IPSDM limits has derived from the compromise between BPL technology promotion and the protection of existing radioservices. Hence, during the proposal of today's IPSDM limits, environmental issues have not seriously been addressed. Nowadays, since the adoption of environmental initiatives becomes urgent, the proposed green factor $\Phi(f)$ aids towards that direction during the proposal of future's IPSDM limits in overhead MIMO/HV/BPL networks. Actually, EE1 –see Figs. 4(a) and 6(a)– and EE6 –see Figs. 4(f) and 6(f)– policies define two extreme state conditions of an interesting SE/EE trade-off.

To highlight this interesting SE/EE trade-off, in Fig. 7(a), the EE capacity of pure scheme configurations of the overhead MIMO/HV/BPL "LOS" case network is plotted versus the corresponding capacity for all continuous EE policies when anthracite electricity production is used. The SE/EE trade-off behavior of the above EE policies is compared against respective results of EE policies whose IPSDM limits range from -100 dBm/Hz to 0 dBm/Hz with step 0.1dBm/Hz (denoted as SISO/CC, SISO/XC, 1×8 SIMO, 8×1 MISO, and 8×8 MIMO curves). Similarly to Fig. 7(a), in Fig. 7(b), curves are drawn in the case of gas electricity production.

Combining Figs. 7(a) and 7(b) with the previous figures, several interesting conclusions may be given:

- The type of the electricity production, say either anthracite or gas electricity production of this paper, has strong effect on the carbon energy footprint.
- Similarly to the vintage trade-off between energy-efficient and SE metrics presented in the literature [7], [68], [126], the trade-off between EE capacity/capacity is also expected to be a quasiconcave function determining a dynamic equilibrium that depends on the EE policy, MIMO configuration scheme and the type of electricity production.

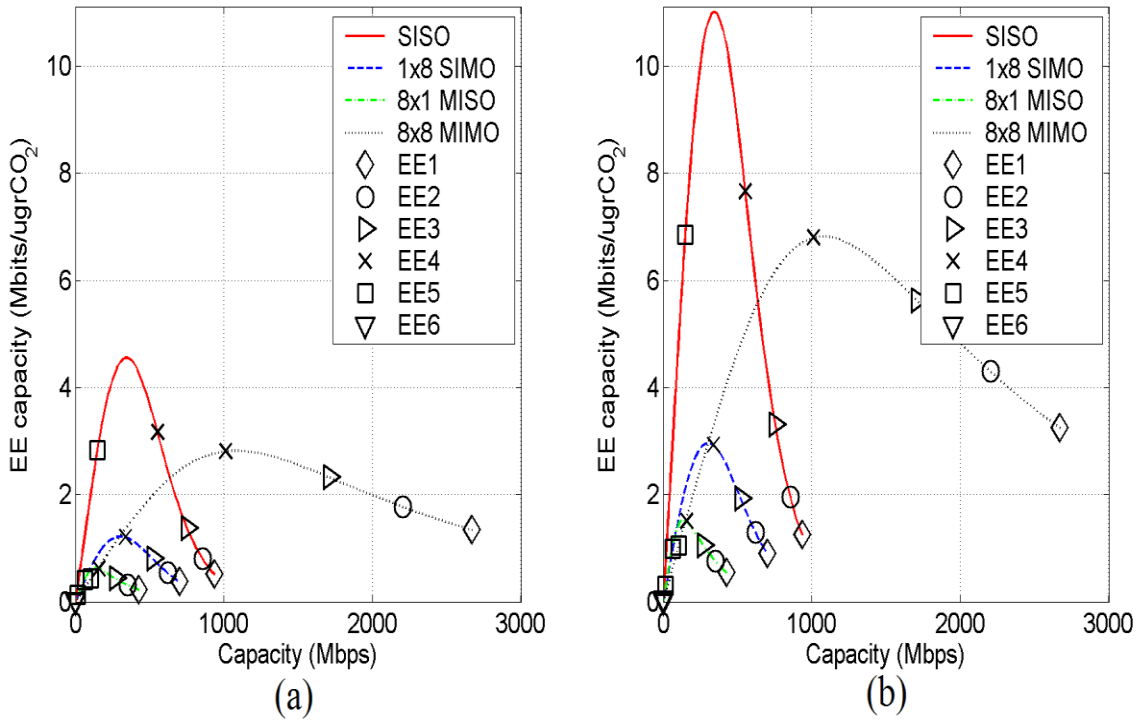

Figure 7. EE capacity and capacity trade-off curves of various single- and multi-port system implementations for the overhead HV/BPL "LOS" case when different EE policies are applied. (a) SISO, 1×8 SIMO, 8×1 MISO, and 8×8 MIMO trade-off curves when anthracite electricity production occurs. (b) SISO/CC, SISO/XC, 1×8 SIMO, 8×1 MISO and 8×8 MIMO trade-off curves when gas electricity production occurs.

- To achieve the best compromise among the different interests of SE- and EE-oriented lobbies, the best proposal is the operation of overhead MIMO/HV/BPL systems near the absolute maxima of trade-off curves presented in Figs. 7(a) and 7(b). Since operation points of today's overhead MIMO/HV/BPL systems are far from the best compromise –see EE1 points of Figs. 7(a) and 7(d)–, imminent IPSDM limits corrections through the proposed greener EE policies are required. In contrast, although very strict IPSDM limits –see EE5 and EE6 points of Figs. 7(a) and 7(d)– facilitate the EMC of BPL networks, the corresponding IPSDM limits push overhead MIMO/HV/BPL networks to operate with poor SE and EE performances. Therefore, observing all the cases examined, regardless of the MIMO configuration scheme and the electricity generation type, EE4 policy offers the best compromise results since its operation points are located at absolute maxima of trade-off curves.
- The countries' strategic frameworks towards cleaner energy sources further improve the SE/EE trade-off curves of overhead MIMO/HV/BPL networks. By interchanging from anthracite electricity production to gas one, EE capacity values get improved by a factor of 2.5 for given EE policy. Moreover, the choice of providers towards distributed energy sources, smart grid solutions and renewable sources tailored to the needs of their countries may, at the same time, skyrocket the EE performance of overhead MIMO/HV/BPL networks.

- The application of well-tuned EE policies combined with the use of adaptive green factor to regulate BPL operation in certain frequency segments according to carbon emission and capacity requirements may provide flexibility in authorities and providers so that the power consumption of overhead MIMO/HV/BPL networks gets reduced with slight deterioration of their capacity. The spectral selectivity is the main advantage of adaptive EE policies against continuous ones.
- Before overhead MIMO/HV/BPL systems interoperate with other broadband technologies –wired, such as fiber and DSL, and wireless, such as WiFi and WiMax–, the overhead HV/BPL systems need to intraoperate with other overhead and underground MV/BPL and LV/BPL that already are installed [5]-[7], [17], [19], [20], [22], [23]. Apart from compatible frequencies, equipment and signaling, BPL standardization and adequate IPSDM limits [26], scalable capacity must be assured taking into account the specific features of MIMO technology, overhead and underground HV/BPL, MV/BPL and LV/BPL transmission and EE issues. Emerging green technology considerations aid towards this direction by introducing suitable EE policies that both respect capacity requirements and ecological awareness.
- Sustainable development and growth is an important issue for countries that historically have been dependent on the exploitation of their natural resources (i.e., forestry, agriculture, mining and fishing) as their economic base [127]. Nowadays, through the prism of the green economy, countries can still commercialize their natural resources in order to financially stimulate their economies [128]. This modern resource harvest can be achieved through microgrids that are owned by the local communities. Microgrids include energy storage systems, distributed generation sources, like microturbines and fuel cell units, renewable energy sources, such as wind turbines and photovoltaic systems and controllable loads [9], [10]. Except for their environmental effect, the operation of microgrids can also significantly improve the SE/EE trade-off curves of overhead MIMO/HV/BPL networks at a local basis. Hence, the future research is going to focus on: (i) the development of new ad-hoc SE/EE trade-off curves of overhead MIMO/HV/BPL networks at a local and daily basis that can combine electricity supply/demand models with the energy source mix of the power grid and the microgrids [129], [130], [131]; and (ii) the stabilization of SE/EE trade-off curves when fluctuations of the energy production in the energy source mix occurs either in the power grid or in microgrids [11], [132]-[134].

VII. Conclusions

This paper has focused on the assessment of the broadband performance of overhead MIMO/HV/BPL networks when environmental policies are adopted. Using suitable SE and EE metrics, major features of today's BPL networks have been reviewed for use in future's greener overhead MIMO/HV/BPL networks. In the light of the information theory, the capacity values of all the considered overhead MIMO/HV/BPL networks revealed that these networks can operate both as a robust broadband platform for SG applications across the transmission power grid and as a green communications solution. In the meanwhile, exploiting the proposed SE/EE trade-offs that determine dynamic equilibrium between capacity and EE capacity of the different overhead MIMO/HV/BPL configurations, a wiser compromise among

transmission rates, EMI regulations and ecology awareness may occur; an important step towards the design and operation of faster, more electromagnetic compatible and greener overhead MIMO/HV/BPL networks in the oncoming SG network.

Conflicts of Interest

The author declares that there is no conflict of interests regarding the publication of this paper.

References

[1] A. G. Lazaropoulos, "Designing Broadband over Power Lines Networks Using the Techno-Economic Pedagogical (TEP) Method – Part I: Overhead High Voltage Networks and Their Capacity Characteristics," *Trends in Renewable Energy*, vol. 1, no. 1, pp. 16-42, Mar. 2015. DOI: 10.17737/tre.2015.1.1.002

[2] A. G. Lazaropoulos, "Designing Broadband over Power Lines Networks Using the Techno-Economic Pedagogical (TEP) Method – Part II: Overhead Low-Voltage and Medium-Voltage Channels and Their Modal Transmission Characteristics," *Trends in Renewable Energy*, vol. 1, no. 2, pp. 59-86, Jun. 2015. DOI: 10.17737/tre.2015.1.1.006

[3] T. A. Papadopoulos, G.K. Papagiannis, and D.P. Labridis, "A generalized model for the calculation of the impedances and admittances of overhead power lines above stratified earth," *Electric Power Systems Research*, vol. 80, no. 9, pp. 1160-1170. DOI: 10.1016/j.epsr.2010.03.009

[4] T. A. Papadopoulos, C. G. Kaloudas, and G. K. Papagiannis, "A multipath channel model for PLC systems based on nodal method and modal analysis," in *Proc. 2007 IEEE Int. Symp. Power Line Communications and Its Applications (ISPLC'07)*, Pisa, Italy, Mar. 2007, pp. 278–283. DOI: 10.1109/ISPLC.2007.371137

[5] A. G. Lazaropoulos, "Broadband Transmission Characteristics of Overhead High-Voltage Power Line Communication Channels," *Progress in Electromagnetics Research B*, vol. 36, pp. 373-398, 2012. DOI:10.2528/PIERB11091408

[6] A. G. Lazaropoulos, "Broadband Transmission and Statistical Performance Properties of Overhead High-Voltage Transmission Networks," *Hindawi Journal of Computer Networks and Commun.*, 2012, article ID 875632, 2012. DOI: 10.1155/2012/875632

[7] A. G. Lazaropoulos, "Green Overhead and Underground Multiple-Input Multiple-Output Medium Voltage Broadband over Power Lines Networks: Energy-Efficient Power Control," *Springer Journal of Global Optimization*, vol. 57, no. 3, pp. 997-1024, Oct. 2012. DOI: 10.1007/s10898-012-9988-y

[8] OPERA1, D44: Report presenting the architecture of plc system, the electricity network topologies, the operating modes and the equipment over which PLC access system will be installed, IST Integr. Project No 507667, Dec. 2005.

[9] P. S. Georgilakis and N. D. Hatziargyriou, "A Review of Power Distribution Planning in the Modern Power Systems Era: Models, Methods and Future

Research," *Electric Power Systems Research*, vol. 121, pp. 89-100, 2015. DOI: 10.1016/j.epsr.2014.12.010

[10] L. Gkatzikis, G. Iosifidis, I. Koutsopoulos, and L. Tassiulas, "Collaborative Placement and Sharing of Storage Resources in the Smart Grid," In *Proc. 2014 IEEE International Conference on Smart Grid Communications (SmartGridComm)*, pp. 103-108, Nov. 2014. DOI: 10.1109/SmartGridComm.2014.7007630

[11] D. I. Giokas and G. C. Pentzaropoulos, "Evaluating productive efficiency in telecommunications: Evidence from Greece," *Telecommunications Policy*, vol. 24, no. 8, pp. 781-794, 2000. DOI: 10.1016/S0308-5961(00)00053-7

[12] L. Wang, G. Avolio, G. Deconinck, E. Van Lil, and L. L. Lai, "Estimation of multi-conductor powerline cable parameters for the modelling of transfer characteristics," *IET Science, Measurement & Technology*, vol. 8, no. 1, pp. 39-45, Jan. 2014. DOI: 10.1049/iet-smt.2012.0123

[13] A. G. Lazaropoulos, "Deployment Concepts for Overhead High Voltage Broadband over Power Lines Connections with Two-Hop Repeater System: Capacity Countermeasures against Aggravated Topologies and High Noise Environments," *Progress in Electromagnetics Research B*, vol. 44, pp. 283-307, 2012. DOI: 10.2528/PIERB12081104, [Online]. Available: http://www.jpier.org/PIERB/pierb44/13.12081104.pdf

[14] A. G. Lazaropoulos, "Overhead and Underground MIMO Low Voltage Broadband over Power Lines Networks and EMI Regulations: Towards Greener Capacity Performances," *Elsevier Computers and Electrical Engineering*, vol. 39, pp. 2214-2230, 2013. DOI: 10.1016/j.compeleceng.2013.02.003

[15] A. G. Lazaropoulos, "Wireless Sensor Network Design for Transmission Line Monitoring, Metering and Controlling Introducing Broadband over PowerLines-enhanced Network Model (BPLeNM)," *ISRN Power Engineering*, vol. 2014, Article ID 894628, 22 pages, 2014. DOI:10.1155/2014/894628. [Online]. Available: http://www.hindawi.com/journals/isrn.power.engineering/2014/894628/

[16] A. G. Lazaropoulos and P. G. Cottis, "Transmission characteristics of overhead medium voltage power line communication channels," *IEEE Trans. Power Del.*, vol. 24, no. 3, pp. 1164-1173, Jul. 2009. DOI: 10.1109/TPWRD.2008.2008467

[17] A. G. Lazaropoulos and P. G. Cottis, "Capacity of overhead medium voltage power line communication channels," *IEEE Trans. Power Del.*, vol. 25, no. 2, pp. 723-733, Apr. 2010. DOI: 10.1109/TPWRD.2009.2034907

[18] A. G. Lazaropoulos and P. G. Cottis, "Broadband transmission via underground medium-voltage power lines-Part I: transmission characteristics," *IEEE Trans. Power Del.*, vol. 25, no. 4, pp. 2414-2424, Oct. 2010. DOI: 10.1109/TPWRD.2010.2048929

[19] A. G. Lazaropoulos and P. G. Cottis, "Broadband transmission via underground medium-voltage power lines-Part II: capacity," *IEEE Trans. Power Del.*, vol. 25, no. 4, pp. 2425-2434, Oct. 2010. DOI: 10.1109/TPWRD.2010.2052113

[20] A. G. Lazaropoulos, "Towards Broadband over Power Lines Systems Integration: Transmission Characteristics of Underground Low-Voltage Distribution Power Lines," *Progress in Electromagnetics Research B*, 39, pp. 89-114, 2012. DOI: 10.2528/PIERB12012409

[21] L. Stadelmeier, D. Schneider, D. Schill, A. Schwager, and J. Speidel, "MIMO for Inhome Power Line Communications," presented at the *Int. Conf. on Source and Channel Coding*, Ulm, Germany, Jan. 2008.

[22] A. G. Lazaropoulos, "Towards Modal Integration of Overhead and Underground Low-Voltage and Medium-Voltage Power Line Communication Channels in the Smart Grid Landscape: Model Expansion, Broadband Signal Transmission Characteristics, and Statistical Performance Metrics (Invited Paper)," *ISRN Signal Processing*, vol. 2012, Article ID 121628, pp. 1-17, 2012. DOI: 10.5402/2012/121628 [Online]. Available: http://www.hindawi.com/isrn/sp/2012/121628/

[23] A. G. Lazaropoulos, "Review and Progress towards the Common Broadband Management of High-Voltage Transmission Grids: Model Expansion and Comparative Modal Analysis," *ISRN Electronics*, vol. 2012, Article ID 935286, pp. 1-18, 2012. DOI: 10.5402/2012/935286 [Online]. Available: http://www.hindawi.com/isrn/electronics/2012/935286/

[24] S. Galli, A. Scaglione, and K. Dostert, "Broadband is power: internet access through the power line network (Guest Editorial)," *IEEE Commun. Mag.*, vol. 41, no. 5, pp. 82–83, May 2003. DOI: 10.1109/MCOM.2003.1200105

[25] M. Götz, M. Rapp, and K. Dostert, "Power line channel characteristics and their effect on communication system design," *IEEE Commun. Mag.*, vol. 42, no. 4, pp. 78-86, Apr. 2004. DOI: 10.1109/MCOM.2004.1284933

[26] S. Galli and O. Logvinov, "Recent developments in the standardization of power line communications within the IEEE," *IEEE Commun. Mag.*, vol. 46, no. 7, pp. 64-71, Jul. 2008. DOI: 10.1109/MCOM.2008.4557044

[27] A. G. Lazaropoulos, "Wireless Sensors and Broadband over PowerLines Networks: The Performance of Broadband over PowerLines-enhanced Network Model (BPLeNM) (Invited Paper)," *ICAS Publishing Group Transaction on IoT and Cloud Computing*, vol. 2, no. 3, pp. 1-35, 2014. [Online]. Available: http://icas-pub.org/ojs/index.php/ticc/article/view/27/17

[28] T. A. Papadopoulos, B. D. Batalas, A. Radis, and G. K. Papagiannis, "Medium voltage network PLC modeling and signal propagation analysis," in *Proc. 2007 IEEE Int. Symp. Power Line Communications and its Applications (ISPLC'07)*, Pisa, Italy, Mar. 2007, pp. 284–289. DOI: 10.1109/ISPLC.2007.371138

[29] A. I. Chrysochos, T. A. Papadopoulos, and G. K. Papagiannis, "Enhancing the frequency-domain calculation of transients in multiconductor power transmission lines," *Electric Power Systems Research*, vol. 122, pp. 56-64, 2015. DOI: 10.1016/j.epsr.2014.12.024

[30] T. A. Papadopoulos, A. I. Chrysochos, A. I. Nousdilis, and G. K. Papagiannis, "Simplified measurement-based black-box modeling of distribution transformers using transfer functions," *Electric Power Systems Research*, vol. 121, pp. 77-88, 2015. DOI: 10.1016/j.epsr.2014.12.003

[31] F. Versolatto and A. M. Tonello, "An MTL theory approach for the simulation of MIMO power-line communication channels," *IEEE Trans. Power Del.*, vol. 26, no. 3, pp. 1710-1717, Jul. 2011. DOI: 10.1109/TPWRD.2011.2126608

[32] D. Schneider, J. Speidel, L. Stadelmeier, and D. Schill, "Precoded spatial multiplexing MIMO for inhome power line communications," in *Proc. IEEE Global Telecommunications Conference*, New Orleans, LA, USA, Nov./Dec. 2008, pp. 1–5. DOI: 10.1109/GLOCOM.2008.ECP.556

[33] V. Oksman and S. Galli, "G.hn: The new ITU-T home networking standard," *IEEE Commun. Mag.*, vol. 47, no. 10, pp. 138–145, Oct. 2009. DOI: 10.1109/MCOM.2009.5273821

[34] M. Tlich, A. Zeddam, F. Moulin, and F. Gauthier, "Indoor power-line communications channel characterization up to 100 MHz–Part I: one parameter deterministic model," *IEEE Trans. Power Del.*, vol. 23, no. 3, pp. 1392–1401, July 2008. DOI: 10.1109/TPWRD.2008.919397

[35] R. Hashmat, P. Pagani, A. Zeddam, and T. Chonavel, "MIMO communications for inhome PLC networks: Measurements and results up to 100MHz," in *Proc. IEEE Int. Symp. Power Line Communications and Its Applications*, Rio de Janeiro, Brazil, Mar. 2010, pp. 120–124. DOI: 10.1109/ISPLC.2010.5479897

[36] A. Canova, N. Benvenuto, and P. Bisaglia, "Receivers for MIMO-PLC channels: Throughput comparison," in *Proc. IEEE Int. Symp. Power Line Communications and Its Applications*, Rio de Janeiro, Brazil, Mar. 2010, pp. 114–119. DOI: 10.1109/ISPLC.2010.5479904

[37] D. Schneider, A. Schwager, J. Speidel and A. Dilly, "Implementation and Results of a MIMO PLC Feasibility Study," in *Proc. IEEE Int. Symp. Power Line Communications and Its Applications*, Udine, Italy, Apr. 2011, pp. 54–59. DOI: 10.1109/ISPLC.2011.5764450

[38] M. Biagi, "MIMO self-interference mitigation effects on PLC relay networks," in *Proc. IEEE Int. Symp. Power Line Communications and Its Applications*, Udine, Italy, Apr. 2011, pp. 182–186. DOI: 10.1109/ISPLC.2011.5764387

[39] M. Biagi, "MIMO self-interference mitigation effects on power line relay networks," *IEEE Commun. Lett.*, vol. 15, no. 8, pp. 866–868, Aug. 2011. DOI: 10.1109/LCOMM.2011.062911.110230

[40] A. Schwager, D. Schneider, W. Bäschlin, A. Dilly, and J. Speidel, "MIMO PLC: Theory, Measurements and System Setup," in *Proc. IEEE Int. Symp. Power Line Communications and Its Applications*, Udine, Italy, Apr. 2011, pp. 48–53. DOI: 10.1109/ISPLC.2011.5764447

[41] F. Versolatto and A. M. Tonello, "A MIMO PLC random channel generator and capacity analysis," in *Proc. IEEE Int. Symp. Power Line Communications and Its Applications*, Udine, Italy, pp. 66–71, Apr. 2011. DOI: 10.1109/ISPLC.2011.5764452

[42] Z. Hasan, H. Boostanimehr, and V. K. Bhargava, "Green cellular networks: A survey, some research issues and challenges," *IEEE Commun. Surveys Tuts.*, vol. 13, no. 4, pp. 524–540, Oct. 2011. DOI: 10.1109/SURV.2011.092311.00031

[43] 3GPP, "Telecommunication management; Study on Energy Savings Management (ESM), (Release 10)," Tech. Rep. TR 32.826, Mar 2010. Available: http://www.3gpp.org/ftp/Specs/html-info/32826.htm

[44] ITU-T Focus Group on Future Networks (FG FN), FG-FN OD-66, Draft Deliverable on "Overview of Energy Saving of Networks", Oct. 2010.

[45] C. Yan, Z. Shunqing, X. Shugong, and G. Y. Li, "Fundamental trade-offs on green wireless networks," *IEEE Commun. Mag.*, vol. 49, no. 6, pp. 30–37, Jun. 2011. DOI: 10.1109/MCOM.2011.5783982

[46] J. Abouei, K. N. Plataniotis, and S. Pasupathy, "Green modulations in energy-constrained wireless sensor networks," *IET Commun.*, vol. 5, no. 2, pp. 240–251, Jan. 2011. DOI: 10.1049/iet-com.2010.0472

[47] S. Ruth, "Green IT More Than a Three Percent Solution?," *IEEE Internet Computing*, vol. 13, no. 4, pp. 74–78, Jul.-Aug. 2009. DOI: 10.1109/MIC.2009.82

[48] Y. G. Li, J. H. Winters, N. R. Sollenberger, "MIMO-OFDM for wireless communications: signal detection with enhanced channel estimation," *IEEE Trans. Commun.*, vol. 50, no. 9, pp. 1471–1477, Sep. 2002. DOI: 10.1109/TCOMM.2002.802566

[49] A. Amanna, A. He, T. Tsou, X. Chen, D. Datla, T. R. Newman, J. H. Reed, and T. Bose, "Green Communications: A New Paradigm for Creating Cost Effective Wireless Systems," Tech. Rep., 2009, [Online]. Available: http://filebox.vt.edu/users/aamanna/web%20page/Green%20Communications-draft%20journal%20paper.pdf

[50] Y. Z. Ying and K. B. Letaief, "An efficient resource-allocation scheme for spatial multiuser access in MIMO/OFDM systems," *IEEE Trans. Commun.*, vol. 53, no. 1, pp. 107–116, Jan. 2005. DOI: 10.1109/TCOMM.2004.840666

[51] S. K. Jayaweera, "Virtual MIMO-based cooperative communication for energy-constrained wireless sensor networks," *IEEE Trans. Wireless Commun.*, vol. 5, no. 5, pp. 984–989, May 2006. DOI: 10.1109/TWC.2006.1633350

[52] R. Eickhoff, R. Kraemer, I. Santamaria, and L. Gonzalez, "Developing energy-efficient MIMO radios," *IEEE Veh. Tech. Mag.*, vol. 4, no. 1, pp. 34–41, Mar. 2009. DOI: 10.1109/MVT.2009.931994

[53] T. Sartenaer, "Multiuser communications over frequency selective wired channels and applications to the powerline access network" Ph.D. dissertation, Univ. Catholique Louvain, Louvain-la-Neuve, Belgium, Sep. 2004.

[54] P. Amirshahi and M. Kavehrad, "High-frequency characteristics of overhead multiconductor power lines for broadband communications," *IEEE J. Sel. Areas Commun.*, vol. 24, no. 7, pp. 1292-1303, Jul. 2006. DOI: 10.1109/JSAC.2006.874399

[55] T. Calliacoudas and F. Issa, ""Multiconductor transmission lines and cables solver," An efficient simulation tool for plc channel networks development," presented at the *IEEE Int. Conf. Power Line Communications and Its Applications*, Athens, Greece, Mar. 2002.

[56] S. Galli and T. Banwell, "A deterministic frequency-domain model for the indoor power line transfer function," *IEEE J. Sel. Areas Commun.*, vol. 24, no. 7, pp. 1304-1316, Jul. 2006. DOI: 10.1109/JSAC.2006.874428

[57] S. Galli and T. Banwell, "A novel approach to accurate modeling of the indoor power line channel-Part II: Transfer function and channel properties," *IEEE Trans. Power Del.*, vol. 20, no. 3, pp. 1869-1878, Jul. 2005. DOI: 10.1109/TPWRD.2005.848732

[58] T. Sartenaer and P. Delogne, "Deterministic modelling of the (Shielded) outdoor powerline channel based on the multiconductor transmission line equations," *IEEE J. Sel. Areas Commun.*, vol. 24, no. 7, pp. 1277-1291, Jul. 2006. DOI: 10.1109/JSAC.2006.874423

[59] T. Sartenaer and P. Delogne, "Powerline cables modelling for broadband communications," in Proc. *IEEE Int. Conf. Power Line Communications and Its Applications*, Malmö, Sweden, Apr. 2001, pp. 331-337.

[60] C. R. Paul, *Analysis of Multiconductor Transmission Lines*. New York: Wiley, 1994.

[61] J. A. B. Faria, *Multiconductor Transmission-Line Structures: Modal Analysis Techniques*. New York: Wiley, 1994.

[62] A. Pérez, A. M. Sánchez, J. R. Regué, M. Ribó, R. Aquilué, P. Rodréguez-Cepeda, and F. J. Pajares, "Circuital and modal characterization of the power-line network in the PLC band," *IEEE Trans. Power Del.*, vol. 24, no. 3, pp. 1182-1189, Jul. 2009. DOI: 10.1109/TPWRD.2009.2014278

[63] H. Meng, S. Chen, Y. L. Guan, C. L. Law, P. L. So, E. Gunawan, and T. T. Lie, "Modeling of transfer characteristics for the broadband power line communication channel," *IEEE Trans. Power Del.*, vol. 19, no. 3, pp. 1057-1064, Jul. 2004. DOI: 10.1109/TPWRD.2004.824430

[64] A. Goldsmith, S. A. Jafar, N. Jindal, and S.Vishwanath, "Capacity limits of MIMO channels," *IEEE J. Sel. Areas. Commun.*, vol. 21, no. 5, pp. 684–702, Jun. 2003. DOI: 10.1109/JSAC.2003.810294

[65] K. Hooghe and M. Guenach, "Toward green copper broadband access networks," *IEEE Commun. Mag.*, vol. 49, no. 8, pp. 87–93, Aug. 2011. DOI: 10.1109/MCOM.2011.5978420

[66] S. Cui, A. J. Goldsmith, and A. Bahai, "Energy-Efficiency of MIMO and Cooperative MIMO Techniques in Sensor Networks," *IEEE J. Sel. Areas Commun.*, vol. 22, no. 6, pp. 1089–1098, Aug. 2004. DOI: 10.1109/JSAC.2004.830916

[67] A. He, S. Srikanteswara, K. K. Bae, T. R. Newman, J. H. Reed, W. H. Tranter, M. Sajadieh, and M. Verhelst, "Power consumption minimization for MIMO systems – A cognitive radio approach," *IEEE J. Sel. Areas Commun.*, vol. 29, no. 2, pp. 469–479, Feb. 2011. DOI: 10.1109/JSAC.2011.110218

[68] C. Isheden and G. P. Fettweis, "Energy-efficient multi-carrier link adaptation with sum rate-dependent circuit power," in *Proc. IEEE Global Telecommunications Conference*, Miami, FL, USA, Dec. 2010, pp. 1-6. DOI: 10.1109/GLOCOM.2010.5683700

[69] DLC+VIT4IP, D1.2: Overall system architecture design DLC system architecture. FP7 Integrated Project No 247750, Jun. 2010.

[70] K. Dostert, *Powerline Communications*. Upper Saddle River, NJ: Prentice-Hall, 2001.

[71] M. Gebhardt, F. Weinmann, and K. Dostert, "Physical and regulatory constraints for communication over the power supply grid," *IEEE Commun. Mag.*, vol. 41, no. 5, pp. 84-90, May 2003. DOI: 10.1109/MCOM.2003.1200106

[72] P. Amirshahi, "Broadband access and home networking through powerline networks" Ph.D. dissertation, Pennsylvania State Univ., University Park, PA, May 2006. [Online]. Available: http://etda.libraries.psu.edu/theses/approved/WorldWideIndex/ETD-1205/index.html

[73] U. A. Bakshi and M. V. Bakshi, *Generation, Transmission and Distribution*. Pune, India: Technical Publications Pune, 2001.

[74] J. C. de Sosa, *Analysis and Design of High-Voltage Transmission Lines*. Bloomington, IN, USA: iUniverse Incorporated, 2010.

[75] J. Kuffel, E. Kuffel, and W. S. Zaengl, *High-Voltage Engineering Fundamentals*. Woburn, MA, UK: Butterworth-Heinemann, 2001.

[76] N. Suljanović, A. Mujčić, M. Zajc, and J. F. Tasič, "Approximate computation of high-frequency characteristics for power line with horizontal disposition and

middle-phase to ground coupling," *Elsevier Electr. Power Syst. Res.*, vol. 69, pp. 17-24, Jan. 2004. DOI: 10.1016/j.epsr.2003.07.005

[77] N. Suljanović, A. Mujčić, M. Zajc, and J. F. Tasič, "High-frequency characteristics of high-voltage power line," in *Proc. IEEE Int. Conf. on Computer as a Tool*, Ljubljana, Slovenia, Sep. 2003, pp. 310-314. DOI: 10.1109/EURCON.2003.1248206

[78] N. Suljanović, A. Mujčić, M. Zajc, and J. F. Tasič, "Power-line high-frequency characteristics: analytical formulation," in *Proc. Joint 1st Workshop on Mobile Future & Symposium on Trends in Communications*, Bratislava, Slovakia, Oct. 2003, pp. 106-109. DOI: 10.1109/TIC.2003.1249100

[79] W. Villiers, J. H. Cloete, and R. Herman, "The feasibility of ampacity control on HV transmission lines using the PLC system," in *Proc. IEEE Conf. Africon*, George, South Africa, Oct. 2002, vol. 2, pp. 865-870. DOI: 10.1109/AFRCON.2002.1160027

[80] M. Zajc, N. Suljanović, A. Mujčić, and J. F. Tasič, "Frequency characteristics measurement of overhead high-voltage power-line in low radio-frequency range," *IEEE Trans. Power Del.*, vol. 22, no. 4, pp. 2142-2149, Oct. 2007. DOI: 10.1109/TPWRD.2007.905369

[81] M. D'Amore and M. S. Sarto, "A new formulation of lossy ground return parameters for transient analysis of multiconductor dissipative lines," *IEEE Trans. Power Del.*, vol. 12, no. 1, pp. 303-314, Jan. 1997. DOI: 10.1109/61.568254

[82] P. Amirshahi and M. Kavehrad, "Medium voltage overhead power-line broadband communications; Transmission capacity and electromagnetic interference," in *Proc. IEEE Int. Symp. Power Line Commun. Appl.*, Vancouver, BC, Canada, Apr. 2005, pp. 2-6. DOI: 10.1109/ISPLC.2005.1430454

[83] M. D'Amore and M. S. Sarto, "Simulation models of a dissipative transmission line above a lossy ground for a wide-frequency range. I: Single conductor configuration," *IEEE Trans. Electromagn. Compat.*, vol. 38, no. 2, pp. 127-138, May 1996. DOI: 10.1109/15.494615

[84] M. D'Amore and M. S. Sarto, "Simulation models of a dissipative transmission line above a lossy ground for a wide-frequency range. II: Multi-conductor configuration," *IEEE Trans. Electromagn. Compat.*, vol. 38, no. 2, pp. 139-149, May 1996. DOI: 10.1109/15.494616

[85] J. Anatory and N. Theethayi, "On the efficacy of using ground return in the broadband power-line communications-A transmission-line analysis," *IEEE Trans. Power Del.*, vol. 23, no. 1, pp. 132-139, Jan. 2008. DOI: 10.1109/TPWRD.2007.910987

[86] J. R. Carson, "Wave propagation in overhead wires with ground return," *Bell Syst. Tech. J.*, vol. 5, pp. 539-554, 1926. DOI: 10.1002/j.1538-7305.1926.tb00122.x

[87] H. Kikuchi, "Wave propagation along an infinite wire above ground at high frequencies," *Proc. Electrotech. J.*, vol. 2, pp. 73-78, Dec. 1956.

[88] H. Kikuchi, "On the transition form a ground return circuit to a surface waveguide," *Proc. Int. Congr. Ultrahigh Frequency Circuits Antennas*, Paris, France, Oct. 1957, pp. 39-45.

[89] R. Pighi and R. Raheli, "On Multicarrier Signal Transmission for High-Voltage Power Lines," in *Proc. IEEE Int. Symp. Power Line Commun. Appl.*, Vancouver, BC, Canada, Apr. 2005, pp. 32-36. DOI: 10.1109/ISPLC.2005.1430460

[90] N. Suljanović, A. Mujčić, M. Zajc, and J. F. Tasič, "Integrated communication model of the HV power-line channel," in *Proc. IEEE Int. Symp. Power Line Communications and Its Applications*, Zaragoza, Spain, Mar/Apr. 2004, pp. 79-84.

[91] F. Issa, D. Chaffanjon, E. P. de la Bâthie, and A. Pacaud, "An efficient tool for modal analysis transmission lines for PLC networks development," presented at the *IEEE Int. Conf. Power Line Communications and Its Applications*, Athens, Greece, Mar. 2002.

[92] W. Villiers, J. H. Cloete, L. M. Wedepohl, and A. Burger, "Real-time sag monitoring system for high-voltage overhead transmission lines based on power-line carrier signal behavior," *IEEE Trans. Power Del.*, vol. 23, no. 1, pp. 389-395, Jan. 2008. DOI: 10.1109/TPWRD.2007.905550

[93] S. G. Lodwig and C. C. Schuetz, "Coupling to control cables in HV substations," in *Proc. IEEE Int. Symp. ElectroMagentic Compatibility*, Montreal, Canada, Mar. 2001, pp. 249-253. DOI: 10.1109/ISEMC.2001.950621

[94] D. Anastasiadou and T. Antonakopoulos, "Multipath characterization of indoor power-line networks," *IEEE Trans. Power Del.*, vol. 20, no. 1, pp. 90-99, Jan. 2005. DOI: 10.1109/TPWRD.2004.832373

[95] S. Barmada, A. Musolino, and M. Raugi, "Innovative model for time-varying power line communication channel response evaluation," *IEEE J. Sel. Areas Commun.*, vol. 24, no. 7, pp. 1317-1326, Jul. 2006. DOI: 10.1109/JSAC.2006.874426

[96] R. S. Prabhu and B. Daneshrad, "Energy-efficient power loading for a MIMO-SVD system and its performance in flat fading," in *Proc. IEEE Global Telecommunications Conference*, Miami, FL, USA, Dec. 2010, pp. 1–5. DOI: 10.1109/GLOCOM.2010.5683485

[97] A. G. Kanatas, D. Vouyioukas, G. Zheng, and L. Clavier, "Beamforming Techniques for Wireless MIMO Relay Networks," *International Journal of Antennas and Propagation*, vol. 2014, Article ID 354714, 2 pages, 2014. DOI: 10.1155/2014/354714

[98] E. Biglieri, J. Proakis, and S. Shamai (Shitz), "Fading channels: Information theoretic and communications aspects," *IEEE Trans. Inform. Theory*, vol. 44, pp. 2619–2692, Oct. 1998. DOI: 10.1109/18.720551

[99] L. M. Kuhn, S. Berger, I. Hammerström, and A. Wittneben, "Power line enhanced cooperative wireless communications," *IEEE J. Sel. Areas Commun.*, vol. 24, no. 7, pp. 1401-1410, Jul. 2006. DOI: 10.1109/JSAC.2006.874407

[100] NATO, "HF Interference, Procedures and Tools (Interférences HF, procédures et outils) Final Report of NATO RTO Information Systems Technology," RTO-TR-ISTR-050, Jun. 2007, [Online]. Available: http://ftp.rta.nato.int/public/PubFullText/RTO/TR/RTO-TR-IST-050/$$TR-IST-050-ALL.pdf

[101] Ofcom, "Amperion PLT Measurements in Crieff," Ofcom, Tech. Rep., Sept. 2005, [Online]. Available: http://www.ofcom.org.uk/research/technology/research/archive/cet/powerline/

[102] NTIA, "Potential interference from broadband over power line (BPL) systems to federal government radio communications at 1.7-80 MHz Phase 1 Study Vol. 1," NTIA Rep. 04-413, Apr. 2004, [Online]. Available: http://www.ntia.doc.gov/ntiahome/fccfilings/2004/bpl/

[103] Ofcom, "DS2 PLT Measurements in Crieff," Ofcom, Tech. Rep. 793 (Part 2), May 2005, [Online]. Available: http://www.ofcom.org.uk/research/technology/research/archive/cet/powerline/ds2.pdf

[104] Ofcom, "Ascom PLT Measurements in Winchester," Ofcom, Tech. Rep. 793 (Part 1), May 2005.

[105] J. Song, C. Pan, Q. Wu, Z. Yang, H. Liu, B. Zhao, and X. Li, "Field Trial of Digital Video Transmission over Medium-Voltage Powerline with Time-Domain Synchronous Orthogonal Frequency Division Multiplexing Technology," in *Proc. 2007 IEEE Int. Symp. on Power Line Communications and its Applications*, ISPLC'07, pp. 559-564, Pisa, Italy, Mar. 2007. DOI: 10.1109/ISPLC.2007.371077

[106] S. Liu and L. J. Greenstein, "Emission characteristics and interference constraint of overhead medium-voltage broadband power line (BPL) systems," in *Proc. IEEE Global Telecommunications Conf.*, New Orleans, LA, USA, Nov./Dec. 2008, pp. 1-5. DOI: 10.1109/GLOCOM.2008.ECP.560

[107] R. Aquilué, I. Gutierrez, J. L. Pijoan, and G. Sánchez, "High-voltage multicarrier spread-spectrum system field test," *IEEE Trans. Power Del.*, vol. 24, no. 3, pp. 1112-1121, Jul. 2009. DOI: 10.1109/TPWRD.2008.2002847

[108] M. Zimmermann and K. Dostert, "Analysis and modeling of impulsive noise in broad-band powerline communications," *IEEE Trans. Electromagn. Compat.*, vol. 44, no. 1, pp. 249-258, Feb. 2002. DOI: 10.1109/15.990732

[109] M. Katayama, T. Yamazato, and H. Okada, "A mathematical model of noise in narrowband power line communication systems," *IEEE J. Sel. Areas Commun.*, vol. 24, no. 7, pp. 1267-1276, Jul. 2006. DOI: 10.1109/JSAC.2006.874408

[110] R. Aquilué, M. Ribó, J. R. Regué, J. L. Pijoan, and G. Sánchez, "Scattering Parameters-Based Channel Characterization and Modeling for Underground Medium-Voltage Power-Line Communications," *IEEE Trans. Power Delivery*, vol. 24, no. 3, pp. 1122-1131, Jul. 2009. DOI: 10.1109/TPWRD.2008.2002963

[111] S. Cui, A. J. Goldsmith, and A. Bahai, "Energy-constrained modulation optimization for coded systems," in *Proc. IEEE Global Telecommunications Conference*, San Francisco, CA, USA, Dec. 2003, pp. 372–376. DOI: 10.1109/GLOCOM.2003.1258264

[112] S. Cui, A. J. Goldsmith, and A. Bahai, "Energy-constrained modulation optimization," *IEEE Trans.Wireless Commun.*, vol. 4, no. 5, pp. 2349–2360, Sep. 2005. DOI: 10.1109/TWC.2005.853882

[113] M. Steyaert, B. De Muer, P. Leroux, M. Borremans, and K. Mertens, "Low-voltage low-power CMOS-RF transceiver design," *IEEE Trans. Microwave Theory Tech.*, vol. 50, pp. 281–287, Jan. 2002. DOI: 10.1109/22.981281

[114] P. J. Sullivan, B. A. Xavier, and W. H. Ku, "Low voltage performance of a microwave CMOS Gilbert cell mixer," *IEEE J. Solid-Sate Circuits*, vol. 32, pp. 1151–1155, July 1997. DOI: 10.1109/4.597309

[115] G. Koutitas, "Green network planning of single frequency networks," *IEEE Trans. on Broadcasting*, vol. 56, no. 4, pp. 541–550, Dec. 2010. DOI: 10.1109/TBC.2010.2056252

[116] International Energy Agency (IEA), "CO_2 emissions from fuel combustion – Highlights," IEA Statistics Rep., 2009.

[117] D. Gesbert, M. Shafi, D. S. Shiu, P. Smith, and A. Naguib, "From theory to practice: An overview of MIMO space-time coded wireless systems," *IEEE J. Sel. Areas. Commun.*, vol. 21, no. 3, pp. 281–302, Apr. 2003. DOI: 10.1109/JSAC.2003.809458

[118] H. Latchman and L. Yonge, "Power line local area networking (Guest Editorial)," *IEEE Commun. Mag.*, vol. 41, no. 4, pp. 32–33, Apr. 2003.

[119] E. Fortunato, A. Garibbo, and L. Petrolino, "An experimental system for digital power line communications over high voltage electric power lines–field trials and obtained results," in *Proc. IEEE Int. Symp. Power Line Communications and Its Applications*, Kyoto, Japan, Mar. 2003, pp. 26-31.

[120] J. Anatory, N. Theethayi, and R. Thottappillil, "Power-line communication channel model for interconnected networks-Part II: Multiconductor system," *IEEE Trans. Power Del.*, vol. 24, no. 1, pp. 124-128, Jan. 2009. DOI: 10.1109/TPWRD.2008.2005681

[121] T. Yoo and A. Goldsmith, "Capacity and Power Allocation for Fading MIMO Channels With Channel Estimation Error," *IEEE Trans. Information Theory*, vol. 52, no. 5, pp. 2203–2214, May 2006. DOI: 10.1109/TIT.2006.872984

[122] M. Antoniali, A. M. Tonello, M. Lenardon, and A. Qualizza, "Measurements and analysis of PLC channels in a cruise ship," in *Proc. IEEE Int. Symp. Power Line Communications and Its Applications*, Udine, Italy, Apr. 2011, pp. 102–107. DOI: 10.1109/ISPLC.2011.5764372

[123] N. Pine and C. Sangho, "Modified multipath model for broadband MIMO power line communications," in *Proc. IEEE Int. Symp. Power Line Commun. Appl.*, Beijing, China, Mar. 2012, pp. 292-297. DOI: 10.1109/ISPLC.2012.6201312

[124] A. Tomasoni, R. Riva, and S. Bellini, "Spatial correlation analysis and model for in-home MIMO power line channels," in *Proc. IEEE Int. Symp. Power Line Commun. Appl.*, Beijing, China, Mar. 2012, pp. 286-291. DOI: 10.1109/ISPLC.2012.6201325

[125] D. Schneider, A. Schwager, W. Baschlin, and P. Pagani, "European MIMO PLC field measurements: Channel analysis," in *Proc. IEEE Int. Symp. Power Line Commun. Appl.*, Beijing, China, Mar. 2012, pp. 304-309. DOI: 10.1109/ISPLC.2012.6201316

[126] C. Xiong, G. Y. Li, S. Zhang, Y. Chen, and S. Xu, "Energy- and spectral-efficiency tradeoff in downlink OFDMA networks," *IEEE Trans. Wireless Commun.*, vol. 10, no. 11, pp. 3874–3886, Nov. 2011. DOI: 10.1109/TWC.2011.091411.110249

[127] G. P. Green, "Amenities and community economic development: Strategies for sustainability," *Journal of Regional Analysis and Policy*, vol. 31, no. 2, pp. 61-76, 2001.

[128] G. T. Heydt, R. Ayyanar, K. W. Hedman, and V. Vittal, "Electric Power and Energy Engineering: The First Century," *Proceedings of the IEEE*, vol. 100, pp. 1315-1328, May 2012. DOI: 10.1109/JPROC.2012.2187130

[129] S. S. Pappas, L. Ekonomou, D. C. Karamousantas, G. E. Chatzarakis, S. K. Katsikas, and P. Liatsis, "Electricity Demand Loads Modeling Using AutoRegressive Moving Average (ARMA) Models," *Energy*, vol. 33, no. 9, pp. 1353-1360, 2008. DOI: 10.1016/j.energy.2008.05.008

[130] I. C. Demetriou, "An Application of Best L1 Piecewise Monotonic Data Approximation to Signal Restoration," *IAENG International Journal of Applied*

Mathematics, to appear. [Online]. Available: http://www.iaeng.org/IJAM/issues_v43/issue_4/IJAM_43_4_09.pdf

[131] I. C. Demetriou, "L1PMA: A Fortran 77 Package for Best L1 Piecewise Monotonic Data Smoothing", *Computer Physics Communications*, vol. 151, no. 1, pp. 315-338, 2003. DOI: 10.1016/S0010-4655(02)00739-7

[132] G. Athanasiou, I. Karafyllis, and S. Kotsios, "Price Stabilization Using Buffer Stocks," *Journal of Economic Dynamics and Control*, vol. 32, no. 4, pp. 1212-1235, 2008. DOI: 10.1016/j.jedc.2007.05.004

[133] S. Kotsios, "Stabilization of Certain Discrete Volterra Systems an Algorithmic Approach," *in Proc. of IEEE 2014 11th International Conference on Informatics in Control, Automation and Robotics (ICINCO*), Vienna, Austria, vol. 1, pp. 629-634, Sep. 2014.

[134] I. C. Demetriou and E. E. Vassiliou, "An algorithm for distributed lag estimation subject to piecewise monotonic coefficients," *IAENG Int. J. Appl. Math*, vol. 39, no. 1, pp. 82-91, 2009.

Trends in Renewable Energy
OPEN ACCESS ISSN: 2376-2144
Peer-Reviewed Article futureenergysp.com/index.php/tre

Synthesis and Characterization of Carbon Nanospheres Obtained by Hydrothermal Carbonization of Wood-derived and Other Saccharides

Qiangu Yan[1*], Rui Li[2]*, Hossein Toghiani[3], Zhiyong Cai[4], Jilei Zhang[1]

1: Department of Sustainable Bioproducts, Mississippi State University, Mississippi State, MS 39762-9820
2: Joint School of Nanoscience and Nanoengineering, North Carolina Agricultural and Technical State University, Greensboro, NC 27411
3: Dave C. Swalm School of Chemical Engineering, Mississippi State University, Mississippi State, MS 39762
4: Forest Products Lab, USDA Forest Service, Madison, WI 53726-2398

Received May 13, 2015; Accepted July 3, 2015; Published July 4, 2015

Carbon nanospheres were synthesized by hydrothermal carbonization (HTC) of four different carbon sources: xylose, glucose, sucrose, and pine wood derived saccharides. The obtained carbon nanospheres were characterized for particle morphology and size, and surface functional groups. Morphological and structural differences among these saccharides derived HTC carbons were clearly observed. Scanning electron microscopy images of carbon nanospheres from HTC of xylose showed uniform spherical particles with diameters around 80 nm, while carbon nanospheres obtained from glucose, sucrose, and pine-derived saccharides had particle size in the range of 100-150 nm, 300-400 nm, and 50-100 nm, respectively. Carbon dioxide and carbon monoxide were primary gaseous phase products during the HTC process. In addition, methane, propane, hydrogen, and benzene were detected in the gas phase.

Keywords: Hydrothermal Carbonization (HTC); Carbon Nanospheres; Carbohydrates; Pine Wood-derived Saccharides; Gas Phase Composition; Mechanism of HTC

1. Introduction

Carbonaceous materials have been widely used in diverse industries due to their superior properties such as good electrical conductivity, high surface area and porosity, and their specific surface chemistry. Carbonaceous materials are produced from carbon-containing compounds by thermal, chemical or hydrothermal processes in gas, liquid, or solid phases [1]. The physical and chemical properties as well as the structure of formed carbons are affected by both reaction conditions and the feedstock [2]. Various feedstocks such as cyclohexane and acetylene have been used to produce nanoscale carbons. However, these raw sources were not sustainable or renewable and these processes were usually expensive. Therefore, the objective of this work is to develop a simple process to produce nanoscale carbon particles with renewable materials such as pine wood-derived saccharides.

In the current effort, the hydrothermal carbonization (HTC) method was examined, and saccharides derived from pinewood were used as the feedstock. A HTC

*Corresponding author: yan@cavs.msstate.edu, rli1@aggies.ncat.edu

Tr Ren Energy, 2015, Vol.1, No.2, 119-128. doi:10.17737/tre.2015.1.2.0012

process with moderate temperatures and self-generated pressures over an aqueous solution of a variety of feedstocks in a dilute acid for hours is a promising process to produce nanostructured carbon materials from woody biomass [3]. The carbon content in wood varies from 47 to 53% due to differences in lignin and extractives contents [4]. Chemical components of loblolly pine woods are 42-46% glucose in cellulose, 1-5% glucose, 10-11% mannose, 7% xylose, 1-2% arabinose, and 1.5-2.5% galactose in hemicelluose, and 27-30% lignin, which makes a total carbon contribution of 66-69% [5]. Almost 30 to 50% of carbon in wood could be converted to the solid char via thermochemical processes.

For this study, highly functionalized carbonaceous materials were synthesized from four different carbon sources (xylose, glucose, sucrose, and carbohydrates derived from pine wood) by using a moderate temperature HTC process. The carbon nanospheres from xylose had a perfect spherical shape with the highest yield among all feedstocks used. The gas phase composition of the reaction effluent was analyzed, and carbonaceous materials were characterized using the scanning electron microscopy (SEM), the transmission electron microscopy (TEM), and the temperature-programmed desorption (TPD). The possible mechanism of the HTC of saccharides was proposed.

2. Materials and Methods

2.1 Materials

All compounds such as xylose, glucose, sucrose, and sulfuric acid (95%) were purchased from Sigma-Aldrich. The wood chips used were raw southern yellow pinewood chips.

2.2 Preparing Pine Wood Derived Saccharides

Saccharides were obtained via sulfuric acid hydrolysis of the southern pine wood chips (<10 mm in length) [6]. The pine wood chips were dried to a moisture content of ~10% in an onsite dryer, and treated with 72% H_2SO_4 (15 g chips in 150 mL acid solution) at 30ºC for 1 h. The mixture of acid treated pine chips was diluted by adding 4,200 mL of water and hydrolyzed at 121ºC for 1 h. Then, the hydrolysate solution was filtered through the crucibles with a filtering disc to separate the filtrate and residues. The filtrate containing saccharides was used to prepare carbon nanoparticles.

An Agilent 1100 high-performance liquid chromatography (HPLC) (Santa Clara, CA) was used to analyze saccharide concentrations in the filtrate. The HPLC consisted of a G1311A liquid chromatograph pump, G1379A online degas unit, G1313A automatic injector with a 20 µl loop, and G1315B diode array detector. The column was Agilent Hi-Plex Ca, 7.7 × 300 mm, 8 µm (p/n PL1170-6810), the mobile phase was de-ionized (DI) H_2O with a flow rate of 0.6 mL/min, and oven temperature was 85ºC. The structural carbohydrates in pine wood were determined according to the standard analytical procedure [6]. The filtrate (*i.e.* the hydrolysate produced from the pine wood) contained 33.3% (w/v) glucose, 4.8% (w/v) xylose, 1.4% (w/v) arabinose, 2.9% (w/v) galactose, and 15.4% (w/v) mannose.

2.3 Synthesis of Carbon Nanospheres by Hydrothermal Carbonization

2.3.1 Preparation of Carbon Nanospheres from Glucose, Sucrose and Xylose

The hydrothermal carbonization of glucose was carried out using following procedures: Sixty gram of glucose was dissolved in 1000 mL DI water and stirred for 0.5 h to form a clear solution. Concentrated sulfuric acid (~95%) was added dropwisely to adjust the pH value of the solution to between 4~5. Then, the solution was transferred to a stainless steel 1 gallon Parr reactor (Moline, IL), and heated and maintained at 180°C with continuous stirring for 12 h. After the hydrothermal carbonization process was completed, the Parr reactor was then cooled to room temperature with continuous stirring. The gas phase (about 5~10 psig) in the Parr reactor was first released and analyzed with a Dycor-Dycor Dymaxion Residual Gas Analyzer (RGA) (AMETEK Process Instruments, Pittsburgh, PA). The obtained black slurry mixture was separated by centrifugation, washed with DI water and ethanol, and dried at 80°C overnight. The procedures for preparing carbon nanospheres from sucrose and xylose were the same as that of glucose.

2.3.2 Preparation of Carbon Nanospheres from Pine-derived Sugars

A 250 mL pine-wood-derived sugar solution, which contained ~30 g saccharides, was used as the starting material. The pH value of the solution was adjusted to 3. The sugar solution was stirred for 0.5 h in a beaker, and then transferred into a Parr reactor. The solution was heated and maintained at 210°C for 12 h. The black solid products were collected and washed with DI water and ethanol to remove soluble ions and sugar residues. The final product was oven-dried at 110°C overnight.

2.4 Characterization of Carbon Materials

The sample morphology was investigated with a Scanning Electron Microscope (SEM) (JEOL JSM-6500F, Peabody, MA). The system was operated with accelerating voltage of 5 kV. All samples were coated with gold. The sample particle sizes were examined with a JEOL JEM-100CX II transmission electron microscope (TEM, Peabody, MA). TEM was operated at accelerating voltage of 100 kV. All samples were sonicated in ethanol solution for 20 min before transferred on copper grid. Thermogravimetric analysis (TGA, Shimadzu TGA-50，Japan) was performed to determine the weight loss during calcination. For each sample, the temperature was ramped at 10 °C/min to 1000°C under atmosphere. Temperature-programmed desorption (TPD) experiments involved heating the carbon nanospheres at 2 °C/min in a helium gas to induce thermal desorption of adsorbed species on the surface. Volatile species were analyzed using an on-line Agilent 7890 GC during the TPD process. A 5 g sample were carried out in a fixed-bed 1/2-inch tubular stainless-steel reactor under N_2 atmosphere (99.999 % purity) at a flow rate of 20 ml/min.

3. Results and Discussion

3.1 Hydrothermal Carbonization of Saccharides

Experimental conditions of the HTC of saccharides including samples, reaction temperature, and reaction time are summarized in Table 1. The results showed that the highest and lowest carbon nanospheres yields were obtained from xylose and sucrose, respectively. The difference in yields may be due to different carbonization tendencies of these saccharides. Xylose began to decompose and carbonize at about 140 °C, while the decomposition temperature for glucose and sucrose was between 160-170 °C. Among all

starting materials studied, xylose was the best raw material to get the highest yield of the carbon nanospheres.

Table 1 Synthesis conditions and product yields for carbon nanospheres obtained from the HTC of saccharides

Sample	HTC temperature (°C)	Reaction time (h)	Yield of nano-materials (g product/100 g saccharides)	Size (nm)
Xylose	180	12	80.2	~80
Glucose	180	12	68.5	100-150
Sucrose	180	12	54.7	300-400
Pine wood derived saccharides	210	12	60.3	50-100

3.2 Gaseous Products from Hydrothermal Carbonization

The composition of gases resulted from the HTC of glucose was analyzed with an on-line RGA (Figure 1). The RGA response showed that significant amounts of CO and CO_2 were released from the glucose. The results were consistent to Xue *et al.* [7], who have studied the pyrolysis of saccharides under different conditions and found that H_2O, CO, and CO_2 were released from the samples. The detection of benzene in the gas phase meant that aromatic species were important intermediates during the HTC process.

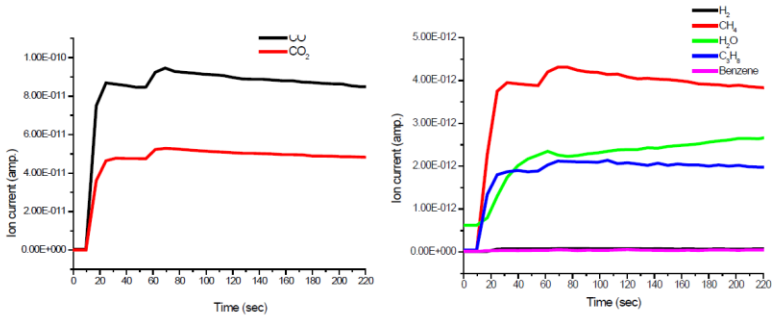

Figure 1 RGA of glucose after the HTC at 180°C.

The gaseous products were further analyzed using an Agilent 7890 GC, and the relative amount of 37.0 % H_2, 10.6 % CO, 45.3 % CO_2, 0.05 % C_2H_6, 0.001 % CH_4, 0.01 % C_3H_8, and 3.8 % N_2 were found in the gas phase. Trace amount of ethylene (less than 0.001 %) was also identified. The results of other saccharides were similar to that of glucose.

3.3 Characterization of Carbon Nanospheres

3.3.1 Scanning Electron Microscopy (SEM) Study

SEM images of carbon nanospheres produced by HTC are shown in Figure 2a-2d. Carbon nanospheres obtained from xylose (Figure 2a) had a higher degree of uniformity in shape and monodisperion compared to those by HTC of other saccharides, while carbon nanospheres derived from glucose and sucrose presented irregular shapes. The carbonaceous products from pine-derived saccharides exhibited a regular morphology (Figure 2d).

Under similar operational conditions, the diameter of nanospheres changed as a function of the type of saccharides used. Thus, the mean diameter followed the tendency: xylose (~80 nm) < glucose (120-150 nm) < sucrose (300-400 nm). This variation may be related to intermediate products decomposed from the different saccharides during the hydrothermal treatment process. The HTC of pentose like xylose proceeds via a furfural route, while hexose HTC occurs via a 5-hydroxymethylfurfural (HMF) route. Disaccharide like sucrose needs to be hydrolyzed into two mono-saccharides in the first step [3].

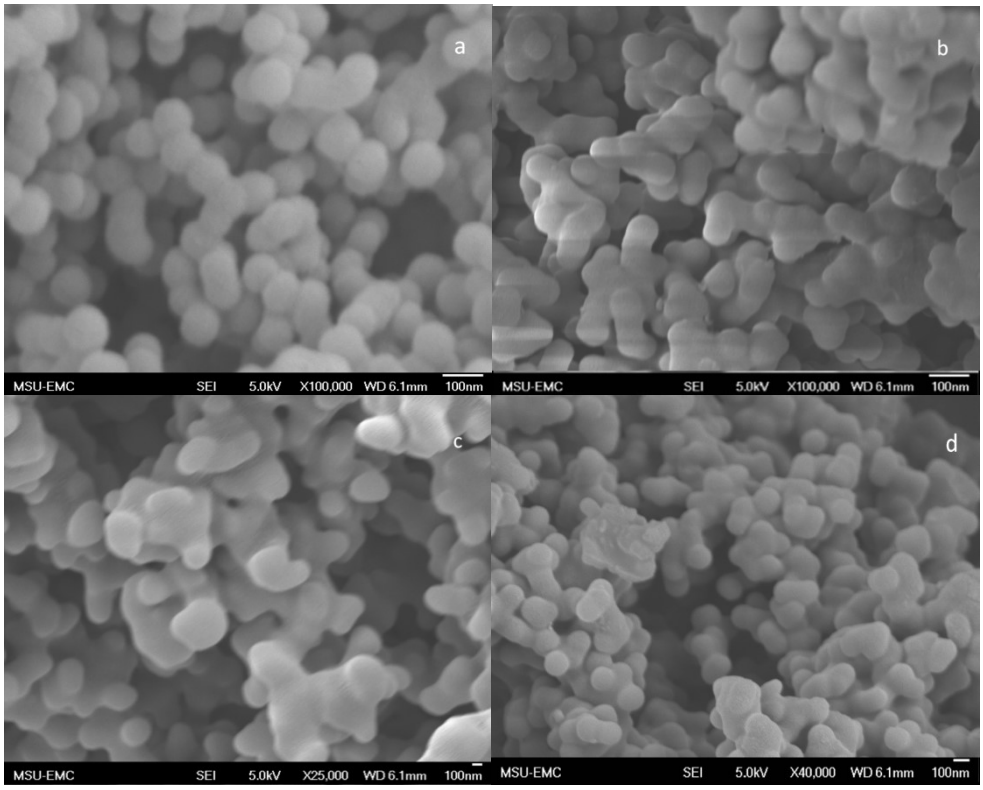

Figure 2 SEM images of carbon nanospheres by the HTC process at 180°C or 210°C. (a) xylose, (b) glucose, (c) sucrose, and (d) pine wood derived sugar solution

3.3.2 Transmission Electron Microscopy (TEM) Study

Figure 3 shows TEM images of carbon nanospheres from saccharides. The products made from xylose exhibited the diameter of approximately 80 nm (Fig. 3a), while glucose HTC products exhibit a tendency to form large agglomerates (Fig. 3b). The particle size from sucrose (400 nm) (Fig. 3c) is larger than that of xylose or glucose (120 to 150 nm). This is attributed to the longer C-C chains in sucrose. Similar to SEM images, TEM images (Figure 3d) show the presence of regularly shaped nanoscale carbons with diameters of 50-100 nm from pine derived sugar solution.

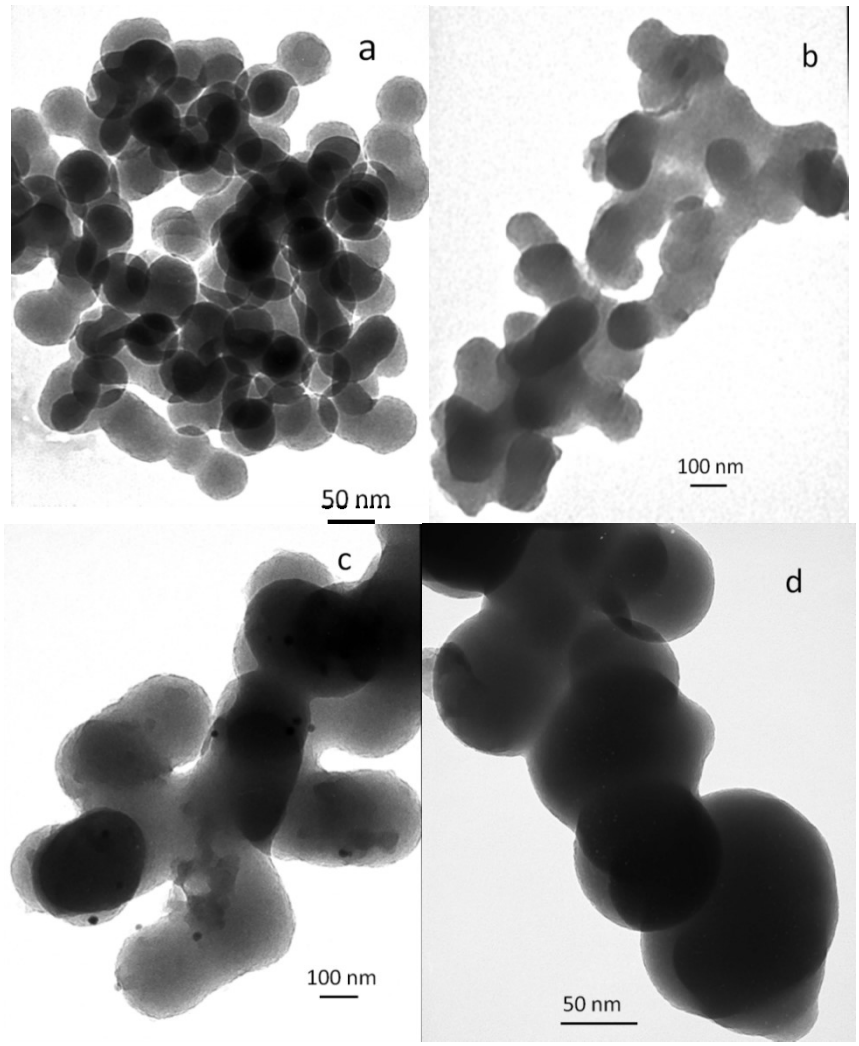

Figure 3 TEM images of carbon nanospheres by the HTC process at 180°C or 210°C. (a) xylose, (b) glucose, (c) sucrose, and (d) pine wood derived sugar solution

3.3.3 Temperature-Programmed Desorption (TPD)

TPD experiments coupled with an on-line GC were conducted to study the thermal desorption. The main decomposition by releasing gaseous compounds from carbon particles starting at 270°C was indicative of a restructuring of carbon motifs. The loss of volatile species such as H_2, CH_4, CO, C_2H_6, C_3H_8, and CO_2 was described by TPD spectra in Figure 4.

Between 400-500 °C, the strongest band intensities corresponded to the loss of CO_2 and CO, which decomposed from oxygenated functional groups. Surface complexes yielding CO_2 groups decomposed at two different temperatures, corresponding to two types of functional groups. Carboxylic acids (-COOH $\rightarrow$ CO_2) were responsible for the low-temperature peak (100-400 °C), and the high-temperature CO_2 evolution was attributed to carboxylic anhydrides and lactones (450-700 °C). The CO-yielding groups were represented by three distinct groups of peaks, and the corresponding peak temperatures of CO desorption centered at 400°C for the anhydride and lactone groups. The CO peak centered at 500°C was assigned to the ether decomposition and the CO peak above 550°C was contributed to the phenols and quinine [8]. Subsequently at 500°C,

the methane peak originated from decomposition of the methylene bridges, which acted as cross-linkers within the HTC carbon framework [9].

Hydrogen on the carbon surface served as chemisorbed water or as surface functionalities (*e.g.*, carboxylic acids, phenolic groups), or was bonded directly to carbon atoms as a part of aromatic or aliphatic structures. The C-H bond is very stable and will not break until 800 °C without catalyst. Heat treatment in an inert atmosphere eliminated part of the hydrogen via surface reduction. The carbonaceous surface contained a lot of oxygen-containing aromatic heterocyclic structures, which decomposed with the formation of carbon monoxide, methane, and other low hydrocarbons. As a consequence of the observed thermal decomposition processes, the structure of HTC carbons underwent a rearrangement process due to ring opening and aromatization.

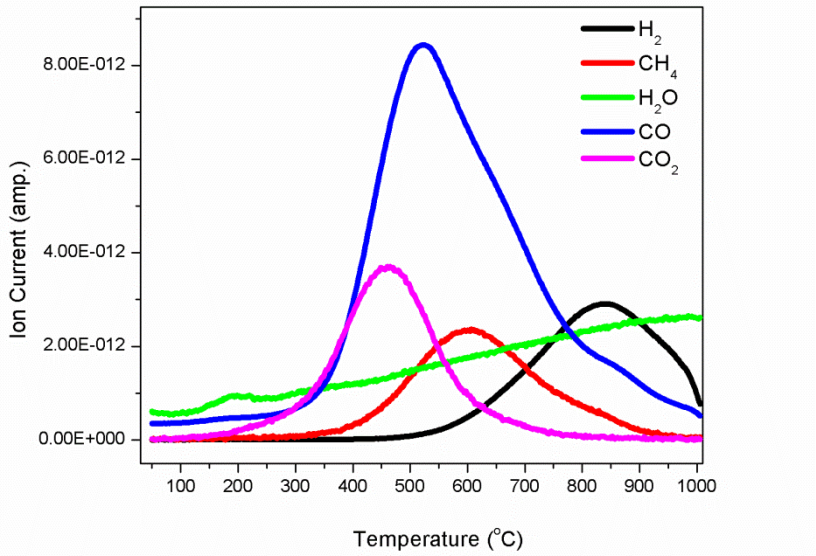

Figure 4 TPD curves for the temperature-programmed calcination of the carbon nanospheres from pine wood derived saccharides

3.3.4 Thermal Gravimetric Analysis (TGA)

Thermoanalytic techniques were used to study the thermal behavior of carbon nanospheres. The TG and DTG curves for the carbon nanospheres from pine-derived saccharides between room temperature and 700°C in N_2 atmosphere are shown in Figure 5. A continuous weight loss with increasing temperature was observed, which denoted breaking of chemical linkages and removal of volatile products from the sample. Three possible steps of weight loss could be observed in Figure 5. The initial weight loss may correspond to the loss of physically adsorbed water and occurred between ambient temperature and 130°C with a peak temperature of 70°C. It was followed by a plateau region for the rate of weight loss from 130°C to 200°C. The strong weight loss observed at around 200°C to 700°C corresponded to the decomposition of all the functional groups in the carbonaceous materials. These results indicated that oxygen functional groups started releasing in this temperature zone, leading to the initialization of aromatization. The most weight loss of carbon nanospheres was in the temperature zone from 350°C to 700°C. This mass loss step mainly attributed to the decomposition of the rest of the carboxylic anhydrides and lactones, part of phenols, quinine, and ether, which were released as volatile products such as CO_2, CO, CH_4, H_2O, and H_2.

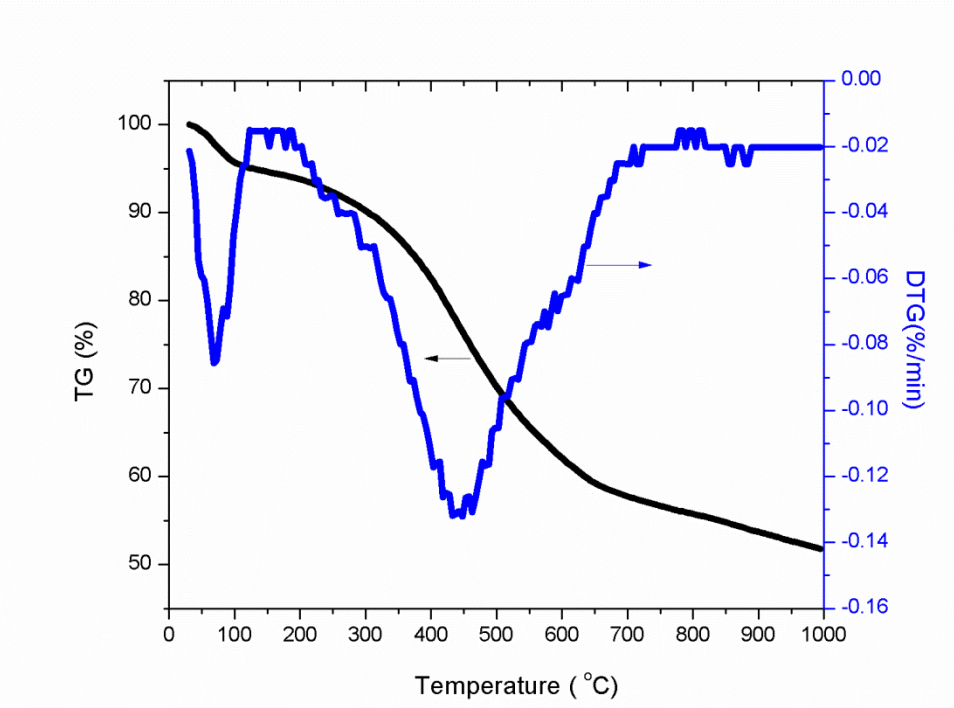

Figure 5 TG and DTG curves of the carbon nanospheres from pine wood derived saccharides

3.4 Possible Mechanism for Formation of Carbon Nanospheres

Based on the TPD spectra and gas phase composition presented upon completion of the HTC reaction, a possible mechanism of this process was proposed. The mechanism comprised two steps. In the first step, when an aqueous sugar solution was hydrothermally treated at 180°C, the sugar molecules (like glucose) hydrolyzed. In the second step, reactions consisted of both polymerization and condensation processes leading to the formation of soluble polymers [10]. Polymerization and condensation reactions may be induced by intermolecular dehydration or aldol condensation [8]. At the same time, the aromatization of polymers took place. The C=O group appeared due to the dehydration of water from the hydroxyl groups in the monomers [11, 12]. Aromatic clusters may be produced by the condensation of the aromatized molecules generated in the decomposition/dehydration of the oligosaccharides or monosaccharides [8]. All RGA results have demonstrated the presence of benzene in the gas phase. When the concentration of aromatic clusters in the aqueous solution reached the critical supersaturation point, the formation of carbon nucleation took place [8, 11]. The formed nuclei of carbon grew by diffusion of the chemical species present in the solution towards the surface [11]. These species were linked to the surface of the spheres via the reactive surface functional groups (hydroxyl, carbonyl, carboxylic, etc.) presented in the particles, which was proved by the experimental TPD spectra. Stable surface functional groups such as ether or quinone were formed. Once the growth process stopped, carbon nanospheres, whose surface contained a high concentration of reactive functional groups, were obtained. The gas phase composition and the TPD spectra of the carbon products were proved almost identical for all the saccharides investigated, indicating the similar mechanism for these saccharides.

4. CONCLUSIONS

This paper presented a systemic study on HTC of model saccharides (xylose, glucose, and sucrose) and carbohydrates derived from pine wood, producing carbon nanospheres with size between 50-400 nm. The carbon nanospheres from xylose had a perfect spherical shape with the highest yield among all feedstocks used. The mixture of saccharides from acid hydrolysis of pine wood can be used as carbon sources to synthesize 50-100 nm carbon nanospheres. The TPD proved that aromatization processes took place during the hydrothermal carbonization, and the carbon nanospheres contained a large number of oxygen functional groups. The shell contained hydrophilic oxygen functional groups (carboxylic, hydroxyl, etc.), while the core had hydrophobic aromatic nucleus with oxygen forming stable groups (ether, quinone, pyrone, etc.). During the thermal decomposition of derived carbon nanospheres, CO_2 and CO first decomposed from oxygenated functional groups, and then CH_4 and H_2 were released. Carbon nanospheres with surface oxygen groups and a controllable size possessed potentials for their further applications in hydrothermal carbon hybrid materials.

CONFLICTS OF INTEREST

The authors declare that there is no conflict of interests regarding the publication of this paper.

REFERENCES

[1] Hu, B., Wang, K., Wu, L., Yu, S.-H., Antonietti, M., and Titirici, M.-M. (2010). Engineering Carbon Materials from the Hydrothermal Carbonization Process of Biomass. *Advanced Materials*, 22(7), 813-828. DOI: 10.1002/adma.200902812

[2] MATERIALS SCIENCE AND PROCESS TECHNOLOGY SERIES. (1993). In: *Handbook of Carbon, Graphite, Diamonds and Fullerenes*, H. O. Pierson, ed., William Andrew Publishing, Oxford, pp: v-vi. DOI: 10.1016/B978-0-8155-1339-1.50003-7

[3] Li, R., and Shahbazi, A. (2015). A Review of Hydrothermal Carbonization of Carbohydrates for Carbon Spheres Preparation. *Trends in Renewable Energy*, 1(1), 43-56. DOI: 10.17737/tre.2015.1.1.009

[4] Ragland, K. W., Aerts, D. J., and Baker, A. J. (1991). Properties of wood for combustion analysis. *Bioresource Technology*, 37(2), 161-168. DOI: 10.1016/0960-8524(91)90205-X

[5] Koch, P. (1972). Utilization of the southern pines. *Asheville, NC: USDA-Forest Service, Southern Forest Experiment Station*, Volume 1, 1-734.

[6] Sluiter, A., Hames, B., Ruiz, R., Scarlata, C., Sluiter, J., Templeton, D., and Crocker, D. (2008). Determination of Structural Carbohydrates and Lignin in Biomass: Laboratory Analytical Procedure (LAP). *http://www.nrel.gov/biomass/pdfs/42618.pdf* (Accessed on 07/03/2015).

[7] Xing, W., Xue, J. S., and Dahn, J. R. (1996). Optimizing Pyrolysis of Sugar Carbons for Use as Anode Materials in Lithium - Ion Batteries. *Journal of The Electrochemical Society*, 143(10), 3046-3052. DOI: 10.1149/1.1837162

[8] Sevilla, M., and Fuertes, A. B. (2009). The production of carbon materials by hydrothermal carbonization of cellulose. *Carbon*, 47(9), 2281-2289. DOI: 10.1016/j.carbon.2009.04.026

[9] Yu, L., Falco, C., Weber, J., White, R. J., Howe, J. Y., and Titirici, M.-M. (2012). Carbohydrate-Derived Hydrothermal Carbons: A Thorough Characterization Study. *Langmuir*, 28(33), 12373-12383. DOI: 10.1021/la3024277

[10] Salak Asghari, F., and Yoshida, H. (2006). Acid-Catalyzed Production of 5-Hydroxymethyl Furfural from d-Fructose in Subcritical Water. *Industrial & Engineering Chemistry Research*, 45(7), 2163-2173. DOI: 10.1021/ie051088y

[11] Bacon, R., and Tang, M. M. (1964). Carbonization of cellulose fibers—II. Physical property study. *Carbon*, 2(3), 221-225. DOI: 10.1016/0008-6223(64)90036-3

[12] Luijkx, G. C. A., van Rantwijk, F., van Bekkum, H., and Antal Jr, M. J. (1995). The role of deoxyhexonic acids in the hydrothermal decarboxylation of carbohydrates. *Carbohydrate Research*, 272(2), 191-202. DOI: 10.1016/0008-6215(95)00098-E

CALL FOR PAPERS

Trends in Renewable Energy

ISSN Print: 2376-2136 ISSN online: 2376-2144
http://futureenergysp.com/index.php/tre/

Trends in Renewable Energy (TRE) is a quarterly, open accessed, peer-reviewed journal publishing reviews and research papers in the field of renewable energy technology and science. The aim of this journal is to provide a communication platform that is run exclusively by scientists. This journal publishes original papers including but not limited to the following fields:

- ✧ Renewable energy technologies
- ✧ Catalysis for energy generation, Green chemistry, Green energy
- ✧ Bioenergy: Biofuel, Biomass, Biorefinery, Bioprocessing, Feedstock utilization, Biological waste treatment,
- ✧ Energy issues: Energy conservation, Energy Resources, Energy transformation, Energy storage
- ✧ Environmental issues: Environmental impacts, Pollution
- ✧ Bioproducts
- ✧ Policy, etc.

We publish the following article types: peer-reviewed reviews, mini-reviews, technical notes, short-form research papers, and original research papers.

The article processing charge (APC), also known as a publication fee, is fully waived for the initial two years for the Trends in Renewable Energy.

Call for Editorial Board Members

We are seeking scholars active in a field of renewable energy interested in serving as volunteer Editorial Board Members.

Qualifications

Ph.D. degree in related areas, or Master's degree with a minimum of 5 years of experience. All members must have a strong record of publications or other proofs to show activities in the energy related field.

If you are interested in serving on the editorial board, please email CV to editor@futureenergysp.com.

Advertise With Us

The rate is $100 per page, $50 for a half-page, and $25 for a quarter-page advertisement for three month. The advertisement will be placed on the additional page of each individual published pdf file.